

Novel lipid-based vesicles for sustained buccal delivery of a local anaesthetic for oral pain relief

Ruba Bnyan

Thesis submitted in partial fulfilment of the requirement of Liverpool John Moores University

for the degree of Doctor of Philosophy

Jan-2020

Dedication

I dedicate all my PhD work to the only one who is behind any success I have or could have achieved in my life...

To the soul of my MOM ... Wafaa Al-Qadri

Mama ... every happiness is incomplete without you!

And...

To my DAD ... Ahmad Nader Bnyan

My Dad is the only person who believed in me more than myself, and who has been to me the model person in sincerity, determination and hardworking.

No acknowledgment or dedication is sufficient to express my gratitude to my dad for the support, encouragement and love I have been receiving from him.

Acknowledgment

- The first and the utmost gratitude is to **Liverpool John Moores University**, Pro Vice Chancellor **Dr. Edward Harcourt**, the **School of Pharmacy and Biomolecular Sciences**, the Director of School, **Prof. Satyajit Sarker**, and **the Doctoral Academy** for generously providing the funding for this research and giving me the opportunity to accomplish my PhD.

- I would like to express my deep gratitude to the **Council for At Risk Academic (CARA)**, which was a great source of support during my research journey.

- Special thanks to the Director of Study **Dr. Matthew Roberts**, without his support, scientific guidance and encouragement this thesis would not have seen the light of day. Dr Matt has an open door and heart policy for discussing any personal or professional issue; his outstanding academic attitude and scientific contribution has left remarkable influences on this research and me personally.

- I would like to thank **my supervisory team (Imran Saleem, Touraj Ehtezazi and Francis O'Neill)**.

- I also genuinely thank **Dr. Iftikhar Khan**. Dr. Ifti provided fantastic scientific guidance, practical suggestions and significant support during this project. I am pleased to say, that through this work, Dr. Ifti and I have developed a strong and trusting friendship that I hope can continue after this work. Deep thanks Ifti, I would not have made it without you.

- I would further like to acknowledge the support, practical training and scientific guidance that I generously received from **Dr. Amos Fatokun** in running the cell culture studies. Dr. Amos' support not only did help me to run the cell-based experiments well, but also he kept me upbeat through all the difficult times I had over a year dealing with repeated contamination of cells and unlucky experimental failures. His encouragement made me more determined to get it right, and only because of him, I can proudly say that I have successfully achieved it.

- I would acknowledge the technical support I got from many staff members including **Dr. James Downing**, who trained me on tissue handling and dissection skills; **Dr. Sarah Gordon**, who was there to discuss a few aspects of my research with generous suggestion. I am grateful for the technical support I got from **Philip Salmon** during the HPLC method development.

- My acknowledgement would be incomplete without mentioning the wonderful environment I was surrounded with, through **lab mates, colleagues, and friends** within LJMU or in the surrounding community.

-Sincere thanks to my old two best friends from Syria, **Noor and Rahaf** who were along the whole journey with me regardless of the distance.

- Last but by no means least, I'd like to acknowledge the love and support I received from **my soulmate sisters, Afraa, Arwa, and Sura, and my brother Mohammad**. I believe I am tremendously fortunate to have had such a supportive, loving and caring family.

Abstract

There is a clinical need for a long acting topical anaesthetic formulation that could be applied by patients themselves, dentists, or health care professionals, therefore the project aim was to develop and prepare a mucoadhesive carrier for the buccal delivery of local anaesthetic (LA), embedded into fast disintegrating film to achieve sustained local pain relief.

Novel transfersomes loaded with LA such as lidocaine could be a superior approach to improve patient compliance and achieve the required level of anaesthesia. Lidocaine-loaded transfersomes were optimised and formulated using a Taguchi design of experiment (DOE) in terms of phospholipid type, type of edge activator (EA) and ratio of phospholipid to EA. Transfersomes were characterised for size, polydispersity index (PDI), charge, and entrapment efficiency (%EE). The obtained transfersomes were 200 nm in size and with a good PDI around 0.3.

A new HPLC method for lidocaine quantification was optimised and validated using a mobile phase of 30 % v/v PBS (0.01 M) and 70 % v/v Acetonitrile at a flow rate of 1 mL/min. Detection was carried out at 255 nm at 30 °C and the retention time was 2.84 minutes. Linearity was obtained over the range 0.1-2 mg/mL (R^2 0.9999). The proposed method was shown to be valid for linearity, accuracy, sensitivity, intermediate precision and repeatability according to ICH guidelines. The %EE was dependent on the formulation parameters and was between 44-56%. Analysing the data by Taguchi DOE showed the effect of factors on both size and %EE were in the following rank order: lipid: EA ratio >EA type >lipid type. The type of lipid (natural or synthetic) showed no significant effect on transfersome size. Increasing the EA concentration reduced transfersome size, however, further increments of EA had an opposite effect, and transfersome size increased. Six transfersome samples were selected based on the analysis of the optimisation results, and their release profiles were assessed. All 6 samples proved that the optimised transfersomes can be used as a sustained release delivery system of LA as they released lidocaine slowly over 24h.

It was believed that incorporation of mucoadhesive polymers into the delivery system would prolong their residence time at the buccal cavity. Thus, three different polymers (HPMC K4M, HPMC K15M, and chitosan HCl) were screened for forming a continuous coating layer, aiming to preserve the uniform nanosize of transfersomes as well as enhancing the %EE. There was

a clear indication of coating layer formation as all formulations showed an increased size afterwards. However, transfersomes coated with HPMC K4M and K15M failed to keep the nanosize or homogenous distribution obtained with the uncoated ones. Although chitosan HCl coated transfersomes showed a slight increment in the size as well, except formulation F5 at low chitosan HCl concentrations (i.e. 0.1 and 0.2 % w/v). Not only did formulation F5 show a non-significant difference in size after coating with chitosan HCl but it also had a higher drug entrapment (84%) compared to the uncoated sample (49%). Therefore, the chitosan-coated formulation (F5-CH) was selected and tested for mucoadhesion and drug release properties. F5-CH exhibited a sustained release profile over 24 h with an immediate release of 23.4% during the first hour, which could guarantee the immediate effect of LA. These findings proposed a novel buccal drug delivery system utilising chitosan HCl coated transfersomes.

Three different cell lines (NOK, MRC5, MRC5-SV2) were employed to confirm the safety of coated transfersomes. Which proved to be completely safe and non-toxic at the intended concentration to be delivered. The *ex vivo* model proved the successful formation of a sustained delivery system, as the drug released from the chitosan coated transfersomes slowly with 80% drug accumulation after 24 h.

Single layer films loaded with the coated transfersomes were successfully developed using a mixture of mucoadhesive polymers (HPC and PVA). A simple casting method was used and the produced films disintegrated on average at 2.75 min. They showed good mechanical properties and flexibility, in addition to have a pH of 7.9 that is well tolerated in the buccal mucosa. The content uniformity was confirmed and the drug release from transfersomes was not affected by their loading into polymeric film.

Contents

DEDICATION.....	II
ACKNOWLEDGMENT.....	III
ABSTRACT	IV
LIST OF ABBREVIATIONS AND ACRONYMS	X
LIST OF FIGURES.....	XII
LIST OF TABLES.....	XVI
CHAPTER 1. INTRODUCTION.....	1
1.1 Buccal delivery.....	2
1.1.1 Buccal mucosa anatomy and physiological properties.....	2
1.1.2 Mucus.....	4
1.1.3 Saliva.....	4
1.1.4 Absorption pathways.....	5
1.1.5 Previous studies of micro/nanoparticle systems for buccal administration	6
1.1.6 Mucoadhesive Films	10
1.2 Lipid-based vesicles	12
1.2.1 Surfactants.....	17
1.2.1.1 Low molecular weight surfactants	18
1.2.1.2 Polymeric surfactants.....	20
1.2.1.3 Surfactant classification depends on HLB	20
1.2.2 Surfactants in lipid-based vesicles	21
1.2.2.1 Surfactant effects on the size and polydispersity index (PDI).....	21
1.2.2.2 Surfactant effects on entrapment efficiency	24
1.2.2.3 Surfactant effects on pharmacokinetics and pharmacodynamics	29
1.2.2.4 Surfactant effects on charge and stability	31
1.2.3 Formulation methods.....	33
1.2.3.1 Conventional methods.....	33
1.2.3.2 Developed methods.....	38
1.3 Local anaesthetics	38
1.3.1 Specific local anaesthetic agents	Error! Bookmark not defined.
1.3.1.1 Lidocaine	41
1.3.1.2 Bupivacaine	Error! Bookmark not defined.
1.3.2 Local anaesthetic delivery	Error! Bookmark not defined.
1.3.2.1 Examples of LAs delivery systems	42
1.3.3 LAs in dentistry	47
1.3.3.1 Methods of LAs delivery in Dentistry.....	48
1.4 Basis for the research project	51
1.4.1 Aim	51
1.4.2 Objectives	51

CHAPTER 2. GENERAL METHODOLOGY	52
2.1 Materials	53
2.1.1 Materials for transfersome formulation and characterisation	53
2.1.2 Materials for cell culture	53
2.1.3 Materials for ex-vivo testing.....	54
2.1.4 Materials for buccal film preparation.....	54
2.1.5 Other materials and solvents	54
2.2 General Methods and main analytical techniques	55
2.2.1 Preparation of transfersomes.....	55
2.2.2 Transfersomes coating	56
2.2.3 Dynamic light scattering (DLS).....	57
2.2.3.1 Size, polydispersity index (PDI), and zeta potential	58
2.2.4 High performance liquid chromatography (HPLC)	58
2.2.4.1 HPLC chromatographic system	60
2.2.5 Entrapment efficiency (%EE)	60
2.2.6 <i>In vitro</i> release study	61
2.2.7 Transfersome morphology	61
2.2.7.1 Transmission electron microscope (TEM).....	62
2.2.7.2 TEM for transfersomes characterisation	62
2.2.7.3 Scanning electron microscope (SEM).....	63
2.2.7.4 SEM for transfersomes characterisation.....	63
2.2.8 Cytotoxicity study	64
2.2.8.1 Cell culture preparation	64
2.2.8.2 Cell treatments and AlamarBlue viability assay	65
2.2.9 <i>Ex-vivo</i> permeability	66
2.2.9.1 Tissue preparation for permeation study	66
2.2.9.2 Permeation experiment using Franz-cell	66
2.2.10 Cell-based model permeation experiment	67
2.2.10.1 Cell-based model preparation	67
2.2.10.2 Permeation through transwell	68
2.2.11 Buccal Film preparation	69
2.2.11.1 Preparation of polymer solutions	69
2.2.11.2 Buccal film casting.....	70
2.2.12 Characterisation of the buccal film.....	70
2.2.12.1 Weight uniformity and thickness	70
2.2.12.2 Film content uniformity	71
2.2.12.3 Film disintegration	71
2.2.12.4 Buccal film Morphology	71
2.2.12.5 pH measurement of the film surface	71
2.2.12.6 Drug release from film	72
2.2.12.7 Tensile strength properties.....	72
2.2.13 Statistical analysis	72
CHAPTER 3. FORMULATION AND OPTIMISATION OF NOVEL TRANSFERSOMES	73
3.1 Introduction	74
3.2 Methods.....	76
3.2.1 HPLC Method development and validation.....	76
3.2.2 Design of experiment (DOE)	77
3.2.3 Formulation and characterisation of transfersomes	80
3.3 Results and discussion	80
3.3.1 HPLC method development.....	80

3.3.2	HPLC method validation	81
3.3.3	Transfersome preparation and characterisation.....	85
3.3.3.1	Zeta potential.....	91
3.3.3.2	Transfersome morphology.....	93
3.3.3.3	<i>In vitro</i> release	94
3.4	Conclusion	97
 CHAPTER 4. TRANSFERSOMES COATING WITH MUCOADHESIVE POLYMER		98
4.1	Introduction	99
4.2	Method.....	101
4.3	Results and discussion	101
4.3.1	Coated transfersomes characterisation	102
4.3.1.1	Size and PDI of the coated formulations.....	102
4.3.1.2	The %EE of the coated Transfersomes.....	110
4.3.1.3	Coated sample selection	111
4.3.1.4	Coated transfersome morphology	116
4.3.2	<i>In vitro</i> release of F5-CH formulation	117
4.4	Conclusion	120
 CHAPTER 5. <i>IN VITRO</i> AND <i>EX VIVO</i> EVALUATION OF LA LOADED TRANSFERSOMES		122
5.1	Introduction	123
5.2	Method.....	125
5.3	Results and discussion	125
5.3.1	Cell viability and transfersomes toxicity.....	125
5.3.2	<i>Ex- vivo</i> permeability	132
5.3.3	Cell-based model development and permeability test	134
5.4	Conclusion	138
 CHAPTER 6. BUCCAL FILM PREPARATION		140
6.1	Introduction	141
6.2	Method.....	142
6.3	Results and discussion	143
6.3.1	Film preparation	143
6.3.2	Characterisation of films.....	149
6.3.3	Film morphology.....	150
6.3.4	Drug release from film.....	153
6.4	Conclusion	154
 CHAPTER 7. GENERAL DISCUSSION AND FUTURE WORK		156
7.1	Research overview	157

7.2	General summary of the research.....	160
7.3	Future work.....	161
	REFERENCES	163
	PUBLICATIONS AND CONFERENCES	180

List of Abbreviations and Acronyms

ACN	Acetonitrile
APIs	Active pharmaceutical ingredients
AB	Alamarblue™
CMC	Carboxymethyl cellulose
CH	Chitosan HCl
DW	Deionized water
DOE	Design of experiment
DMPC	Dimyristoyl phosphatidylcholine
DAD	Diode-array detector
DMEM	Dulbecco's modified eagle medium
DLS	Dynamic light scattering
EA	Edge activator
EPC	Egg phosphatidylcholine
%EE	Entrapment efficiency
EC	Ethyl cellulose
FBS	Fetal bovine serum
HPLC	High performance liquid chromatography
h	Hour
MRC5	Human lung fibroblasts
HLB	Hydrophobic lipophilic balance
HPC	Hydroxypropylcellulose
HPMC	Hydroxypropylmethylcellulose
MRC5- SV2	Immortalized human fibroblasts
ICH	International Conference on Harmonisation
LOD	Limit of Detection
LOQ	Limit of Quantification
LA	Local anaesthetic
MeOH	Methanol
μL	Microliter

μm	Micrometre
MPs	Microparticles
mL	Millilitre
mm	Millimetre
mM	Millimolar
Min	Minute
MW	Molecular weight
nm	Nanometre
NPs	Nanoparticles
NOK	Normal oral keratinocytes
n	Number of samples
PBS	Phosphate buffered saline
PVA	Poly(vinyl alcohol)
PAA	Polyacrylic acid
PC	Polycarbonate
PDI	Polydispersity index
R²	Regression value
Rt	Retention time
RPM	Revolution per minute
SEM	Scanning electron microscope
S/N	Signal to noise ratio
SDC	Sodium deoxycholate
mm²	Square millimetre
SD	Standard deviation
SC	Subcutaneous
Tc	Transition temperature
TEM	Transmission electron microscope
UV	Ultraviolet
V/V	Volume /volume
w/v	Weight / volume
w/w	Weight/ weight

List of Figures

Figure 1.1 Structure of buccal mucosa ¹³	3
Figure 1.2 Schematic diagram for the penetration routes in the buccal mucosa ²²	6
Figure 1.3 A) The dispersion of drug molecules within the lipid-based vesicles, B) comparison between conventional liposome on right half and transfersome (elastic liposome) left side, C) surfactant monomer with one tail, D) surfactant monomer with two hydrocarbon tail, E) micelle (surfactant assembly) in aqueous medium, F) micelles in non-aqueous medium ⁵⁵ ..	13
Figure 1.4 Illustrated diagram of surfactant classification based on molecular weight and hydrophilic lipophilic balance ⁵⁵	18
Figure 1.5 General chemical structure of local anaesthetics ¹⁶³	40
Figure 1.6 Skeletal formula of lidocaine molecule.	42
Figure 2.1 Schematic diagram of transfersomes preparation method ²⁰⁵	56
Figure 2.2 Schematic drawing showing the instrumentation of DLS; (A) process of size measurement and (B) zeta potential measurement ²¹⁰	58
Figure 2.3 Schematic diagram of Franz cell	67
Figure 2.4 Schematic diagram of a transwell set up with inserted cells. The insert has a microporous membrane allowing nutrition medium to freely move between the upper and lower compartment. The cells are seeded on the upper face of the membrane, the drug will be placed on top of the cells (upper part) and the accumulative drug concentration (lower compartment) will be measured as indication of drug permeability through the cells and membrane ²²⁶	69
Figure 2.5 Schematic diagram of film thickness measurements.	70
Figure 3.1 Representative lidocaine HPLC chromatogram obtained using method M11.....	84

Figure 3.2 HPLC calibration curve over the linear range (0.1-2 mg/ml).....	84
Figure 3.3 Graphical representation of transfersomes size of all 18 formulations, n=3, mean values \pm SD.....	89
Figure 3.4 Effect of studied parameters using the mean of S/N ratios.....	91
Figure 3.5 Transfersomes morphology, TEM images (top), and SEM images (bottom) of transfersomes.....	94
Figure 3.6 Release profile of lidocaine permeated across dialysis bag from 6 different transfersomes formulations versus the free drug (control) over 24h, n=3 \pm SD.....	96
Figure 4.1 Results of HPMC K4M coated transfersomes characterisation for size, n=3, mean values \pm SD.....	104
Figure 4.2 Results of HPMC K15M coated transfersomes characterisation for size, n=3, mean values \pm SD.....	106
Figure 4.3 Results of chitosan coated transfersomes characterisation for size, n=3, mean values \pm SD.....	108
Figure 4.4 %EE for Formulations (F2, F5, F8, F11, F14, and F17) after coating with HPMC K4M with concentrations 0.1, 0.2, 0.3, 0.4 and 0.6 % w/v, stars are to flag levels of significant differences compared to uncoated (*, ** and *** represents P<0.05, P<0.01 and P<0.001 respectively), n=3, mean values \pm SD.....	113
Figure 4.5 %EE for Formulations (F2, F5, F8, F11, F14, and F17) after coating with HPMC K15M with concentrations 0.1, 0.2, 0.3, 0.4 and 0.6 % w/v, stars are to flag levels of significant differences compared to uncoated (*, ** and *** represent P<0.05, P<0.01 and P<0.001 respectively), n=3, mean values \pm SD.....	114
Figure 4.6 %EE for Formulations (F2, F5, F8, F11, F14, and F17) after coating with Chitosan HCl with concentrations 0.1, 0.2, 0.3, 0.4 and 0.6 % w/v, stars are to flag levels of significant	

differences compared to uncoated (*, ** and *** represents $P < 0.05$, $P < 0.01$ and $P < 0.001$ respectively), $n=3$, mean values \pm SD.115

Figure 4.7 SEM images of chitosan coated transfersomes (F5-CH).....116

Figure 4.8 SEM images of untreated tissue (top) and after tissue after treating with F5-CH (bottom).....117

Figure 4.9 Release profile of lidocaine permeated across dialysis bag from chitosan coated formulation (F5-CH) versus the free drug (control) over 24h, $n=3$, mean values \pm SD.118

Figure 4.10 Percentage cumulative drug release permeated across dialysis membrane from chitosan coated formulation (F5-CH) versus the uncoated transfersome (F5) over 24h, $n=3$, mean values \pm SD.119

Figure 5.1 MRC5 cell viability measured by AB assay after 24 h exposure to the ingredients, data represent mean \pm SD, $n=3$. Stars are to flag levels of significant differences compared to control (*, ** and *** represents $P < 0.05$, $P < 0.01$ and $P < 0.001$, respectively).....127

Figure 5.2 MRC5-SV2 cell viability measured by AB assay after 24 h exposure to the ingredients, data represent mean \pm SD, $n=3$. Stars are to flag levels of significant differences compared to control (*, ** and *** represents $P < 0.05$, $P < 0.01$ and $P < 0.001$, respectively).127

Figure 5.3 Cell viability measured by AB assay after 24 h exposure to blank and loaded transfersomes F2, and F5. Data represent mean \pm SD, $n=3$. The level of significant differences compared to control or for the comparison of each pair of formulations for the same131

Figure 5.4 A and B- images of fresh oesophagus tissue; C and D- images of epithelium mounted onto Franz diffusion cells before and after permeability study, respectively.....133

Figure 5.5 Permeation profiles (up to 24 h) of F5 and F5-CH formulations using pig oesophagus epithelium as an ex vivo model, Values are mean \pm SD for $n=3$ independent experiments. 134

Figure 5.6 Optical microscope (bright-field) images of NOK cells acquired during the development of the cell-based model. A) Cultures in an open well, B) Cultures in a transwell 24 h after seeding, C) Cultures in a transwell after 28 days from seeding, and D) fixed cells in cell-based model after 24 h of treatment.135

Figure 5.7 Permeation profiles (over 24 h) of F5 and F5-CH formulations using a cell-based model in comparison to the release profile from the ex vivo (tissue) model. Values are mean \pm SD for n=3 independent experiments.....136

Figure 6.1 SEM images of produced film, top) images showed film edge confirming two layers, bottom) polymeric smooth surface with transfersomes embedded (left) and transfersomes rough surface (right).152

Figure 6.2 SEM images revealed the existence of intact transfersomes in two different dissolved film samples.153

Figure 6.3 Release profile from film loaded with F5-CH transfersomes using Franz diffusion cell with fresh animal oesophagus epithelium and comparison with release from coated transfersomes (not from film) , n=3, mean values \pm SD.154

Figure 7.1 Schematic conclusion of the research.160

List of Tables

Table 1.1 Summary of some reported studies of micro/nanoparticles preparation for buccal delivery.....	8
Table 1.2 Summary of the main lipid-based vesicular systems, with their main constituents, distinctive properties and disadvantages.	14
Table 1.3 Chemical structures of the most commonly used non-ionic surfactants ⁵⁵	19
Table 1.4 Short review of the conventional methods for lipid-based vesicles with their advantages and drawbacks.....	35
Table 1.5 Summary of some studies that aimed to develop lidocaine delivery systems, the method of preparation, main carrier of the system and the achieved outcome.	44
Table 1.6 Summary of the reported method used for LAs delivery in dentistry.....	49
Table 2.1 Transfersome components with their concentrations (a, b and c representing high, medium and low concentrations, respectively) that were assessed for toxicity	66
Table 3.1 Parameters used in HPLC method development of lidocaine	77
Table 3.2 Taguchi design of experiment including various factors and levels.	78
Table 3.3 . Summary of the composition of each formulation with different types of lipid (SPC, DMPC), EA (Span 80, Tween 80 and SDC) and their ratios (95:5, 75:25 and 55:45 w/w) with each other.	79
Table 3.4 List of methods tested in the HPLC method development study including different mobile phase composition, flow rate and detection wavelengths, with the obtained results including their Rt, symmetry, and shape.	82
Table 3.5 HPLC method validation parameters of lidocaine free-base	85
Table 3.6 Accuracy and precision (intermediate precision and repeatability).....	85

Table 3.7 Transfersome formulation (F1-F18) characterisation results; size, polydispersity index (PDI), zeta potential, and entrapment efficiency (%EE), n=3 ±SD.	87
Table 3.8 Response table for Signal to Noise ratios (S/N), showing the rank of the factors X1, X2 and X3 as they affect transfersome size.	91
Table 4.1 Results of HPMC K4M coated transfersomes characterisation for size, PDI, and %EE, n=3, mean values ± SD, stars are to flag levels of significant differences compared to uncoated (*, ** and *** represents P<0.05, P<0.01 and P<0.001 respectively).	103
Table 4.2 Results of HPMC K15M coated transfersomes characterisation for size, PDI, and %EE n=3, mean values ± SD, stars are to flag levels of significant differences compared to uncoated (*, ** and *** represents P<0.05, P<0.01 and P<0.001 respectively).	105
Table 4.3 Results of chitosan coated transfersomes characterisation for size, PDI, and %EE, n=3, mean values ± SD, stars are to flag levels of significant differences compared to uncoated (*, ** and *** represents P<0.05, P<0.01 and P<0.001 respectively).	107
Table 6.1 Mixture of polymeric solutions screened for film preparation	143
Table 6.2 Descriptive results of film formation trials.	146
Table 6.3 Results of film characterisations including weight uniformity, thickness, content uniformity, disintegration time, pH, and tensile strength, n=12, mean values± SD.	150

Chapter 1. Introduction

1.1 Buccal delivery

The buccal region of the oral cavity is an attractive site for drug delivery as it offers several advantages over the parenteral and oral routes. Both the non-invasive administration and the ease of application improve patient compliance in comparison with the non-oral routes¹⁻³. Parenteral drug administration could be difficult for patients who suffer from needle phobia, which is defined as an extreme patient fear and anxiety associated with needles^{4,5}. Needle-fear is usually related to consequences of serious symptoms such as hypoxemia, tachycardia, and change in hormone levels that could also result in patients avoiding the healthcare system^{6,7}. Therefore, a non-invasive route of administration is commonly reported to be more patient friendly due to the reduced side effects that usually accompany all type of treatments with injection^{8,9}. Systemic delivery of the drug could be intended via transmucosal application because the buccal cavity is highly vascularised, has approximately neutral pH, and reduced enzymatic activities². Additionally, higher bioavailability could be achieved since the drug avoids hepatic first pass metabolism, and bypasses the hostile environment of the gastrointestinal tract¹⁰. Furthermore, the treatment of local lesions, dental pain, localised infection or inflammation in the mouth can be achieved through direct drug administration with an advantage of minimising the systemic side effects^{2,11}.

1.1.1 Buccal mucosa anatomy and physiological properties

The buccal mucosa represents only one third of the total oral mucosa, and it refers to the lining of cheeks, the upper and lower lips. It is composed of three distinct layers (Figure 1.1), the outermost layer which is the stratified squamous epithelium with a distinctive basement membrane separating it from the lamina propria, that is followed by the submucosa¹¹. The buccal epithelium is non-keratinised and has approximately 40-50 cell layers resulting in a

thickness of 500-600 μm , its turnover time has been estimated between 5-6 days, and it contains polar lipids mainly cholesterol sulfate and glucosyl ceramides ¹².

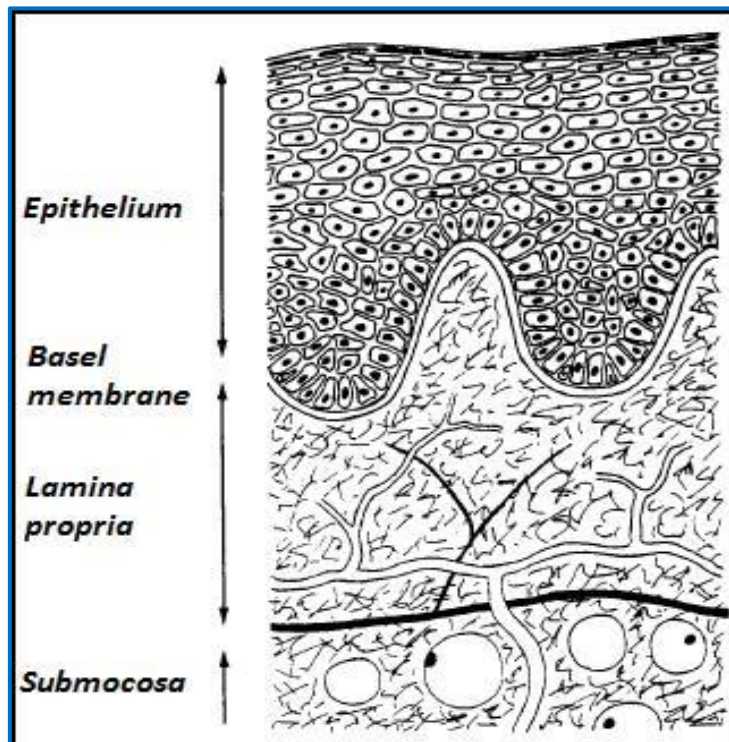


Figure 1.1 Structure of buccal mucosa ¹³

The buccal epithelium is considered to be the main barrier for systemic transmucosal drug delivery due to many reasons. Firstly the presence of the membrane coating granules (MCG), which are small organelles containing some of the intracellular lipid that migrate to the cell surface where their membrane fuses with the cell membrane and their lipid content is extruded into the extracellular space ². Secondly, the existence of enzymes such as aminopeptidase, carboxypeptidase, esterase and hydrogenase, which represents the major barrier especially for peptide delivery. Although some studies showed that these enzymes have weak activities and the most active one among them is the N-aminopeptidase, they still need to be considered during the design of a drug delivery system. Finally, the basement membrane, which is the complex interface zone between the overlying squamous epithelium and the underlying connective tissue stroma. However, the structure of the basement

membrane was not considered dense enough to exclude relatively large molecules, but it was suggested that the surface charge on the molecule surface may bind non-specifically to the basal membrane ^{2,12}. The lamina propria is immediately beneath the epithelium. It is a loose papillary layer containing fibrocollagenous, vascular channels, and peripheral nerves. Finally, the submucosal layer consists of broad bands of fibrocollagenous and elastic tissue containing the blood vessels and nerves. However, some unmyelinated axonal endings of the stromal neural elements project upward and penetrate the epithelium to function as sensory receptors, while others such as efferent autonomic fibres terminate in the lamina propria ¹².

1.1.2 Mucus

The buccal mucosa is covered by a cohesive gel-like layer (mucus) with a thickness between 40-300 μm . The mucus is negatively charged at physiological salivary pH of 5.8-7.4 and it is believed to play a major role in the adhesion of mucoadhesive drug delivery systems ^{10,14}. Mucus turnover rate is thought to be another important factor to be considered while planning the residence time of the delivery system, which was reported to range between 12-24 h in human ¹⁵⁻¹⁷.

1.1.3 Saliva

Saliva is considered another barrier for buccal delivery for many reasons. The continuous secretion of saliva (0.5 -2 L per day) could lead to subsequent dilution of the drug, plus the risk of premature swallowing of the drug or the whole delivery system before effective absorption occurs through the buccal mucosa. In addition to the presence of some functional enzymes such as lysozyme, lipase and α -amylase, which makes saliva a considerable barrier for buccal delivery especially of large molecular weight drugs such as protein and peptides ¹⁰.

1.1.4 Absorption pathways

Drug molecules or drug carriers can cross the epithelium either by passive diffusion, carrier mediated transport or endocytosis depending on the nature, size and charge of the drug/carrier ¹⁸. For example, a study conducted by Roblegg et al. showed that negatively charged nanoparticles with a size of 200 nm formed aggregates with the mucus and did not penetrate ¹⁹. However, nanoparticles with a 20 nm size permeated the mucus layer regardless of their charge and penetrated into the stratum superficial of the top third region of the epithelium through the transcellular route. Positively charged nanoparticles with a size of 200 nm permeated the mucus layer and penetrated into deeper regions of the tissue¹⁹. Similarly, many studies have reported the employment of liposomes for buccal administration, where the liposomes size was reported to range between 100-300 nm to permeate through the paracellular route. However, it was claimed that the liposome permeation through the buccal mucosa isn't based on their size only, it could be also related to the penetration enhancing effect of phospholipid and other ingredients included such as surfactants ^{20,21}. Generally, passive diffusion is considered the predominant pathway and absorption may occur via the paracellular route for hydrophilic drugs (Figure 1.2), while the transcellular route for more hydrophobic drugs or both depending on the physicochemical properties of the drug and the carrier ²².

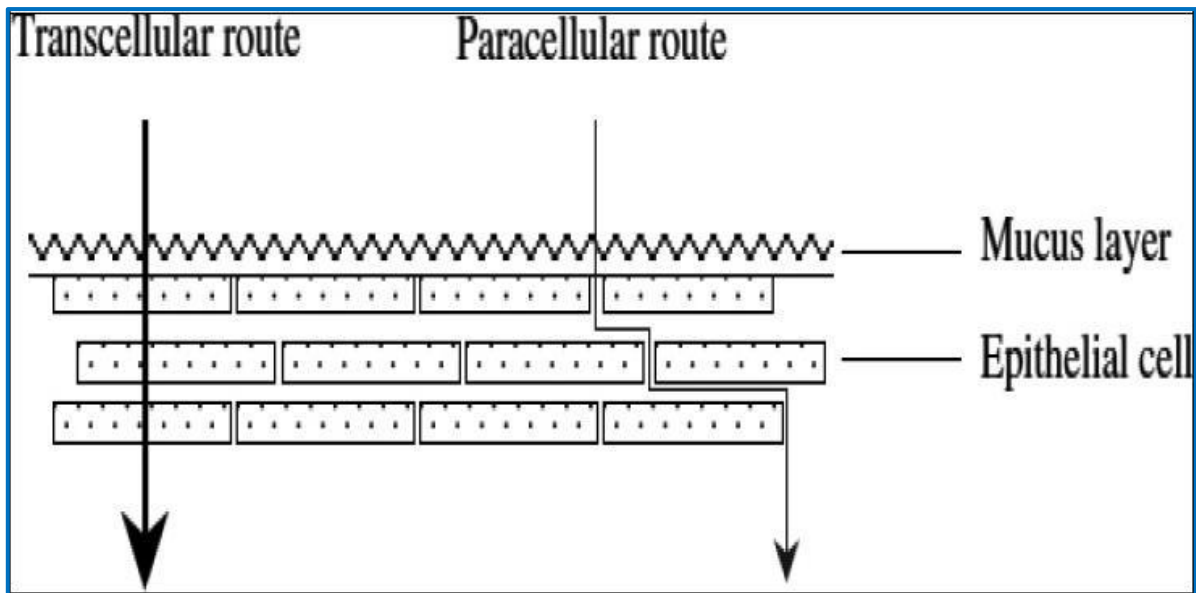


Figure 1.2 Schematic diagram for the penetration routes in the buccal mucosa ²²

1.1.5 Previous studies of micro/nanoparticle systems for buccal administration

There have been many attempts to deliver drugs, therapeutic peptides, proteins, and vaccines through the buccal cavity to gain the previously discussed advantages for either local or systemic effect. However, in recent years, the general trend has been toward the development of either micro-(MPs) or nano-(NPs) particulate systems for drug delivery. Both MPs and NPs have several advantages for buccal drug delivery, such as reducing the risk of local irritation and decreasing the uncomfortable sensation of foreign objects. Additionally, they distribute over a larger area of the mucosal surface, leading to higher drug uptake ²³. The major challenge facing such delivery systems is their retention in the oral cavity for the desired time ², therefore, many technologies have been investigated to overcome this obstacle such as using absorption enhancers or mucoadhesive systems. Although particulate systems have many advantages, they still face the risk of being washed away with the saliva. Hence, most of the developed MPs/NPs systems were either directly prepared using material of mucoadhesive properties and utilised in their suspension form or alternatively, further

incorporated in a mucoadhesive dosage form such as mucoadhesive patches, films or tablets.

Table 1.1 shows some examples of previously completed studies.

Table 1.1 Summary of some reported studies of micro/nanoparticles preparation for buccal delivery

Drug	Delivery system	Dosage form	Target	Ref.
Piroxicam	Eudragit microparticles	Fast-dissolving mucoadhesive MPs	systemic	24
Nifedipine	Methyl methacrylate microparticles	Fast-dissolving mucoadhesive MPS	systemic	25
Metformin hydrochloride	Chitosan microparticles	Bioadhesive chitosan-based MPs	systemic	26
Atenolol	poloxamer 407 microparticles	Sublingual Tablet	systemic	27
Insulin	PEG-b-PLA nanoparticles	Mucoadhesive chitosan film	systemic	28
Lidocaine	Compritol solid dispersion microparticles	Patch/ and bi-layered patch	systemic	29

Drug	Delivery system	Dosage form	Target	Ref.
Acyclovir	PLGA nanospheres	Buccoadhesive film	local	30
Lignocaine base/diclofenac diethylamine	free drug /Solid lipid nanoparticles	Transmucosal patch	local	31
Heparin	Polymethacrylate nanoparticles	Mucoadhesive NPs	systemic	32
Propranolol hydrochloride	Chitosan/gelatin microparticles	Mucoadhesive tablets	systemic	33

1.1.6 Mucoadhesive Films

Most buccal formulations do not allow achieving a prolonged effect especially when they are meant for local activity, due to either the flushing by saliva or ingestion of foods and continuous jaw movement. This usually leads to an increase in the frequency of treatment, but this can be overcome by producing mucoadhesive dosage forms that could be retained within the oral cavity and prolong the drug release such as tablets^{34,35}, gels³⁶, patches^{37,38} and films³⁹.

Among the buccal dosage forms, films and patches have gained increasing attention due to their small size and reduced thickness in comparison with tablets and lozenges, which reflects improved patient compliance. Besides patient satisfaction, buccal films provide an advantage of delivering a measured dose of drug in comparison with the inaccuracy of ointment and gel forms²². Buccal films are laminates consisting usually from a backing layer, which ensures unidirectional drug delivery and protects it from environmental factors such as salivary pH and enzymes. The second layer often has mucoadhesive properties and represents a drug reservoir¹⁰.

Mucoadhesion is defined as an interaction between the mucus surface and a surface of synthetic or natural macromolecule. The mucoadhesion phenomenon has been explained by many models such as adsorption, wetting, diffusion, electronic and fracture theories. The adhesion occurs either through chemical interaction such as electrostatic, hydrophobic, hydrogen bonding, and van der Waals' interactions or physical entanglement⁴⁰. Several polymers have been employed as they meet the requirements for being mucoadhesive such as having many hydrogen bond functional groups, suitable wetting properties, strong anionic

or cationic charges, sufficient flexibility for cross-linking with the tissue mucus network, swelling properties, and high molecular weight ^{16,41}.

The polymers are classified into: i) natural polymers such as chitosan, gelatin, pectin, and sodium alginate, ii) synthetic polymers such as polyacrylic acid derivatives (PAA), polycarbonate (PC), and cellulose derivatives (carboxymethyl cellulose CMC, hypromellose HPMC, hydroxypropyl cellulose HPC). However, the choice of the polymer depends mainly on its distinctive properties. For example, some polymers have aqueous solubility such as sodium alginate, PAA, and CMC, whilst others are water insoluble such as PC, chitosan and ethyl cellulose (EC), the latter being the most extensively used polymer in forming the backing layer. Moreover, polymers such as PAA display enzyme inhibition properties, which makes them preferable for the delivery of peptides and proteins. Chitosan and its derivatives such as thiolated chitosan have shown superior mucoadhesive properties, increased solubility and permeation properties ^{16,40-42}.

Generally, buccal films are either prepared by solvent casting or hot melt extrusion techniques. Although the solvent casting method is the most widely used to prepare buccal films, the content uniformity of the drug within the dosage unit was the major challenge especially with monolayered film preparation. Hot melt extrusion was also introduced to prepare buccal films offering more uniformity in drug dispersion within the molten polymer. However, it is not suitable for thermolabile drugs or carriers, which sometimes require the inclusion of protectant excipients to decrease drug degradation ^{16,41}. Several studies reported film preparation and loading with MP and NP systems for controlled buccal delivery as summarised in Table 1.1.

1.2 Lipid-based vesicles

Improving patient compliance is one of many drivers for research through achieving a good therapeutic profile and reducing unwanted side effects. Substantial attempts have been made to alter drug pharmacokinetic and pharmacodynamic properties such as solubility, permeability, release profile and targeting^{43,44}. This has been achieved by designing delivery systems such as particulates, polymeric micro/nano spheres, and vesicular systems^{43,45,46}. Vesicular systems usually consist of amphipathic lipids which are self-assembled in aqueous media to form one or multi bilayers enclosing a hydrophilic core⁴⁷. They are employed as a carrier for both hydrophilic and lipophilic active pharmaceutical ingredients (APIs). Hydrophilic drugs are usually encapsulated in the aqueous core or adsorbed on the surface of the polar head part of the lipid, whereas the lipophilic drugs are encapsulated between the concentric bilayer (lipid tails form a suitable lipophilic environment)^{48,49} (Figure 1.3, A).

Lipid-based vesicular systems may be classified depending on many factors such as their constituents, size and number of bilayers, which accumulatively affect the final vesicle properties in several ways^{50,51} (Table 1.2). However, in order to enhance lipid-based vesicular system properties, a new generation of liposomes was developed to be flexible and ultra-deformable (Figure 1.3, B).

Alterations to the conventional liposome composition were reported, since surfactants were incorporated into their structure as well as the lipid component (Table 1.2). Transfersomes were considered a new generation of liposome with a high deformability, which allows them to squeeze easily through biological barriers⁵². The presence of surfactants in the composition of lipid-based vesicular systems has been stated as the reason for the improvement in many properties such as the entrapment efficiency (EE), stability and

permeability^{53,54}. However, the vesicle composition may vary depending on the properties of the surfactants used⁵⁵.

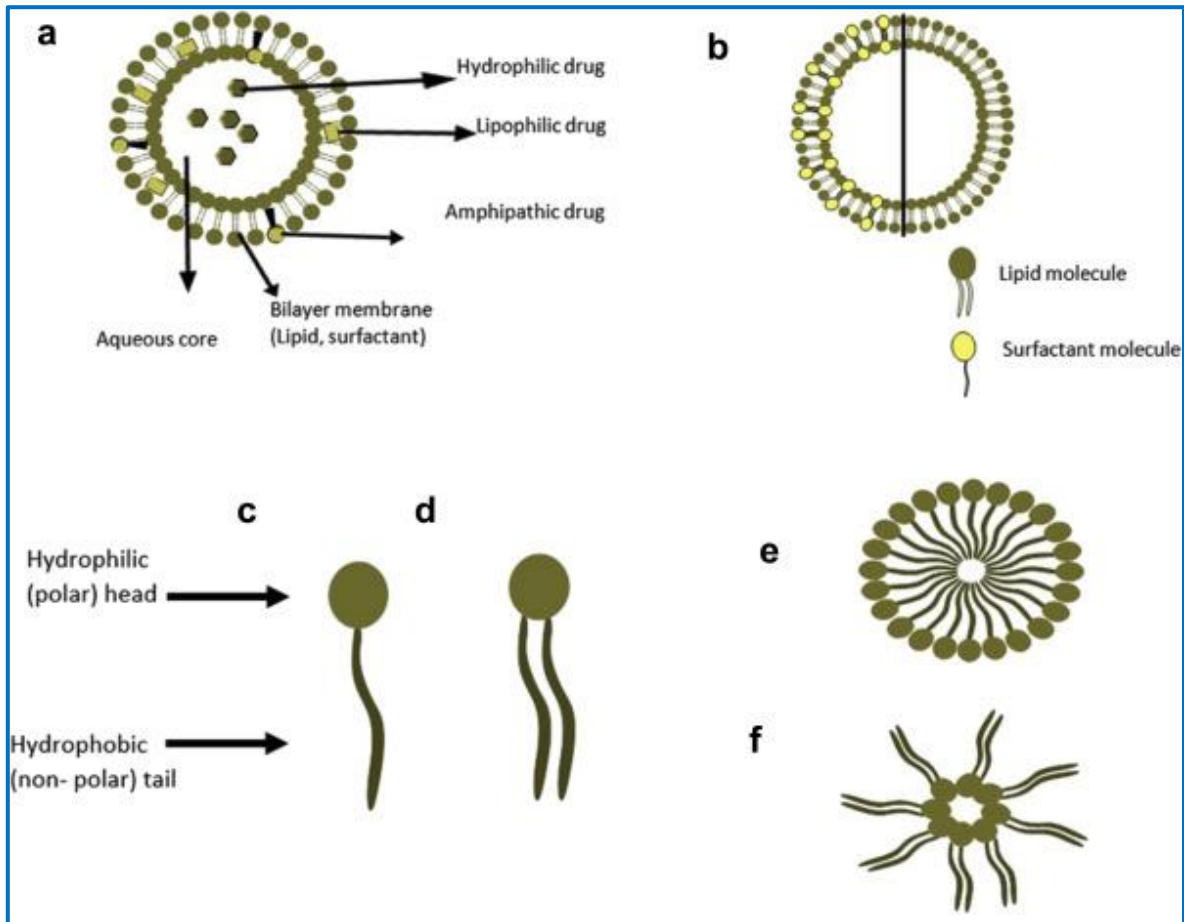


Figure 1.3 A) The dispersion of drug molecules within the lipid-based vesicles, B) comparison between conventional liposome on right half and transfersome (elastic liposome) left side, C) surfactant monomer with one tail, D) surfactant monomer with two hydrocarbon tail, E) micelle (surfactant assembly) in aqueous medium, F) micelles in non-aqueous medium⁵⁵.

Table 1.2 Summary of the main lipid-based vesicular systems, with their main constituents, distinctive properties and disadvantages.

Vesicular system	Main constituents	Distinctive properties	Ref.
Liposomes (Figure 1.3)	<ul style="list-style-type: none"> • Natural or synthetic Phospholipids (neutral or charged). • Cholesterol. 	<ul style="list-style-type: none"> • Sizes vary between 25-2500 nm • Suitable for both hydrophilic, lipophilic, small molecular weight and macromolecular drugs. • Reduced toxicity. • Targeted drug could be achieved. <p>Disadvantages</p> <ul style="list-style-type: none"> • Drug leakage. • Expensive. • Low stability. • Low encapsulation of hydrophilic drugs. 	50,56,57
Niosomes	<ul style="list-style-type: none"> • Non-ionic surfactant (uncharged single-chain surfactant). • With/or without cholesterol. 	<ul style="list-style-type: none"> • Microscopic lamellar vesicles. • More stable than liposome. • Osmotically active. • Suitable for loading drugs with wide range of solubility. • Relatively less expensive than liposome. 	58,59

		Disadvantages <ul style="list-style-type: none"> • Aggregation. • Fusion. • Drug leaking. 	
Transfersomes/ Deformable or Ultra-deformable liposome (Figure 1.3)	<ul style="list-style-type: none"> • Surfactant (edge activator). • Natural or synthetic Phospholipids (neutral or charged). 	<ul style="list-style-type: none"> • High deformability. • Show very high encapsulation for lipophilic drugs. • More stability. Disadvantages <ul style="list-style-type: none"> • Difficulty of loading lipophilic drug without compromising their deformability. • Expensive to formulate. • Chemically unstable as they are more prone to oxidation. 	60-62
Ethosomes/ Elastic vesicles	<ul style="list-style-type: none"> • Ethanol (20-45%) as permeation enhancer or surfactant. • Phospholipid. 	<ul style="list-style-type: none"> • Increase cell membrane lipid fluidity due to the presence of ethanol. • Enhanced permeation profile, especially for dermal application. • Low risk profile or toxicity. • Relatively simple to manufacture. 	63-67

		Disadvantages <ul style="list-style-type: none"> • Poor encapsulation/yield. • Possibility of vesicles disruption. 	
Pro-vesicular system (Proliposomes/ proniosomes)	<ul style="list-style-type: none"> • Water-soluble porous carrier (solid particles). • In addition to the same ingredients of the liposome or niosome respectively. 	<ul style="list-style-type: none"> • Mainly to overcome the disadvantages of liposome /niosome. • Free flowing dry form that enhance the stability. 	68,69
Other: e.g. Herbosomes/ Sphingosomes/ Genosomes	<ul style="list-style-type: none"> • Similar to liposomes, where lipid charge, type, or nature determine the type of the vesicles. 	<ul style="list-style-type: none"> • Improved stability, e.g. herbosomes as they have phytochemical water-soluble particles that form stronger bonds with phospholipids in comparison with liposomes. • Provide selective passive targeting, e.g. sphigosomes as they contain sphingolipid which improves targeting. • Suitable for delivering specific substances such as gene, e.g. genosomes. 	46,50,70

1.2.1 Surfactants

Surfactants, also referred to as surface-active agents or edge activators, are amphipathic molecules and composed mainly of two main moieties; the polar hydrophilic part, which is attached to the non-polar lipophilic part ^{71,72}. The lipophilic part is usually a straight or branched hydrocarbon chain (tail) consists of eight to eighteen carbon atoms ⁷³ (Figure 1.3 C and D). At low concentrations surfactants exist as monomers, and usually in aqueous medium they adsorb on the interfacial surfaces (solution- air interface) and consequently they displace some surface molecules and reduce the intermolecular forces, thus lowering the surface tension ^{74,75}. However, above a certain concentration (critical micelle concentration, CMC) they aggregate and form micelles (Figure 1.3, F and E). The CMC value for each surfactant may vary as it depends on the method of and determination and other factors such as surface tension, viscosity, temperature and conductivity ^{76,77}. Additionally, many studies reported that CMC is not a precise value, but represents a range of concentrations over which the self-assembly of surfactant molecules to form micelles are induced ⁷⁸. It was also reported that increasing the temperature of the system could cause a reduction in the CMC value, which was explained by the destruction of the hydrogen bonds that usually form between the hydrophilic groups of surfactants and the water molecules ⁷⁹⁻⁸¹. However, surfactants form micelles due to the hydrophobic effect, and they could adopt several arrangements ^{82,83}. In aqueous medium, the hydrophilic heads face the aqueous surroundings and the lipophilic tails are directed toward the non-aqueous medium. However, in a non-polar medium, they work similarly but the micelles form in an opposite arrangement where the polar groups face each other and the tails project out towards the non-aqueous medium ⁷⁵ (Figure 1.3 F and E).

Surfactants may be classified depending on either their molecular weight or their hydrophilic-lipophilic balance (HLB) ⁸⁴ (Figure 1.4). Moreover, they are further categorised into several sub-groups based on the properties such as charge of the hydrophilic head group ⁸⁴.

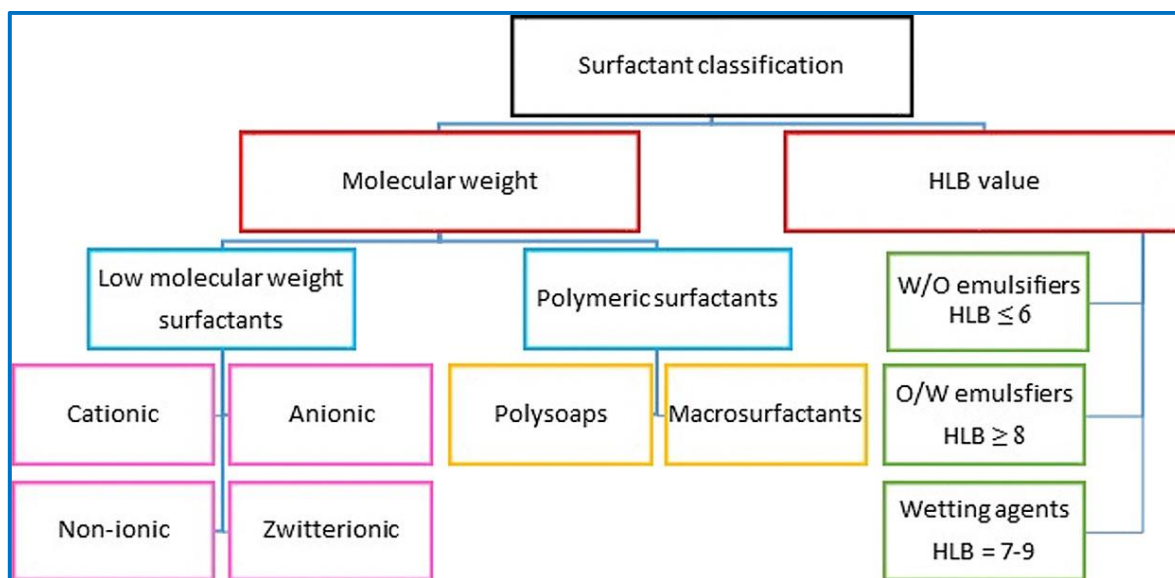


Figure 1.4 Illustrated diagram of surfactant classification based on molecular weight and hydrophilic lipophilic balance ⁵⁵.

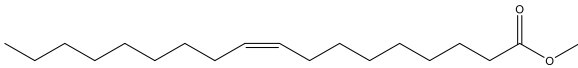
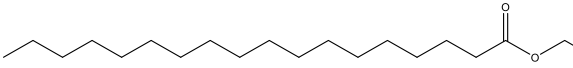
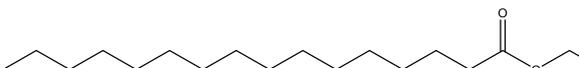
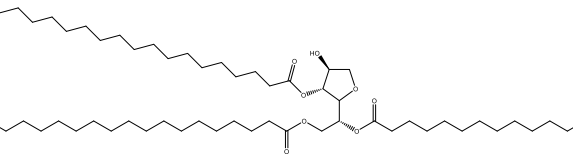
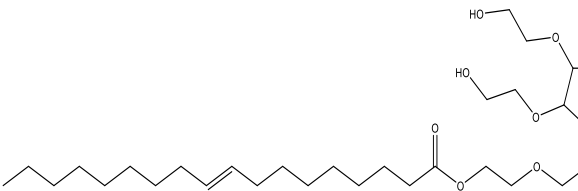
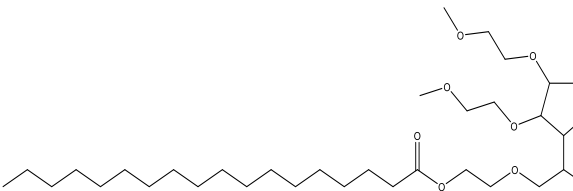
1.2.1.1 Low molecular weight surfactants

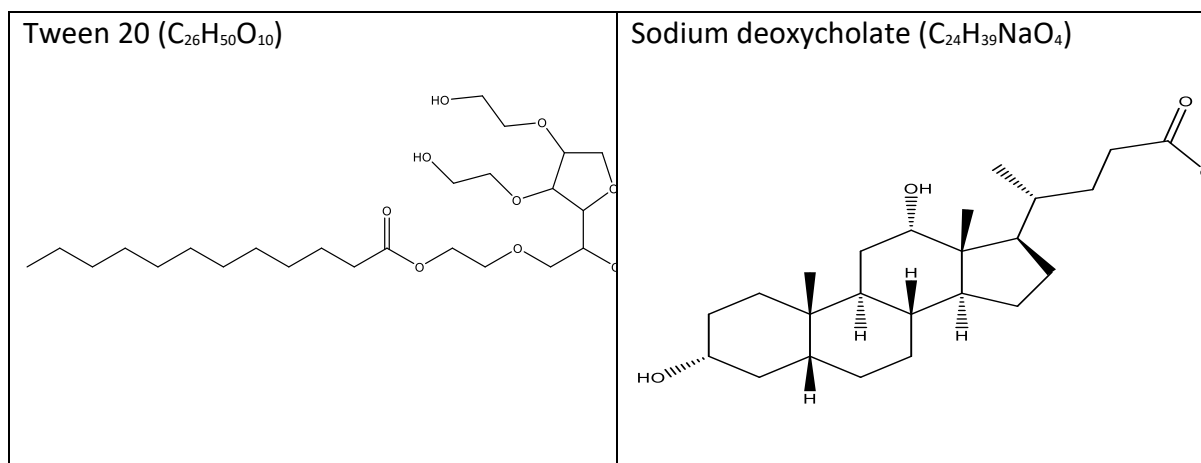
There are four major types of low molecular weight surfactants where the classification depends on the nature of the hydrophilic parts. **Anionic surfactants** have negatively charged hydrophilic parts. They are widely used due to their low cost. Generally, they could be carboxylates ($C_nH_{2n+1}COO^{-x}$), sulphates ($C_nH_{2n+1}OSO_3^{-x}$), sulphonates ($C_nH_{2n+1}SO_3^{-x}$), or phosphates ($C_nH_{2n+1}OPO(OH)O^{-x}$), where n is the number of carbon atoms (i.e. n = 8-18) ^{71,84}.

Cationic surfactants have positively charged hydrophilic parts and often a natural fatty acid. Quaternary ammonium compounds are the most commonly used cationic surfactants such as alkyl dimethyl benzyl ammonium chloride (benzalkonium chloride), which is widely used as a preservative in pharmaceutical formulation (i.e. bactericidal) ^{71,85}. **Amphoteric surfactants (zwitterionic)** contain both cationic and anionic groups and their behaviour is

dictated by the pH of the medium in which they are dissolved. They act as anionic surfactants in alkaline pH due to their acquisition of a negative charge, whereas in acidic medium they gain a positive charge and behave like cations. They show good water solubility, improved stability, and better compatibility with other surfactants and within different media in comparison with the cationic and anionic surfactants. **Non-ionic surfactants** are characterised by the presence of uncharged hydrophilic groups that do not dissociate in aqueous solution such as alcohol, ether, ester or amide groups (Table 1.3). They contain wide range of classes such as alcohol ethoxylate, sorbitan esters ethoxylate, and fatty acid ethoxylates. Additionally, there are multihydroxy products such as glycol esters, glycerol esters, glucosides and sucrose esters ^{71,84,85}.

Table 1.3 Chemical structures of the most commonly used non-ionic surfactants ⁵⁵.

<p>Span 80 (C₂₄H₄₄O₆)</p> 	<p>Span 60 (C₂₄H₄₆O₆)</p> 
<p>Span 40 (C₂₂H₄₂O₆)</p> 	<p>Span 65 (C₆₀H₁₁₄O₈)</p> 
<p>Tween 80 (C₃₂H₆₀O₁₀)</p> 	<p>Tween 60 (C₃₅H₆₈O₁₀)</p> 



1.2.1.2 Polymeric surfactants

Polymeric surfactants have been developed in the last two decades and can assemble into one or several macromolecular structures that have hydrophilic and lipophilic character. They are now commonly employed due to their wide application as stabilizers in emulsion and suspension formulation. Several modifications have been carried out on these surfactants to improve their properties and get molecules that are effective in several pH conditions, temperature, and media ^{71,85}. The number of the hydrophilic and lipophilic groups as well as their distribution along the carbon chain is considered to be a distinctive property of the polymeric surfactants. The high structural complexity of the polymeric surfactants exhibit several behavioural differences in comparison with low molecular weight surfactants ⁸⁶. Depending on the distribution of the hydrophilic and lipophilic moieties, these polymeric surfactants are usually sub-categorised into two main classes; polysoaps and macrosurfactants ⁸⁷.

1.2.1.3 Surfactant classification depends on HLB

The hydrophilic-lipophilic balance classification system was first developed by Griffin in the last century, and it is a scale that represents the percentage of hydrophilic to lipophilic groups in surfactant molecules ⁸⁸. HLB is subdivided into several categories based on the range of

HLB value, each represents a group of surfactants with similar behaviour^{71,84}. Surfactants with HLB values of 3-6 show more lipophilicity and they tend to form W/O emulsion, and micelles/vesicles that are more soluble in non-aqueous media. While HLB values of 8-18 represent O/W emulsifiers or solubilisers, which are more hydrophilic and water-soluble. However, surfactants with HLB values between 7-9 are considered as wetting agents and therefore exhibit both properties. Sometimes it is possible to use two or more emulsifying agents (surfactants) at once to achieve the desired solubilisation effect. For example, mixing Tween 80 (i.e. polysorbate with a HLB value of 15) with Span 80 (sorbitane monooleate, which has a HLB value of 4.3) in different proportions may cover a range of HLB values in order to choose better composition to achieve the desired properties^{71,85}. Therefore, the optimum use of the HLB value is to enable the selection of the surfactant composition.

1.2.2 Surfactants in lipid-based vesicles

The uses of surfactants in lipid-based vesicles has progressed over the last few decades⁸⁹. One study has focused on using surfactants from one group e.g. studying the non-ionic surfactants in case of niosomes⁹⁰, whereas others have investigated the effects of using several surfactants with different characteristics on vesicle properties. Additionally, most studies have aimed to maximise the effect of the chosen surfactant in order to optimise the formation of the lipid vesicles to achieve the desired size, drug loading and physiochemical properties.

1.2.2.1 Surfactant effects on the size and polydispersity index (PDI)

The presence of surfactants in lipid-based vesicle systems has a noticeable effect on their size. In 2016, Singh et al studied the role of surfactant in the formulation of elastic liposomes for the transdermal delivery of the opioid analgesic tramadol. The effect of several surfactant (i.e.

Span 80, Tween 80, and sodium deoxycholate) was investigated in liposome formulations, where an indirect relationship was observed between liposomes vesicle size and surfactant concentration ⁹¹. It was suggested that the higher surfactant concentration covered the surfaces of the liposomes and therefore prevented them from aggregation ^{91,92}. A small polydispersity index was also reported with the higher surfactant concentration and the consistent size distribution was thought to be an important factor in reducing interfacial tension and producing a homogeneous emulsion ⁹³. The same three surfactants were also used by Jain et al to prepare transfersomes and no significant differences in vesicle size was expected, as a result of the homogenization method (through polycarbonated membrane) used during the preparation of the formulations ^{60,94}. However, a reduction in vesicle size was noted when higher surfactant concentrations were used, it might be attributed to the fact that surfactant with concentration more than 15% induce micelle formation rather than vesicle formation ⁶⁰. A similar study of the influence of several surfactants on elastic liposome properties was carried out by Barbosa et al. ⁹⁵. They investigated the incorporation of the non-ionic surfactants that have either one hydrophobic chain (such as octaethylene glycol laurate (PEG8L), polyoxyethylene glycol-4-laurate (PEG4L), and pentaethylene glycol monododecyl ether (C12E5)) or two hydrophobic chains (such as polyoxyethylene glycol-8-dilaurate (PEG8DL), and polyoxyethylene glycol-4-dilaurate (PEG4DL)). The study revealed similar results, exhibiting higher surfactant concentration lead to the formation of smaller vesicles ⁹⁵. Additionally, surfactants with two hydrophobic chains exhibited better and homogeneous PDI in comparison to those with one carbon chain, which could be explained by their better capability to anchor within the lipid bilayer ⁹⁵⁻⁹⁷. However, not only does the number of the hydrophobic chains affect the vesicle size, but also the length of the carbon chain of the surfactant. Duangjit et al. studied the effect of carbon chain length and content

of the surfactant on meloxicam loaded liposomes ⁹⁸. The size of the obtained liposomes decreased as the length of carbon chain of the surfactant increased from C4 to C16. This was attributed to the rise of the surfactant hydrophobicity as its carbon chain length increased, which in turn improved the solubility of the surfactant molecules within the lipid bilayer ^{98,99}. Moreover, a reduction in vesicle size was also reported to be influenced by the hydrophilicity of the head group of the surfactant, which was thought to be due to the shortness of the hydrophobic backbone in comparison to the hydrophilic head group, which was asparagine grafts in that case ⁹⁸⁻¹⁰⁰. Similar results were achieved during niosomes loading with a β -carotene as a model of lipophilic moiety, with the more hydrophilic surfactant (higher HLB value) producing smaller vesicles ⁶⁶. In contrast, the size of elastic transfersomes optimized with several surfactants for the transdermal delivery of pentoxifylline increased as the HLB of the surfactants increased. The surfactants were ranked as they formed larger transfersomes in the following order Span 80 < Span 20 < Tween 21 < Tween 20 ⁹⁴. Similar ranking of several Spans on the niosomes size were obtained, since the size of the vesicles increased as the HLB progressively increased, Span 20 (HLB= 8.6) showed larger niosomes size, after that the size gradually decreased with Span 40 (HLB= 6.7), Span 60 (4.7) and Span 80 (HLB= 4.3) ¹⁰¹. This could be due the effect of the surface free energy, which might decrease as the hydrophobicity increases ¹⁰². Some researchers have investigated the effect of the lipid type on vesicle size. The inclusion of some lipids, for example, an anionic lipid such as dicetylphosphate (DCP) with Span 20-based niosomes reduced vesicle size. The reduction was explained by the increased curvature of the bilayer caused by the electrostatic repulsion between the ionized head group of both the lipid (DCP) and the surfactant ¹⁰³. It has been also suggested that the lipid to surfactant ratio can affect vesicle size. Using cholesterol at higher concentrations than usually specified was observed to increase niosomes size ¹⁰⁴. Parallel

results have been obtained by many studies, where the incorporation of cholesterol in niosomes or liposomes at higher concentration than the surfactant leads to increased vesicle size. It was suggested that the competition between cholesterol and surfactant to keep their place in the lipid bilayer may increase the size of vesicle ¹⁰³⁻¹⁰⁶. In summary, the inclusion of surfactants within lipid-based vesicles has an obvious effect on vesicle size and many factors need to be considered when a surfactant is incorporated into the formulation. Parameters such as surfactant concentration, number of carbon chains, carbon chain length, and the hydrophilicity of the head groups have an inverse effect on vesicle size. While the competition of other moieties with the surfactant molecules during the arrangement of the lipid bilayer clearly showed an increase in lipid vesicle size.

1.2.2.2 Surfactant effects on entrapment efficiency

Achieving a good EE is considered to be the main goal during the developing of any vesicular delivery system. Many researches have tried to incorporate surfactants into lipid-based vesicles in order to improve the encapsulation of both hydrophobic and hydrophilic drugs as well as reduce drug leakage in liposome formulations ^{66,99,100}. Although many attempts have been carried out to investigate surfactants effects on improving the EE, there is still no definitive proof that specific surfactant properties could lead to certain entrapment. It may entail many surfactant properties, such as the type and concentration, that could have an effect on the EE of a certain drug within a certain lipid composition ¹⁰⁴. General trends could be observed from a set of surfactant properties on a hydrophilic drug entrapment, but that effect could be totally different when a hydrophobic drug is encapsulated. The effect of various parameters on the EE are discussed in more details below.

1.2.2.2.1 Surfactant concentration

Many researchers have studied the effect of surfactant concentration on vesicle's EE and it has been commonly reported that higher surfactant concentration reduce the EE. This effect has been explained by the possible formation of micelles when the surfactant concentration in the bilayer exceeds a critical lamellar/micellar transition temperature ^{60,91,92,107}. Furthermore, the permeability of the vesicles membrane might increase due to the arrangement of surfactant molecules within the lipid bilayer structure, which could introduce pores within the membrane and increase its fluidity ¹⁰⁸. Overall, this will prompt entrapped drug leakage ^{91,109,110}. Additionally, it is thought that the optimum amount of surfactant depends on the packing density of the phospholipid used and the surfactant-phospholipid interaction. When the surfactant concentration increases and it is known to have a high tendency to interact with the lipid, this leads to a reduction in entrapment due to competition on the loading within the bilayer ^{105,110,111}. For example, transfersomes were prepared and loaded with dexamethasone as a model lipophilic drug to evaluate sodium deoxycholate (SDC), Tween 80 and Span 80 as edge activators at five different lipid-surfactant ratios (95:5, 90:10, 85:15, 80:20, 75:25) ⁶⁰. The study revealed that encapsulation efficiency decreased as the concentration of the surfactant increased. Transfersomes prepared with SDC showed the lowest encapsulation of dexamethasone, as both surfactant and drug possess similar steroidal structure and therefore competing with each other for their entrapment ⁶⁰. Similarly, Patel et al. studied the effect of surfactant concentration on the entrapment of a lipophilic drug (i.e. curcumin) in lipid-based vesicles and demonstrated that higher surfactant concentration lowered the entrapment ¹¹⁰. Conversely, other researchers have reported that increasing surfactant concentration will increase the number of vesicles formed, which consequently leads to a higher volume of the hydrophobic bilayer domain available to house a hydrophobic

drug^{101,112,113}. The impact of surfactant concentration was similar when a low concentration was used to prepare Span-based niosomes, a small number of niosomes was obtained, and it was recommended that a higher surfactant concentration may improve drug entrapment¹⁰⁹.

1.2.2.2.2 Surfactant structure (carbon chain length, saturation, hydrophilic head group) and transition temperature (T_c)

Generally, it is suggested that by increasing the carbon chain length of the surfactant, the solubility of a lipophilic drug in the lipid bilayer should increase and consequently the entrapment efficiency will increase^{114,115}. On the other hand, a point not to forget is that a surfactant with a long carbon chain might compete with a lipophilic drug as they assemble themselves within the lipid bilayer, and excluding the drug and thus reducing its entrapment^{91,116}. Similar results were observed when niosomes were formulated with different types of Span. All Span surfactants have similar head groups and only differ by their hydrophobic chain. Niosomes that were prepared with Span 60 showed the highest entrapment as it has the longest carbon chain^{101,109}. In contrast, Span 80 resulted in the lowest entrapment efficiency, which was suggested to be related to the unsaturated double bond in its alkyl carbon chain. The presence of the double bond within the carbon chain might make it bend and thus would make the niosomes bilayer to be more permeable as the packing of the adjacent molecules may not be tight^{101,109}. Comparable outcomes were observed by El-Laithy et al., when they prepared proniosomes by using several non-ionic surfactants such as Tween (80 and 20) , Span (80 and 20) and sugar esters (such as, sucrose stearate, sucrose palmitate, sucrose myristate, and sucrose laurate)¹¹².

Although the Tween-based proniosomes showed the lowest entrapment efficiency, Tween 80 revealed better encapsulation due to its long carbon chain. Moreover, all sugar ester

surfactants showed good encapsulation due to their long carbon chains in spite of their high HLB values ^{112,117}. Additionally, it was proposed that not only the properties of tail but also the head group of the surfactant might influence drug entrapment within vesicles. The physiochemical properties of Span 60/Tween 60 niosomes with ellagic acid as a drug were evaluated ¹¹⁸. The study revealed that entrapment efficiency increased with Tween 60 niosomes, possibly due to the nature of the surfactant head group. The head group of Tween 60 (polyoxyethylene groups) is larger than the head group of Span 60, which in turn could help solubilize more ellagic acid ¹¹⁸. In addition, the formation of hydrogen bonds may be possible between the head group of Tween and the phenolic groups and lactone moiety of the ellagic acid ^{118,119}.

Furthermore, the phase transition temperature (T_c) of the surfactant could be an important factor in explaining surfactant effects on EE of lipid-based vesicles. It was reported that the higher the surfactant transition temperature, the better their ability to form a more ordered gel structure and a less leaky bilayer, which may further improve the entrapment efficiency ^{112,115,120}. While surfactants with a lower T_c could be more liquid in form, leading to irregular structural formation and increased fluidity of the vesicles bilayer, that in turn reduces the drug entrapment ^{102,109,121,122}. For example, Gupta et al. showed that Span 80 gave the lowest entrapment as it has the lowest transition temperature ($T_c = -12^\circ\text{C}$) in comparison to Span 60, 40, and 20 since their transition temperatures are 53°C , 42°C and 16°C respectively ¹⁰¹. These results were consistent with several other studies where the highest entrapment of drug was obtained from vesicles prepared using Span with the highest transition temperature ^{109,123,124}.

1.2.2.2.3 Surfactant HLB value and surfactant physical state

Evaluating surfactant effects on vesicle entrapment efficiency not only depends on its chemical structure, but also requires an understanding of the influence of the hydrophilic-lipophilic balance (HLB). However, the effect of the surfactant HLB value on the entrapment still depends on the drug lipophilicity^{60,125}. Literature suggested that the maximum entrapment of a lipophilic drug could be achieved by using a surfactant with a low HLB value^{104,126,127}. For example, Tween 60 was reported to give better encapsulation of β -carotene (a model lipophilic drug) when compared to Tween 20 since their HLB values are 14.9 and 16.7 respectively⁶⁶. Niosomes showed a lower tendency to entrap the lipophilic carvedilol, as the HLB value of the surfactant used increased^{104,128}. Chaudhary et al., obtained a higher encapsulation of curcumin from transfersomes prepared using Span 80 (HLB value 4.3) as an edge activator compared with Tween 80 (HLB value 15)⁹¹. Similar findings were also exhibited when dexamethasone loaded transfersomes were prepared, with both Span 85 and Span 80, with HLB values of 1.8 and 4.3 respectively, showed higher encapsulation than Tween 80 (HLB 15) and sodium deoxycholate (HLB 16)⁶⁰.

On the other hand, surfactants with high HLB values are thought to give better encapsulation of hydrophilic drugs^{129,130}. This was proved by Shaji et al., who prepared piroxicam loaded-transfersomes as sodium deoxycholate based transfersomes, highest encapsulation was obtained in comparison to Tween 80, Span 80 and Span 65¹²⁹. Surprisingly, contrasting results were obtained when the hydrophilic drug diclofenac sodium was loaded within transfersomes using different types of surfactant¹²⁵. The surfactants used were ranked according to their ability to give the highest encapsulation as: Span 85 > Span 80 > sodium cholate > sodium deoxycholate > Tween 80. Although Tween 80 did not show higher encapsulation than sodium

cholate or sodium deoxycholate, Span-based transfersomes showed the highest EE regardless of their low HLB values ¹²⁵.

Moreover, the physical state of the surfactant could have an effect on vesicles EE ¹⁰³. Surfactants could be solids, such as sodium deoxycholate, gel form such as Span 60 and 40 or a liquid such as Span 80. Gel-type surfactants are likely to produce less permeable vesicles than liquid surfactants. Several types of surfactant were used in the preparation of insulin-loaded niosomes and the presence of the gel-type surfactants such as Span 60 and Span 40 were found to improve drug entrapment. Whereas niosomes prepared using liquid surfactants such as Span 20 and Span 80 were thought to be more permeable and showed lower entrapment efficiency ¹⁰³.

1.2.2.3 Surfactant effects on pharmacokinetics and pharmacodynamics

There are many claims that the presence of surfactant could have an effect on the pharmacokinetic and pharmacodynamics properties of lipid-based delivery systems, such as enhancing drug release, permeability through the route of administration, circulation time and cellular uptake. For example, in surfactant-based liposomes, increasing surfactant concentration enhanced the release of the encapsulated drug (ciprofloxacin) from the delivery system. However, the amount of ciprofloxacin released was dependant on the type of surfactant used and using Tween 80 significantly enhanced release ¹¹⁶. Similar results were obtained in other studies, where the use of Tween 80 in liposomal formulations enhanced the flux of drug through the skin ^{131,132}. Although Tween 80 enhanced the skin permeation of celecoxib-loaded liposomes, it did not show any enhancement of celecoxib cellular uptake in comparison to conventional celecoxib liposomes ¹³². Niosomes were prepared with several types of Span for the delivery of the antitumor agent 5-fluorouracil (5-FU) and the release rate

from formulations prepared using Span 40 and Span 60 was slower than those prepared using Span 20 and Span 80 ¹³³. This trend could be due to the difference in the rigidity and permeability of the formed bilayer, since both Span 40 and Span 60 have a high Tc and form a less permeable bilayer than Span 20 and Span 80. Additionally, in comparison with free drug solution, all surfactant-based vesicles of 5-FU showed higher concentrations of drug in several organs for a longer duration that could enhance the possibility of the preferential phagocytic uptake and reduce its cytotoxicity ¹³³. Also, the pharmacokinetic studies of the 5-FU vesicles reported an increase in the half-life and a decrease in the clearance, which in turn maintained a sustained action of 5-FU ¹³³. Similarly, paclitaxel was also formulated in niosomes with several surfactants for oral delivery to slow release rate and reduce the toxic side effects ¹²⁶. Moreover, Span 40-based niosomes were more efficient in protecting paclitaxel from degradation by the gastrointestinal enzymes ¹²⁶. Span 60-based vesicles were also prepared to deliver doxorubicin, showed prolonged release, doubled its therapeutic effect (tumoricidal effect) and reduced the drug clearance ^{134,135}. Similar results were achieved when several Spans were used to prepare ketoprofen loaded vesicles and Span 60 was reported to be superior in maintaining the anti-inflammatory effect of ketoprofen for a longer time with slower release rate in comparison to Span 40 ¹³⁶. Confalonieri et al. carried out a comparison between surfactant-based vesicles and non-niosomal formulations for the delivery of flurbiprofen ¹³⁷. After IV administration to dairy cattle, there was no immunogenical reaction. Furthermore, the surfactant-based niosomes showed longer circulation time in the vascular space, which could improve the flurbiprofen distribution into the required organs/ tissue as well as its short half-life ¹³⁷. In addition, a high permeation through the skin with an improved pharmacological activity and reduced side effects were reported after applying meloxicam-loaded niosomes during in vivo animal studies, which

were prepared using both Span 60 and ethanol as surfactants ¹³⁸. A significant enhancement in the cellular uptake of gene-loaded niosomes were reported in comparison to a conventional liposomal delivery ¹³⁹. Span 60 and Span 40 were more effective in mediating the cellular uptake of the gene (antisense oligonucleotides) during the in vitro study using a COS-7 cell line ¹³⁹. Similarly, it was reported that the permeability and the flux of lidocaine hydrochloride through the porcine buccal tissue was enhanced by the presence of the surface active agent such as oleic acid in comparison with a standard lidocaine solution. However, that was concentration dependant, where increasing the surfactant concentration showed higher drug flux through the buccal mucosa ¹⁴⁰. Previous studies suggested its permeability could be improved due to the disruptive effect of the surfactant on both the hydrophilic and hydrophobic region of the membrane lipids ^{140,141}. In summary, surfactants have a clear influence on the pharmacokinetic and pharmacodynamic properties of lipid delivery systems, such as sustaining release, enhancing circulation time, targeting and cellular uptake. Nevertheless, the impact is not always constant and could alter depending on the properties of the surfactant.

1.2.2.4 Surfactant effects on charge and stability

Measuring the electrostatic charge of lipid vesicles is an important factor in order to evaluate their surface properties, as it might play a crucial role in their stability by either creating repulsive forces or agglomeration ^{94,129}. The net charge on the vesicle surfaces was thought to be the combination of both lipid and surfactant charge. However, it was reported that the type of surfactant could greatly affect the zeta potential. For example; between several types of surfactant-based transfersomes, cholate-based transfersomes exhibited the highest negative zeta potential value. Additionally, as the concentration of the surfactant increased,

the net charge of the transfersomes increased as well ¹²⁹. This high negative charge was considered to be advantageous as the research aimed to prepare transfersomes for transdermal drug delivery ⁹⁴. Since it was thought to enhance the transfersomes permeability and stability due to the repulsive forces between the charge of the vesicles and skin surface ^{94,111}. On the other hand, the same research revealed that all Tween-based transfersomes showed positive charge and the greater the hydrophilicity of the Tween (i.e. HLB value) the larger the positive charge on the vesicle surfaces ^{94,111}. Similarly, many studies have reported that as the surfactant concentration increases, the vesicles hold a larger zeta potential. Generally, the high charge could improve vesicles stability by reducing aggregation due to the electrostatic repulsions that could occur between them when they bear similar charge on their surfaces ^{92,93,134,142}. On the other hand, some studies suggested that increasing the surfactant concentration may reduce the physical stability by forming several types of aggregates such as elongated vesicles or tubules due to the fusion of the spherical vesicles ¹⁴³. That could be related not only to the surfactant concentration but also to the medium pH, since it was reported that at high pH surfactant monomers might have looser packing and form more elongated and aggregated vesicles ¹⁴³.

Additionally, the surfactant transition temperature was also reported to have an effect on the vesicular system stability. It was thought that the surfactant with higher transition temperature could be useful to prepare more stable vesicles ^{101,144,145}. Moreover, it was claimed that a surfactant molecular structure such as polyoxyethylene alkyl ether could enhance the stability of liposomes, since its large hydrophilic group induced a steric hindrance which impaired liposome aggregation and improved the stability ¹⁴⁶. Similar findings were reported when sodium 3,6,9,12,15-pentaoxaheptacosanoate (AEC4-Na), which is a weak acid type anionic surfactant, was used to form vesicles. Inhibition of aggregation and the stability

were enhanced because of the steric repulsion which was induced by the hydrophilic oxyethylene unit of AEC4-Na ¹⁴⁷.

1.2.3 Formulation methods

Lipid-based vesicles can be prepared using a wide range of methods, which combine several techniques, and ingredients (i.e. lipids, organic or aqueous media). The choice of the method of preparation could have an effect on the properties of the produced vesicles such as the size and entrapment efficiency. The methods range from conventional to developed and more advanced methods which could enable large scale production ¹⁴⁸.

1.2.3.1 Conventional methods

The most commonly used methods for the preparation of lipid-based vesicles. Generally share the same four stages ¹⁴⁸:

- A) Lipids dissolution in organic solvent.
- B) Forming a dry lipid film by evaporating the organic solvent.
- C) Rehydration and annealing of the lipids.
- D) Vesicles harvesting.

However, there are some specific detailed differences between the applied methods based on the properties of the constituents used such as drug solubility (i.e. lipophilic or hydrophilic), drug stability and the possibility of using temperature (considering heat sensitive drugs), the desired output style (i.e. liposome, ethosome, transfersomes, etc.). Table 1.4 summarises the most reported methods, describing the main differences between the techniques as well as their advantages and drawbacks.

Although conventional methods for lipid-based vesicles preparation are considered simple on small-scale preparations, they have shown few drawbacks such as broad size distribution, inconsistent drug entrapment and the presence of harsh conditions (i.e. high temperature and presence of organic solvents), which make them not convenient for industrial production.

Table 1.4 Short review of the conventional methods for lipid-based vesicles with their advantages and drawbacks.

Technique (short description)	Advantages	Drawbacks	Ref.
<p>Thin lipid film hydration method</p> <p>(The general 4 steps in addition to size reduction step: by either extrusions through a polycarbonate membrane, probe sonication, or water bath sonication)</p>	<ul style="list-style-type: none"> - Straightforward process. - Help in forming multilamellar (MLVs) or giant/small unilamellar vesicles. - Used for preparation of liposomes, transfersomes and proliposomes. - More suitable for lipophilic drugs. 	<ul style="list-style-type: none"> - The use of organic solvent and mechanical agitation. - Production of large particles with no control on size. - Poor encapsulation efficiencies of hydrophilic materials - Time consuming. 	<p>149-151</p>
<p>Reverse phase evaporation method</p> <p>(Achieved by forming inverted micelles water-in-oil emulsions, then by slow evaporation of organic solvent, conversion</p>	<ul style="list-style-type: none"> - Simple. - Results in higher internal aqueous loading capacity. - More suitable for water soluble drugs. 	<ul style="list-style-type: none"> - The use of large quantity of organic solvent. - Time consuming. - Adverse effects of trace elements of the organic solvent that may remain. 	<p>148,152</p>

Technique (short description)	Advantages	Drawbacks	Ref.
of the system into a viscous gel results in liposome).			
<p>Solvent injection</p> <p>(involves quick injection of phospholipids dissolved in ethanol/ether into drug containing aqueous phase, followed by evaporation and size reduction)</p>	<ul style="list-style-type: none"> - Simple approach. - Results in the formation of a heterogeneous species of liposomes. - Formation of ethosomes. 	<ul style="list-style-type: none"> - Remaining residues and trace of organic solvent. - Possible nozzle blockage. - High temperature especially during ether injection. 	152-154
<p>Detergent depletion</p> <p>(formation of detergent-lipid micelles, followed by detergent removal by dialysis or size exclusion gel chromatography)</p>	<ul style="list-style-type: none"> - Produces homogenous vesicles size. - Suits more hydrophilic drugs. 	<ul style="list-style-type: none"> - The presence of organic solvent traces and detergent residue. - Time consuming. - Low entrapment efficiency of hydrophobic drugs. - General poor liposomal yield. 	51,148,15 5

Technique (short description)	Advantages	Drawbacks	Ref.
<p style="text-align: center;">Heating method</p> <p>(Simply lipids are hydrated followed by heating for a specific time above phospholipids Tc in the presence of a hydrating agent)</p>	<ul style="list-style-type: none"> - Organic solvent free - Simple and fast process. - Possible scale up manufacturing. 	<ul style="list-style-type: none"> - The need of high temperature. - The uses of hydrating agents such as glycerine. - Not suitable for thermosensitive drugs. 	<p style="text-align: center;">156,157</p>

1.2.3.2 Developed methods

New methods have been explored for the production of lipid-based vesicles employing the recent advances in technology. Developing the preparation methods have helped in producing a new generation of vesicles, which may be scaled up and produced on an industrial level ¹⁴⁸.

Microfluidic methods were among the novel techniques that were established to produce unilamellar vesicles with homogeneous size ^{158,159}. They include micro hydrodynamic focusing method (size ranged between 40-140 nm), microfluidic droplets method (giant vesicles with size of 4-20 μm), and pulsed jet flow microfluidic method (larger vesicles of 200–534 μm but remarkable %EE). The method flexibility and adaptability offer the possibility of vesicles preparation with a wide range of sizes. However, similar to conventional method the excessive use of organic solvent and harsh agitation makes microfluidic methods unsuitable for industrial production ¹⁶⁰. Supercritical fluidic method was developed as free organic solvent method proposing many other advantages such as the option of large scale up production, as well as the use of a cheap and environmentally friendly solvent (i.e. CO_2). Yet it suffers from some downsides, especially the low vesicle yield, the use of high pressure, which requires special infrastructure with overall high costs. Thus, the method has not been widely employed and has a limited application ^{148,155}.

1.3 Local anaesthetics

Local anaesthetics (LA) block the transmission of painful stimuli to the brain by acting on ion channels of nociceptor fibres, to achieve a control for both acute and chronic pain ¹⁶¹. Although researcher have indicated that LA mechanism of action is complicated, but the general mechanism is by blocking the voltage-gated sodium channels and preventing the

inward Na^+ current during the depolarization. That is basically achieved due to the ability of LAs to cross the lipid bilayer of neuronal membrane and inactivate the sodium channel from the inside of the axoplasm. Hence, no further conduction of impulses happens and in turn prevents the propagation of the axonal action potential and stop the pain stimuli transmission¹⁶². Local anaesthetics are weak bases, they generally consist of three main parts a lipophilic ring, an intermediate link, and a hydrophilic amine, which are mostly tertiary amines (**Error! Reference source not found.**). LAs are classified based on the nature of the intermediate link, amide and esters LAs¹⁶². The ester-based LAs include cocaine, procaine, chlorprocaine and amethocaine. While LAs containing amide groups are considered the most commonly used and include lidocaine, bupivacaine, and ropivacaine, the intermediate link does not only define LA classes but also determines the pathway of metabolism. While plasma pseudocholinesterases metabolise ester LAs, the amide-based ones are mainly metabolised by the cytochrome family of enzymes in the liver^{162,163}. Furthermore, there are many factors affecting the physiological activities of LAs including the pH of the tissue environment, LAs properties such as pKa, as well as the bond and length of the intermediate chain. For example, it was reported the longer the intermediate chain the more potent the LA, which explains why bupivacaine is three to four times more potent than lidocaine¹⁶⁴.

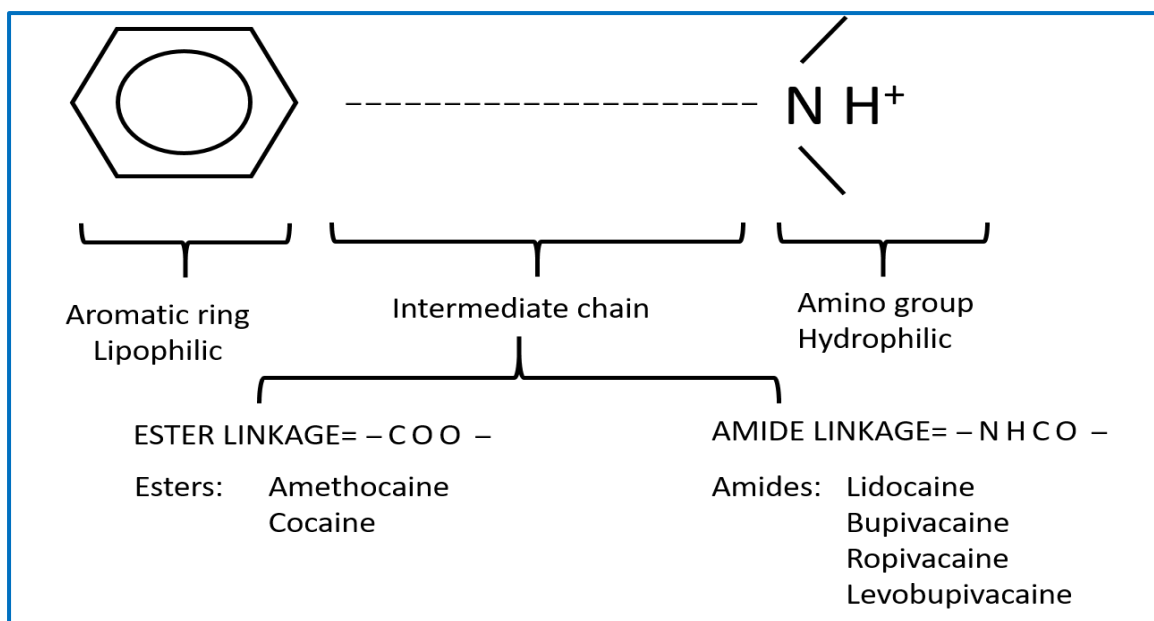


Figure 1.5 General chemical structure of local anaesthetics ¹⁶³.

In general, the difference between ester and amide LAs depends mainly on the mechanisms by which they get metabolised, excreted, and their potential to produce allergic reactions ¹⁶⁴.

There are many reported incidences to prove that ester-based LAs have higher risk of showing allergic reactions or systemic toxicity. For example, cocaine was reported to cause major side effects as it is a potent vasoconstrictor, additionally, it could show a fatal toxicity for patients with reduced plasma cholinesterase activity. Therefore, amide-based LAs are considered safer and more commonly used in clinical practice.

1.3.1 Local anaesthetic delivery

Generally, in order to improve LAs pharmacokinetic properties, prolong their pharmacological activity and minimise their toxicity, numerous studies have been conducted to formulate LAs in different forms. Additionally, the technology of scaling down to micro- and nanoscale in the formulation of LAs has significantly enhanced pain management, and helped to overcome some of the limitations of the traditional LA delivery tools.

These micro- and nano- carriers have then delivered in several forms such as injectable implants, films, patches, depof foam, microstructural systems, liposomes, and nanogels (self-assembly, pH- responsive, or natural polymer-based nanogels) ^{165,166}. There were many efforts to formulate LAs, manipulate their safety, efficacy, and release profiles using many approaches. Starting from formulating an oil depot formulation (which is considered the simplest delivery system) to producing more advanced delivery system to control release of the drug. Larsen et al. tried to enhance the release profile by formulating parenteral and intraocular delivery systems of both lidocaine and bupivacaine ¹⁶⁷⁻¹⁶⁹.

Nowadays, controlled release systems are intensively considered because of their enhanced properties. The prolonged action makes them the preferable candidates in the production of any delivery system. Achieving a controlled release of LAs from a delivery system was and still is a challenging topic and the only current controlled release local anaesthetic available in the market is Exparel[®] (Pacira Pharmaceuticals Inc.), which is a depof foam formulation of liposomal bupivacaine. Although, it succeeded in reaching the market due to the good sustained release profile of bupivacaine, the method of administration is by using an infiltration technique through multiple injections ¹⁷⁰, which could be considered a main limitation of Exparel[®].

1.3.2 Lidocaine

Lidocaine or 2-(diethylamino)-N-(2,6-dimethylphenyl)acetamide, also referred to as lignocaine, is the general prototype of amide LAs (Figure 1.6). It was the first amide LA to be introduced in 1948. Adjacent to its anaesthetic activity, it was reported to show analgesic effects and anti-inflammatory properties. It is also classified as Class 1B antiarrhythmic drug. Therefore It is considered the most widely used anaesthetic as it can be administered

intravenously (IV), intrathecally, subcutaneously (SC) as local infiltration. Lidocaine was claimed to have fast onset of action. Additionally as weak base with pK_a of 7.9¹⁶³, it was categorised as a poorly water-soluble drug with a pH dependent solubility¹⁷¹. It also exhibits lipophilic properties with log P of 2.33, and low protein-binding capacity of 64%¹⁶³. The low protein-binding capacity results in a moderate duration of action which marks lidocaine as the least toxic of all amide LAs¹⁶³. After systemic administration, some side effects ranging from moderate to severe have been reported. Symptoms such as metallic taste, slurred speech, diplopia (double vision), light headache, tinnitus (buzzing in the ears), confusion, agitation, muscular spasm were all reported as lidocaine side effects. Additionally, seizures were also reported at high plasma concentration (i.e. >5-8 $\mu\text{g}/\text{mL}$)¹⁷².

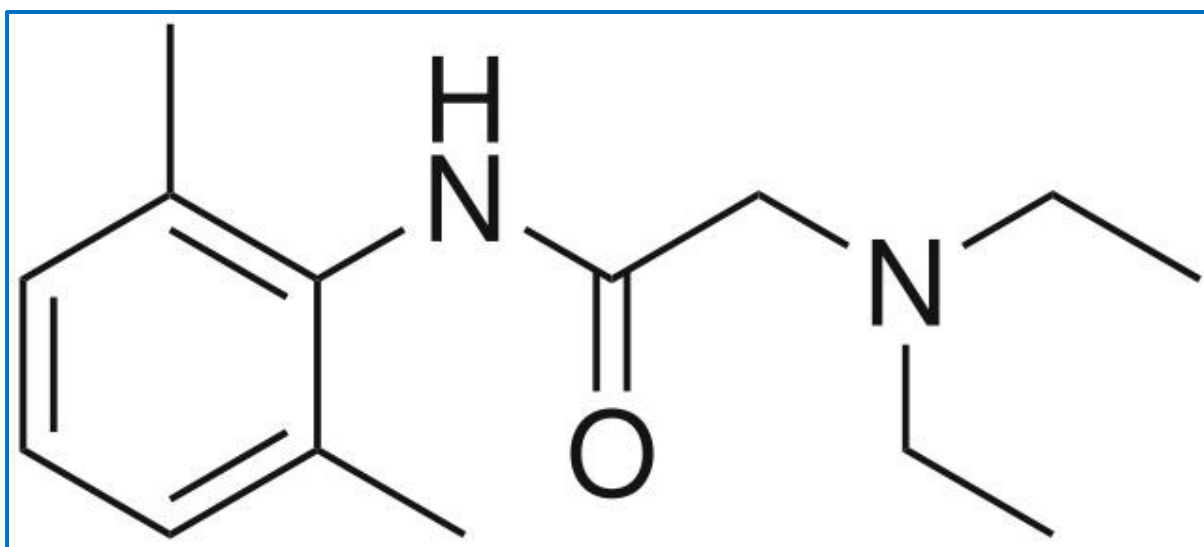


Figure 1.6 Skeletal formula of lidocaine molecule.

1.3.2.1 Examples of delivery systems of lidocaine

Table 1.5 reviews some of the delivery systems, which have been developed to deliver LAs mainly lidocaine, showing the exerted efforts over the last few decades to incorporate several materials, many methods of preparation, combinations of several carriers as well as

employing stimuli responsive materials. Overall, these numerous studies emphasise the real necessity for developing a successful delivery system of local anaesthetic.

Table 1.5 Summary of some studies that aimed to develop lidocaine delivery systems, the method of preparation, main carrier of the system and the achieved outcome.

Category	Delivery system/ Dosage form/ (method of preparation)	Main Carrier	Outcome	Ref.
Polymeric delivery systems	Microparticles (flow focusing)	PLGA	Higher drug encapsulation and slower release kinetics was obtained.	173
	Porous microparticles (double emulsion)	PLGA	Very fast drug release was achieved due to particle porosity.	174
	Microparticles (microfluidics)	PLA and polycaprolactone	The study produced a controlled and sustained drug release up to 130 h.	175
	Nanospheres (emulsion solvent evaporation)	PLA and poly (d,l-lactic acid)– poly(ethylene glycol), poly(ε-caprolactone) (PCL)	The developed nanosphere reduced the toxicity of lidocaine and prolonged its anaesthetic action.	176-179

Category	Delivery system/ Dosage form/ (method of preparation)	Main Carrier	Outcome	Ref.
	Lipid- polymer hybrid nanoparticles (solvent extraction/evaporation method)	1,2-dilauroyl-sn-glycero-3- phosphocholine (DLPC), chitosan (CS), cholesterol, and 1,2-Distearoyl-sn- glycero-3-phosphoethanolamine-N- [methoxy(polyethylene glycol)-2000] (DSPE-PEG2000)	The delivery system showed better permeation (via skin), hence increases in vivo lidocaine anaesthetic effects.	180
Hydrogel-based delivery systems	pH/thermoreponsive microspheres (chemical cross linking) injectable emulsion	Poly(N-isopropylacrylamide-co- acrylamide) copolymer	A delayed release of lidocaine was achieved by increasing temperature to 37 °C.	181,18 2
	Microspheres (emulsion solvent evaporation method) injectable hdyrogel system	Chitosan-glyceryl monooleate (GMO)	The carrier increased the system viscosity which led to reduced drug burst effect and retarded its release up to 80%.	183

Category	Delivery system/ Dosage form/ (method of preparation)	Main Carrier	Outcome	Ref.
Lipid-based delivery systems	Liposome (freeze drying)	Egg phosphatidyl choline	The study revealed the insertion of lidocaine within the bilayer and inducing less tight packing of the lipid in the vesicles.	184
	Nanoethosomes (modified ethanol injection method)	Cholesterol and Rhodamine B	The ethosome delivery system showed by in vitro and in vivo assay an enhanced lidocaine penetration into a deep skin layers.	185- 187
	Transfersomes (thin-film hydration method) HPMC k15 topical gel	Soybean phosphatidylcholine, cholesterol, sodium cholate (SC), span 80 (sorbitan monostearate), and brij 35	Transfersomes showed enhanced drug permeation effect (skin) and prolonged local anaesthetic action of lidocaine, without any alteration to the skin structure or irritation.	188

1.3.3 LAs in dentistry

A number of intra-oral conditions can be painful and long lasting, including recurrent aphthous stomatitis, lichen planus, vesiculobullos disorders, atypical odontalgia, burning mouth syndrome, and postoperative dental pain. Treatment of these conditions is unsatisfactory and often relies on repeated application of very short lasting numbing agents such as sprays, mouth rinses or creams, which are easily and rapidly washed away by the action of saliva and swallowing. Local anaesthetic was considered the foundation of pain control in dentistry¹⁸⁹, and the development of safe and effective LA agents has been considered the most important progression in dental science over the last few decades. However, both systemic administration and the overuse of short acting topical local anaesthetics have been linked with serious side effects and even death^{190,191}. To avoid the systemic adverse effects whilst achieving longer-term pain relief may require submucosal injection of LA, but there is a high prevalence of anxiety and fear of dental injections in the population and injections may have further complications such as mucosal irritation, hematoma, infection, nerve trauma, and muscle spasm^{189,192,193}. For instance, Exparel® is widely used nowadays by dentists to produce buccal anaesthesia, however the injection side effects are still an issue to consider as well as improving overall patient satisfaction¹⁹⁴. Other systems were also developed to treat pain after tooth extraction, such as developing sponge like hydrogel fillers incorporating lidocaine cross-linked within a polymeric matrix, or by mixing common bone putty with LA and using it to fill the bone gap^{195,196}.

1.3.3.1 Methods of LAs delivery in Dentistry

Developing newer methods for the delivery of LAs was believed to enhance the general pain relief with diminished pain from injection and reduced side effects (both systemically and locally).

Some of these methods were reviewed by Second et al ¹⁹⁷ (Table 1.6). Nonetheless, all reported methods were only under investigations and none of them has yet been adopted by dentists to induce anaesthesia as a pre injection or a substitute to injection.

Table 1.6 Summary of the reported method used for LAs delivery in dentistry.

Method	Mechanism/ advantages	Limitations	Ref
Electronic Dental Anesthesia (EDA)	<ul style="list-style-type: none"> Depends on the principle of Trans-cutaneous Electrical Nerve Stimulation (TENS). TENS is a noninvasive, low-risk nerve stimulation to relieve the pain. 	<ul style="list-style-type: none"> Increased salivary flow in oral cavity Inability to use metal instruments freely. <p>Contraindicated in heart diseases, neurological disorders, brain tumors, seizures, and patients wearing pacemakers and cochlear implants.</p>	198
Iontophoresis	<ul style="list-style-type: none"> Using a constant low-voltage direct current, enhancing ion transport through the barrier. Painless 	<ul style="list-style-type: none"> Irritation at higher current densities or with longer duration. 	197,199
Eutectic Mixture of Local Anesthetics (EMLA)	<ul style="list-style-type: none"> A mixture of lignocaine and prilocaine mixed in equal 	<ul style="list-style-type: none"> Rapid wash. 	200

Method	Mechanism/ advantages	Limitations	Ref
	<p>weight quantities that form a eutectic mixture.</p> <ul style="list-style-type: none"> • Used prior to needle insertion as this reduces the incidence of injection pain. 		
Jet Injection	<ul style="list-style-type: none"> • Uses a high-pressure narrow jet of the injection liquid. • A small amount of local anesthetic is pushed as a jet into the submucosa. 	<ul style="list-style-type: none"> • Surface anaesthesia • traditional LAs infiltration was more effective. 	201

1.4 Basis for the research project

There is a clinical need for a long acting topical anaesthetic formulation that could be applied by patients themselves, dentists, or health care professionals. The topical formulation should show sustained release properties with the aim to minimise the risk of systemic side effects. The ideal goal is to achieve pain free dental practice and improve patients' satisfaction.

1.4.1 Aim

This project aims to develop and prepare mucoadhesive transfersome formulations for the buccal delivery of local anaesthetics, embedded into fast disintegrating film to achieve sustained local pain relief.

1.4.2 Objectives

- 1) To prepare and optimise LA loaded transfersomes using Taguchi design of experiment approach, by screening many formulation parameters that would affect the delivery system properties such as size and entrapment efficiency.
- 2) To prepare coated transfersomes by assessing several mucoadhesive polymers.
- 3) To characterise transfersomes (uncoated and coated) for size, PDI, charge, morphology, drug entrapment efficiency, as well as drug release by employing a developed and validated (HPLC) method.
- 4) To evaluate the toxicity of the developed transfersomes using cell viability assay.
- 5) To quantify the drug permeability by comparing the results of using fresh animal tissue for an *ex-vivo* test as well as a cell-based developed model.
- 6) To prepare and characterise fast disintegrating polymer films incorporating the optimised transfersomes.

Chapter 2. General Methodology

2.1 Materials

2.1.1 Materials for transfersome formulation and characterisation

Egg phosphatidylcholine (EPC), sodium deoxycholate (SDC), Tween 80 and Span 80 were purchased from Sigma Aldrich, UK. Lidocaine (free-base, $\geq 97.5\%$) and phosphotungstic acid were obtained from Fisher Scientific, UK. 1,2-Dimyristoyl-sn-glycero-3-phosphorylcholine (DMPC) was purchased from Lipoid, Switzerland. Chitosan hydrochloride (Chitoscience[®]) was purchased from Hepe Medical Chitosan HMC⁺ GmbH, Germany. Hydroxypropyl methylcellulose (HPMC) Methocel[®]K4M and Methocel[®] K15M were obtained from Colorcon, UK. Whatman[®] polycarbonate filter membranes of 25 mm diameter and 0.2 μm pore size were purchased from Sigma Aldrich, UK. Spectra/Pro[®]3 dialysis membrane tubing of MW 3.5 kDa with diameter of 11.5 mm was purchased from Fisher Scientific, UK.

2.1.2 Materials for cell culture

Normal oral keratinocytes (NOK) was a kind gift from Dr. Janet M. Risk (University of Liverpool). Two lung cell lines, the human lung fibroblasts (MRC5) and immortalized human fibroblasts (MRC5-SV2, derived from the parental MRC-5) were both obtained from the European Collection of Animal Cell Cultures (ECACC), UK. Dulbecco's Modified Eagle Medium (DMEM) with high glucose, TrypLE[™] Express Enzyme (1X) with phenol red, L-glutamine, Antibiotic-Antimycotic and AlamarBlue[™] (AB) cell viability reagent were purchased from Gibco/Thermofisher, UK. Fetal Bovine Serum (FBS) was obtained from Sigma Aldrich, UK. Black 96-well plates (sterile, tissue culture-treated, microclear) were purchased from Greiner Bio-One (UK). Tissue culture inserts for 24-well plates (PET membrane bottom, transparent, pore size 0.4 μm) were purchased from Sarstedt Ltd, UK.

2.1.3 Materials for ex-vivo testing

Porcine oesophaguses were freshly obtained from a local abattoir (C S Morphet & Sons Ltd, Widnes, UK). Krebs bicarbonate Ringer's solution was freshly prepared and gassed with 5% CO₂: 95% O₂.

2.1.4 Materials for buccal film preparation

Poly(vinyl alcohol) (PVA) (MW 9,000-10,000, 80% hydrolysed) and glycerine were purchased from Sigma Aldrich, UK. HPMC Metolose[®] 603, and Metolose[®] 606 were obtained from Shin-Etsu Chemical Co. Japan. Hydroxypropylcellulose (HPC) (Klucel[®] EXF) was gifted from Ashland, UK.

2.1.5 Other materials and solvents

Phosphate buffered saline (PBS, pH7.4) tablets purchased from Sigma Aldrich, UK. Di-Potassium hydrogen orthophosphate anhydrous was purchased from BDH Chemicals Ltd, UK. Acetonitrile (ACN), methanol (MeOH), and absolute ethanol were obtained from Fisher Scientific, UK. All solvents used were of HPLC grade. Deionised water (DW) was provided by LJMU.

2.2 General Methods and main analytical techniques

2.2.1 Preparation of transfersomes

Lipid-based film hydration method was adopted to produce both blank and loaded transfersomes²⁰²⁻²⁰⁴ (Figure 2.1). In the loaded transfersomes, the drug (i.e. lidocaine) was used in each formulation as the equivalent molar ratio to both phospholipid and EA ratio, and all components were dissolved in 12 mL of absolute ethanol. The mixture was sonicated for 5 minutes to ensure complete dissolution of all components using a water bath sonicator (Model U500D, Ultrawave, UK). This was followed by the evaporation of ethanol using a rotary evaporator (Heidolph Laborota 4000 efficient, Germany) at 60 °C under reduced pressure. A continuous thin lipid film was obtained upon rotation (at 250 rpm) and after the complete evaporation of the ethanol. The lipid film was hydrated using 9 mL of PBS (pH 7.4). The hydrated formulation was left to anneal for 30 minutes. Subsequently, formed transfersomes were extruded (Liposofast LF 50, Avestin, Germany), for 5 cycles at 45 °C using 200 nm membrane filters.

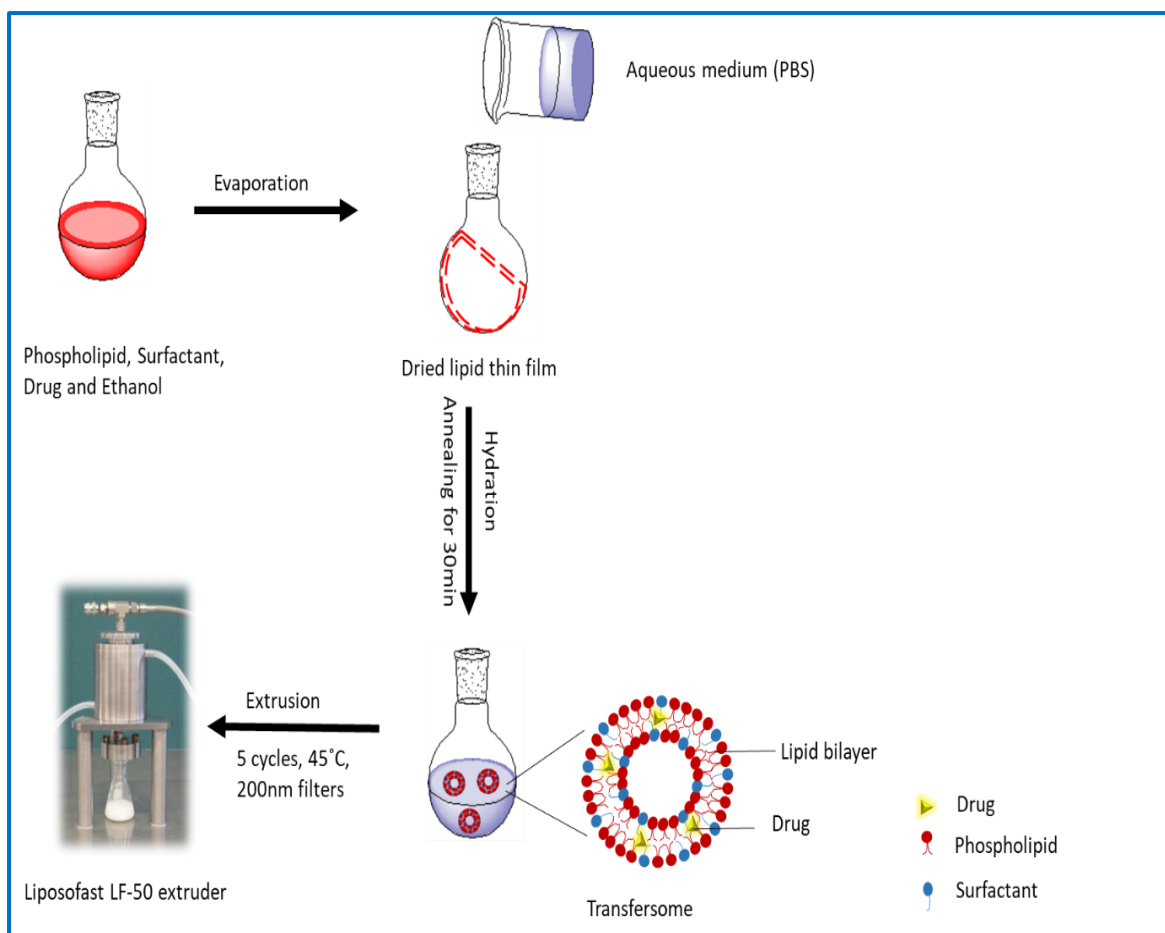


Figure 2.1 Schematic diagram of transfersomes preparation method ²⁰⁵.

2.2.2 Transfersomes coating

Transfersome coating was completed using three different water-soluble polymers chitosan HCl, HPMC K4M, or K15M. Solutions of five different concentrations (0.1, 0.2, 0.3, 0.4, and 0.6 % w/v) were prepared from each polymer ^{206,207}. Transfersomes for coating were prepared using the same method (Section 2.2.1), except that the lipid film was hydrated using half of the original volume of PBS (i.e. 4.5 mL). The extruded transfersomes were coated by dropwise addition of equal volume 4.5 mL of each polymer whilst under magnetic stirring (400 rpm). The samples were then left stirring for a further 5 minutes.

2.2.3 Dynamic light scattering (DLS)

Dynamic light scattering is a measurement technique commonly used for particle size and size distribution analysis in the sub-micron range (i.e. between 1 nm to 1 μm)^{208,209}. DLS measures particle size based on Brownian motion principle. Brownian motion is the random and uncontrolled movement of particles in a fluid due to the constant bombardment with the other molecules. Smaller particles move rapidly as they are easily kicked by the solvent molecules, while slower Brownian motion is obtained with larger particles. In DLS, the speed at which the particles diffuse within the solvent due to Brownian motion is measured and reflects their size (Stoke- Einstein equation)²⁰⁹. This is achieved by directing light through the colloid, which is scattered by the particles and the signal is detected at a certain angle. The detected signal represents the fluctuation amplitude of the scattered light intensity, which is associated with the particle size (Figure 2.2). For example, if small particles are measured they will move quickly and as a result, the scattered light will fluctuate rapidly. In contrast, the intensity of the scattered light will fluctuate slowly due to the slow motion of the large particles^{208,209}. The same principle applies in order to measure the polydispersity index (PDI). PDI reflects the uniformity of the particle size in the characterised sample^{208,209}.

Some DLS instrument can also be used to measure the zeta potential (the particle charge). Zeta potential is not an absolute value, but an estimation of the surface charge. As the charged particles in a dispersion move towards the opposite electrode under the effect of an electrical field, a potential difference is obtained between the electrophoretically mobile particles and the layer of dispersant around them. This potential difference is known as Zeta potential (ZP), which is not a measure of the charge or charge density. So ZP provides an indicator of the surface charge (positive or negative) but it is not definitive and there are many

exceptions to this assumption, therefore only the magnitude of ZP should be considered regardless of its positive or negative value ²¹⁰ (Figure 2.2).

Temperature and dispersion viscosity are important factors to be considered when using DLS to measure size and PDI, while pH and ionic strength are more influential for ZP measurement ^{209,210}.

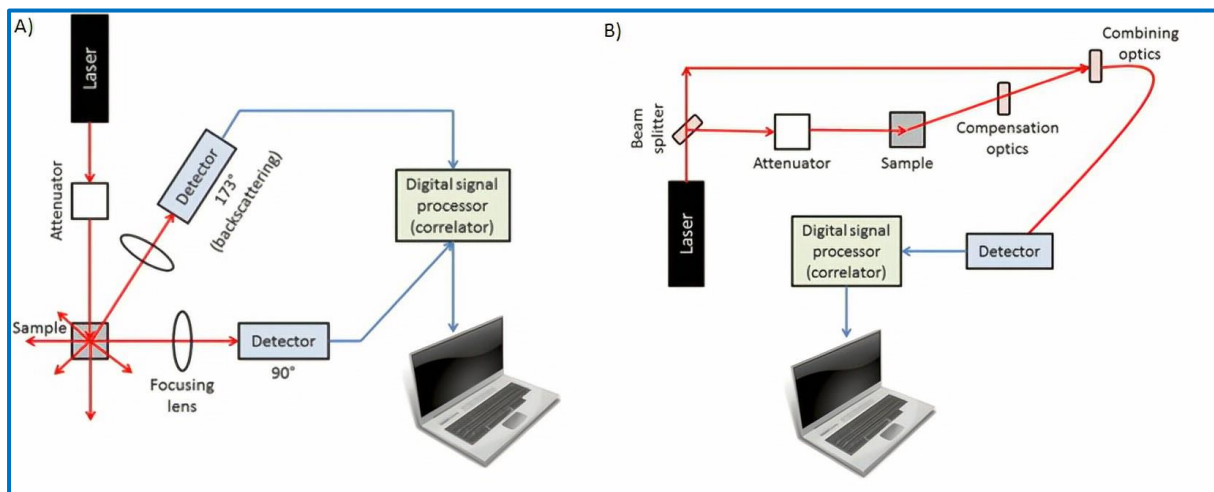


Figure 2.2 Schematic drawing showing the instrumentation of DLS; (A) process of size measurement and (B) zeta potential measurement ²¹⁰.

2.2.3.1 Size, polydispersity index (PDI), and zeta potential

Transfersomes were characterised for particle size, polydispersity index, and zeta potential using a dynamic light scattering (DLS) instrument (Zetasizer Nano; Malvern Instruments Ltd., UK). In this respect, 1 mL of each formulation was transferred into the transparent Malvern zeta potential cuvette and placed in the instrument.

2.2.4 High performance liquid chromatography (HPLC)

HPLC is an essential analytical technique for assessing drug content. Nowadays, HPLC is predominantly employed in research laboratories and in the pharmaceutical industry for the evaluation of a huge variety of samples. HPLC is used for checking the purity of new chemical

substances, monitoring changes in synthetic procedures, evaluation new formulations, conducting quality assurance testing of drug product from its raw ingredients to the final dosage and stability. Adjacent to the pharmaceutical applications, it has also been employed for clinical and forensic applications (e.g. urine analysis and quantification of drugs in biological samples, etc.), food and environmental applications as well ²¹¹⁻²¹³.

The same basic principle of all chromatographic separation applies to HPLC. The separation of a sample into its major components based on the relative affinity of different molecules for the mobile phase and stationary phase used in the separation. There are several types of HPLC systems based on the employed stationary phase. HPLC systems that use separation method based on the polarity are classified into normal phase and reverse phase. While ion exchange HPLC and size exclusion systems separate samples based on their charge and size respectively ²¹³.

Development of a valid HPLC method plays a critical role in the drug discovery and formulation development, as the HPLC method will be used to ensure the identity, purity, and potency of the drug product ²¹⁴. There are many factors to be considered during the method development process. Primarily factors related to HPLC conditions such as selecting the detector (i.e. wavelength), selecting the type and temperature of the column, the mobile phase composition and pH, and the separation technique (i.e. isocratic or gradient). Then, factors related to the drug and sample preparation, as some of its physicochemical properties such as solubility is crucial to be identified in order to prepare the sample and achieve high-resolution chromatograph (i.e. sharp, symmetrical peaks, short retention times with low detection limits) ^{214,215}.

Similar to most analytical methods, any developed HPLC method is required to be validated as a part of the quality assurance process as recommended by most regulatory authorities such as International Conference on Harmonisation (ICH) ²¹⁶. Although method validation is time consuming, it is an essential process and a systematic way to prove the suitability of the method to provide useful and consistent data.

Full details about the HPLC method development for Lidocaine analysis and validation are mentioned in chapter 3, section 3.2.1. However, only the general system details are provided in the following section.

2.2.4.1 HPLC chromatographic system

An HPLC system (1200 series) from Agilent Technologies, UK, was used with diode-array detector (DAD) and variable wavelength detector. An Agilent C18 column with dimensions of 4.6 x 150 mm, and a particle size of 5 μm , was employed (Agilent Technologies, USA). The column oven temperature was set at 30 °C with an injection volume of 10 μL . The final composition of the mobile phase was optimised with ACN and 0.01 M phosphate buffer (70 : 30, v/v) at a flow rate of 1 mL/min (the total run time was 5 min), and a UV detection wavelength of 255 nm.

2.2.5 Entrapment efficiency (%EE)

The total drug concentration contained within each formulation was measured using a 0.5 mL aliquot, which was diluted with MeOH until a clear transparent solution was obtained. The drug concentration was then measured using the developed HPLC method. Another 0.5 mL of the formulation was placed in a centrifugal filter tube of 3 kDa pore size (Amicon® Ultra, Merck Millipore Ltd, Ireland) and centrifuged for 30 minutes with centrifugal force of 15.6 rcf (13000 rpm) using benchtop centrifuge (Eppendorf Centrifuge 5415 D, Germany). The filtrate

at the bottom was diluted with MeOH, and the untrapped drug concentration was measured via HPLC. The %EE was then calculated using equation 2.1

$$\%EE = \frac{(total\ drug\ conc. - untrapped\ drug\ conc.)}{Total\ drug\ conc.} \times 100 \quad (2.1)$$

2.2.6 *In vitro* release study

The release profiles of some samples based on DOE results, and 0.1 % CH-coated sample were studied *in vitro* at 37 ± 0.5 °C in addition to a control sample containing free lidocaine only. The release study was carried out in a 500 mL beaker filled with 150 mL PBS (pH 7.4) on a magnetic stirrer at speed of 250 rpm. Transfersome samples were sealed inside dialysis cellulose membrane with 3.5 kDa molecular exclusion pores, measuring 12 cm, which were suspended in the PBS medium and incubated at 37 ± 0.5 °C. Aliquots of 0.5 mL of each sample were withdrawn at time intervals 0, 1, 3, 5, 7, 16 and 24 h. and replaced with a fresh PBS solution. The aliquots were then analysed using the developed HPLC method for the lidocaine content. A plot of the cumulative amounts of drug against time was then obtained.

2.2.7 Transfersome morphology

Electron microscopes have been established as a powerful technique for the characterisation of a wide range of materials especially at micro and nanoscale levels. Their extremely high resolution made them a very important tool for many applications. The main two types are Transmission Electron Microscope (TEM) and Scanning Electron Microscope (SEM) and both instruments were employed for transfersome characterisation in this study. Therefore, the general principle of each and the main differences between them are briefly described below as well as their application in visualising transfersomes.

2.2.7.1 Transmission electron microscope (TEM)

TEM has been widely employed to examine very fine materials and structures to an atomic scale, which are difficult to be observed by conventional optical microscope. Materials with dimensions of 100 nm or even lower such as the micro and nanoscale features of membranes or the crystalline structure of particles incorporated in membranes are now widely characterised by TEM ^{217,218}.

The basic principle of TEM as suggested by its name is to use transmitted electrons that travel through a vacuum column and then pass through the sample after being focused into a very thin beam by electromagnetic lenses. The transmitted electrons are then refocused by the electromagnetic lenses and projected on a phosphor detector, to convert the electron image information to a visible form ²¹⁸. Therefore, it is believed that TEM provides more information about the inner structure of the sample. However, sample preparation is the key aspect in TEM analysis, as the sample must be thin enough to allow the transmitted electrons to pass through with minimum energy loss. Samples are loaded onto grid, which is usually coated with a thin layer of amorphous carbon to provide a low electron density support to the samples ²¹⁹.

2.2.7.2 TEM for transfersomes characterisation

Transfersomes morphology was observed under a TEM using a FEI Morgagni Transmission Electron Microscope (Philips Electron Optics BV, Netherlands). A drop of the transfersome suspension was placed on the copper grid and left for a few minutes. A drop of negative stain solution (phosphotungstic acid, 1%) was then added to the sample grid. The grid was then rinsed with distilled water to wash off the excess stain, and placed in the TEM sample chamber for visualisation.

2.2.7.3 Scanning electron microscope (SEM)

SEM is considered one of the most important techniques in the characterisation of surface morphology and has numerous applications. SEM utilizes the interaction between the electron and the sample to generate a topographical image with higher magnification and observes finer details of the sample than light microscope ²²⁰.

SEM uses a focused beam of high energy electrons that react with the sample to give an overview image of the sample topography, texture, relative composition, crystalline structure and orientation of materials. The focused beam at the surface of the sample produce several signals (i.e. secondary electrons, backscattered electrons, and characteristic X-ray) which are then collected by a detector and finally displayed on the monitor ²²¹.

Samples must be solid and dry for SEM examination and most samples are required to be coated with an electrically conductive material such as carbon or gold. The choice of the coating material usually depends on the required data, gold coating is usually employed when high resolution electron imaging is required while carbon coating is preferable for elemental analysis of the sample ²¹⁹⁻²²¹.

2.2.7.4 SEM for transfersomes characterisation

Transfersome samples (both uncoated and coated) were observed using SEM (FEI – Quanta™ 200 ESEM, Holland) after preparing the stubs. The samples were placed at the top of aluminium stubs (pin stubs, 13 mm) and left to dry completely. Then the stubs were gold coated using a sputter coater (EmiTech K 550X Gold Sputter Coater, 10-15 nm) before the examination with the SEM ^{222,223}.

SEM imaging was also employed to prove the concept of mucoadhesive properties of the coated transfersomes. The method was adapted with some modifications from the

bioadhesion study conducted by Refai et al. ²²⁴. Aliquots of 1 mL of the coated transfersome sample (F5-CH) were placed on freshly desiccated epithelium over a microscope slide that was positioned in angle of 45°. After 5 minutes, the sample was washed with PBS by continuous dropping of approximately 8 mL at a rate of 10-15 drops per minute. Then the treated tissue was placed and left to dry on the SEM stub before gold coating.

2.2.8 Cytotoxicity study

2.2.8.1 Cell culture preparation

NOK, MRC-5 and MRC-5 SV2 cells were cultured in DMEM supplemented with 10% FBS, 1% L-glutamine (2 mM) and 1% antibiotic-antimycotic solution. Cells were used at passage numbers 8-23 (NOK), 26-45 (MRC-5) and 25-33 (MRC-5 SV2). All cell lines were maintained in 75 cm² T-flasks and incubated in a humidified atmosphere at 37 °C and 5% CO₂. The cells were passaged and cultured at approximately 80-90% confluency. To do this, the growth medium was aspirated, the cell culture was rinsed with 5 mL PBS, and the rinse was then discarded. 3-5 mL of TrypLE solution was added to the flask and decanted after 1 minute. After that, the flask was incubated for about 5 minutes at 37 °C. Then the cells were flooded with growth medium and triturated in order to disperse any cell clumps and obtain a homogeneous suspension of single cells for plating or establishment of a maintenance culture. Plating cells for experiments involved estimating the cell density of the suspension using the haemocytometer, preparing from that stock suspension a diluted suspension at a desired cell density based on the type of experiments to be carried out later, seeding the cells into a 96-well plate and putting the plate in the incubator until needed for experiments. Maintenance cultures for further use were prepared by diluting the stock suspension (between 1:10 and 1:5) to an optimal density and introducing about 10 mL of the diluted suspension into a new

T75 flask, which was then placed in the incubator. The cultures were fed with fresh growth medium every 3-4 days, as necessary, until they were needed for passaging.

2.2.8.2 Cell treatments and AlamarBlue viability assay

The toxicity profile of all transfersome components were assessed over 24 h using both MRC5 and MRC5-SV2 cells by employing the AlamarBlue (AB) assay. Each component was assessed at 3 different concentrations (Table 2.1). Additionally, the 24 h toxicity profiles of the transfersome/coated transfersome samples were evaluated in the three cell lines (NOK, MRC5, and MRC5-SV2) using the AB assay. Black, microclear 96-well plates of cells were prepared for each cell line by adding into each well of the plate 90 μL of the cell suspension with a density of 1×10^4 cells/mL and incubating the plates at 37 °C and 5% CO_2 . After 24 h, the cultures were confirmed to be free from microbial contamination by examining them under the microscope and then treated in triplicate with the different concentrations of the samples (each concentration prepared as a 10x strength and 10 μL of it was added to 90 μL of growth medium in each well to make 100 μL). The treated plates were incubated for another 24 h before viability was assessed with the alamar blue (AB) reagent. 10 μL (10% of total medium volume in each well) of pre-warmed AB was added to each well, and the plate was incubated for 3 h at 37 °C. The fluorescence of resorufin (reduced, fluorescent alamar blue) in each well was then measured using a microplate reader Clariostar plate reader (BMG Labtech, UK) ²²⁵. The percentage cell viability was then calculated as the ratio, expressed as a percentage, between the average fluorescence of each sample-treated triplicate and the average fluorescence of the negative control triplicate.

Table 2.1 Transfersome components with their concentrations (a, b and c representing high, medium and low concentrations, respectively) that were assessed for toxicity

Transfersome component	Concentration (mM)		
	a (high)	b (medium)	c (low)
Tween 80	8.33	2.77	0.92
Span 80	8.32	2.77	0.92
SDC	8.32	2.77	0.92
Lid	33.28	8.53	4.26
DMPC	24.98	8.32	2.77
EPC	25	8.33	2.77

2.2.9 Ex-vivo permeability

2.2.9.1 Tissue preparation for permeation study

Porcine oesophagus was obtained from a local abattoir after the pigs were freshly slaughtered. The tissues were transported to the laboratory in ice, and used within 2 h. The tissues were rinsed with ringer's solution a few times. The majority of the underlying connective tissue was detached with the help of scalpel blade and scissors. However, to fully separate the epithelial layer from the connective tissue, heat separation method was adopted rather than the surgical method to maintain the epithelial integrity. Pieces of the oesophagus were immersed into pre-warmed deionised water at 65-70 °C for 1 minute. Then the epithelial layer was easily peeled off. The obtained tissues were either immediately used for permeability study or dried with a tissue paper, wrapped with aluminium foil and stored in the fridge at 4 °C for further use, in both ways the obtained epithelial was clear from any mucous after the treatment in warmed water. The integrity of the tissue was visualised each time before the experiment. The thickness of the tissue was also measured with a digital calliper and recorded in order to minimize variation between studies.

2.2.9.2 Permeation experiment using Franz-cell

The permeation of transfersomes through the tissue was carried out using Franz diffusion cells (Soham Scientific, UK), with 176.71 mm² of permeation area and a receiver compartment

of 5 mL (Figure 2.3). The oesophagus epithelium was gently mounted between the receptor and donor chambers to avoid any damage that could alter the permeation. Transfersome/coated transfersome samples of 1 mL were placed in the donor chamber. The receptor chamber was filled with 4.5 mL of PBS and magnetically stirred. Both donor chamber and the sampling port were sealed with laboratory film to avoid any evaporation over the time of study. The experiment was conducted at 37 °C, aliquots of 0.5 mL of each samples were withdrawn at time intervals of 0, 1, 3, 5, 7, 24 h and replaced with fresh PBS. The aliquots were then analysed using HPLC for drug content, and the cumulative amounts of drug in the receptor solution were plotted against time.

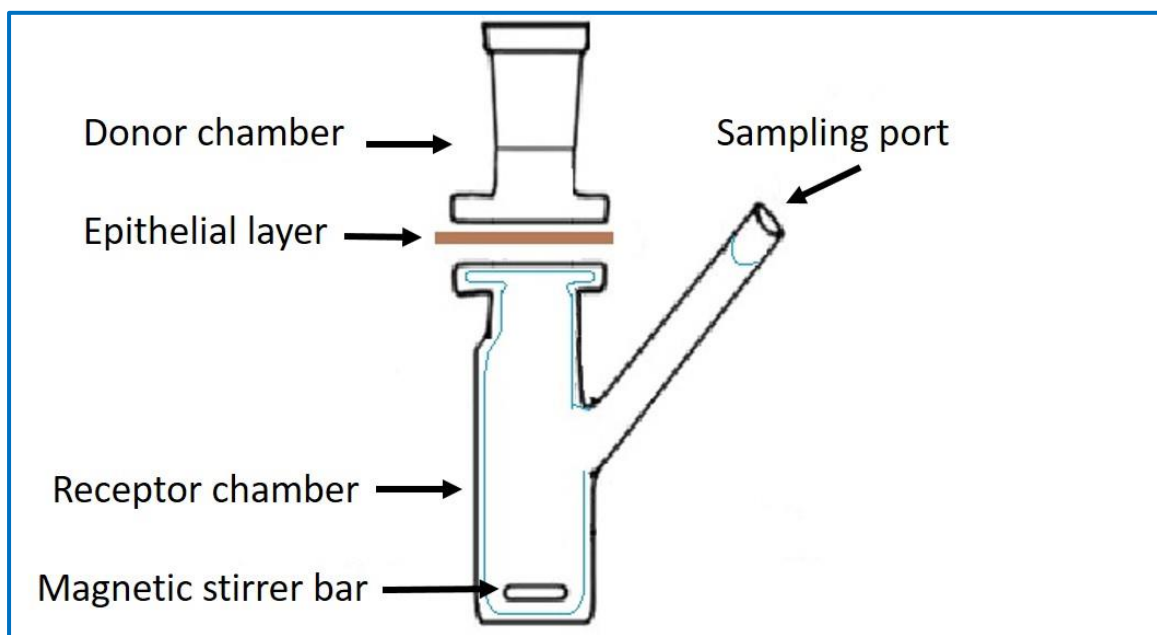


Figure 2.3 Schematic diagram of Franz cell

2.2.10 Cell-based model permeation experiment

2.2.10.1 Cell-based model preparation

A cell-based model was developed in-house using NOK cells, which were cultured in 24-well plate tissue culture (transwell) inserts (Figure 2.4). Each transwell insert with PET membrane

bottom was first soaked for 10 minutes in growth medium pre-warmed to 37 °C. NOK cells of 3 different passages were then seeded at a density of 2×10^5 cells/cm², with 100 µL placed in each transwell. Fresh growth medium was added to both apical and basolateral chambers to achieve a full volume of 1000 µL (i.e. the total volume in the apical part was 200 µL, and 800 µL in the basolateral part). To control for confluency, NOK cells at the same density as those seeded onto the transwells were also seeded into an adjacent well without the transwell. The plate was then incubated at 37 °C and 5% CO₂. The medium was freshly replaced every other day. Cell confluency was checked every day and once a fully confluent layer was obtained, the full culturing time to achieve approximately 5-7 layers was estimated (usually 25-28 days).

2.2.10.2 Permeation through transwell

After 28 days of incubation, 100 µL from the apical part was withdrawn and discarded. The volume was replaced with 100 µL of transferrin-coated transferrin samples. 500 µL aliquot of each sample was withdrawn from the basolateral part at time intervals of 0, 1, 3, 5, 7, 24 h and replaced with the same volume of fresh pre-warmed growth medium. The aliquots were placed in centrifugal filter tubes of 3 kDa pore size and centrifuged for 5 minutes using benchtop centrifuge. The filtrate at the bottom was diluted with MeOH and analysed using HPLC for drug content, and the cumulative amounts of drug in the basolateral part were plotted against sampling time intervals.

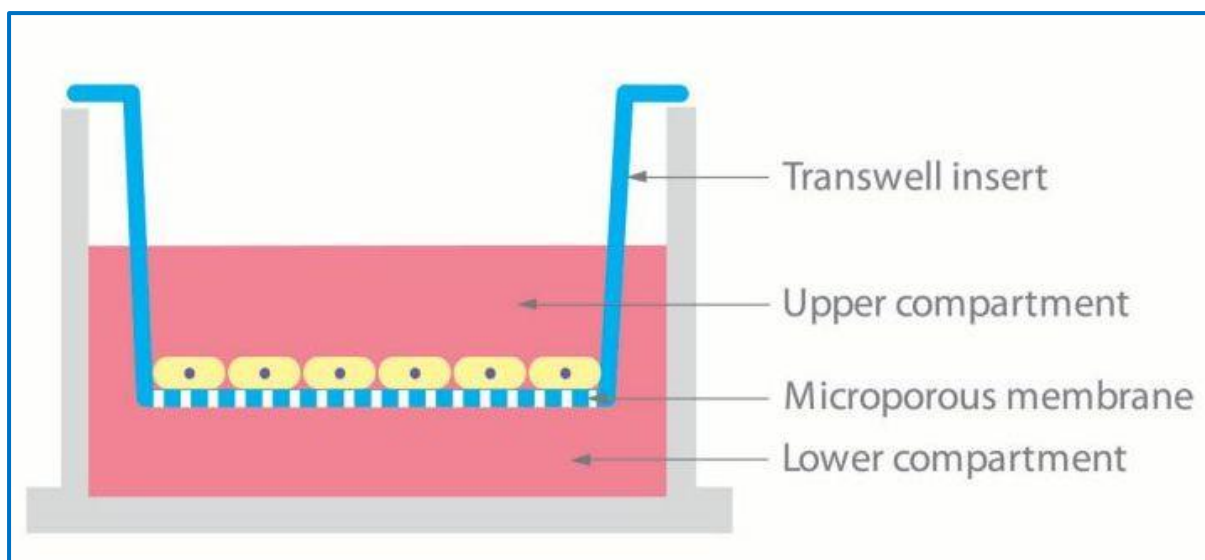


Figure 2.4 Schematic diagram of a transwell set up with inserted cells. The insert has a microporous membrane allowing nutrition medium to freely move between the upper and lower compartment. The cells are seeded on the upper face of the membrane, the drug will be placed on top of the cells (upper part) and the accumulative drug concentration (lower compartment) will be measured as indication of drug permeability through the cells and membrane ²²⁶.

2.2.11 Buccal Film preparation

2.2.11.1 Preparation of polymer solutions

Aqueous solutions of five polymers (HPMC 603, HPMC 606, HPC, PVA low molecular weight) were prepared in concentration of 15% w/v and mixed in several combinations (full details are provided in Chapter 6, section 6.2). The required quantity of each polymer was dispersed into the required volume of DW in a glass bottle using a magnetic stirrer to avoid the powder clumping; however, a very low speed was used to prevent bubble formation (i.e. 150 rpm). The dispersion was mixed until the polymer completely dissolved and a clear solution was obtained. The solution clarity was tested by visual inspection of the poured solution from a metallic spatula. Similarly, solutions of glycerine were prepared by mixing the required weight of glycerine with DW. However, some polymer solutions such as HPC solution was left to stir overnight at 70 °C in order to achieve a clear solution and completely solubilise the polymer. Mixtures of the polymer solutions individually, with and without the plasticiser (i.e. glycerine)

and transfersomes were casted and screened for film producibility (section 6.2). However, before casting, each mixture was blended for 5 minutes using low speed magnetic stirrer.

2.2.11.2 Buccal film casting

The mixture was poured into a glass petri dish (90 x15 mm) slowly to avoid air entrapment. The petri dish was gently tapped and mixed in a circular pattern to ensure the spread of the homogenous mixture. The casting plate was dried in a Technico™ vacuum oven at 65 °C and pressure of 400-600 mbar. After drying to a constant weight (i.e. after 4 h), the film was peeled off the petri dish using a tweezer. The film was stored for further characterisation.

2.2.12 Characterisation of the buccal film

Cast films were sliced into 2cm x 2cm square pieces using a scalpel, where each piece was considered as a final dosage form. Several films from the same casted batch and from several batches were considered for characterisations using a variety of techniques.

2.2.12.1 Weight uniformity and thickness

The weight and thickness of each film was determined. Films were weighed using an analytical balance (Mettler AT400, UK). The thickness of individual film was measured using a digital calliper at 4 cross sections as illustrated in Figure 2.5.

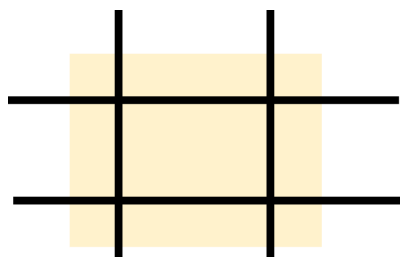


Figure 2.5 Schematic diagram of film thickness measurements.

2.2.12.2 Film content uniformity

The content uniformity of each film was determined by dissolving it completely in 2 mL mixture of MeOH: DW in 1:1 ratio. After complete film solubilisation, HPLC was employed to measure the drug content.

2.2.12.3 Film disintegration

Disintegration time of each film was determined in distilled water at 37 °C using a DTG 1000 disintegration tester (Copley Scientific, UK). The time was recorded when the film began to disintegrate, and when the film completely disintegrated and passed through the wire mesh.

2.2.12.4 Buccal film Morphology

SEM images of the surface and edges of films were obtained by sticking small pieces onto carbon adhesive tape on the top of the stub. Further samples were prepared by hydrating films with 1 mL of DW on a glass slide. Samples of the formed hydrated mass were applied onto the top of the stub and left to dry. All prepared stubs were then visualised by SEM as detailed in Section 2.2.4.4.2.

2.2.12.5 pH measurement of the film surface

Surface pH was evaluated by placing the films into a glass petri dish, adding an aliquot of 1 mL of PBS onto the film surface, and leaving to hydrate for a few minutes. pH value was taken as the average of several readings across the film surface using pH meter (pH 211 microprocessor pH meter, Hanna Instrument, UK). The test was repeated on both faces of the films and from several batches.

2.2.12.6 Drug release from film

The permeation of drug released from the films through tissue samples was determined using the Franz diffusion cell model as reported in Section 2.2.6.1.2. The film was mounted gently in the donor chamber on top of the porcine tissue with the lipid surface facing the tissue and 1 mL of PBS was then added. The experiment was then completed as mentioned in Section 2.2.6.1.2 and the cumulative amount of drug released from the film were plotted against time.

2.2.12.7 Tensile strength properties

Tensile strength testing was performed using a TA-XT-Plus® texture analyser (Texture Analyser, Stable Microsystems, UK). Each film was placed between the tensile grips. The force at break (N) was collected and the tensile strength (N/cm²) was calculated using equation 2.2.

$$\text{Tensile strength (N/cm}^2\text{)} = \frac{\text{Force at break (N)}}{\text{Cross sectional area of sample (cm}^2\text{)}} \quad (2.2)$$

2.2.13 Statistical analysis

All experiments were prepared in triplicates or more and all data are presented as mean values \pm standard deviation (SD). Statistical analyses were performed on the data using one-way ANOVA with Tukey post-test or unpaired t-test analysis employing GraphPad Prism 8 software to determine any significant differences between the studied variables. The level of significance in difference was considered as $p < 0.05$.

Chapter 3. Formulation and optimisation of novel transfersomes

3.1 Introduction

Several advantages offered by buccal mucosa of oral cavity make it an attractive site using non-invasive administration for drug delivery with improved patient compliance when compared to parenteral or oral routes ^{2,227}. There is a clinical need for a long acting topical LA preparation, which could be applied by the patient directly to the buccal region and have sustained release properties that allow maximum local effect with minimum risk of systemic side effects.

There are few licensed LA solution formulations for subcutaneous (SC) infiltration to produce a prolonged effect allowing for a decreased frequency of injection. The prolonged effect is mainly gained by either the addition of a vasoconstrictor e.g. epinephrine, which prevents the leakage of the LA to the blood stream, or through liposomal and lipid-based Depofoam formulations ^{161,228}.

To our knowledge, several attempts have been made to formulate LAs as polymeric or lipid-based microspheres and nanoparticles for injectable or transdermal drug delivery. However, most of these developed systems were not intended for non-injectable oral mucosal administration.

Novel transfersomes loaded with LA such as lidocaine and intended to be a sustained release delivery system for the treatment of oral pain could be a better approach to improve patient compliance and achieve the required level of anaesthesia. However, the properties of drug loaded transfersomes usually vary with several parameters such as the nature and concentration of lipid and EA component, and the preparation process parameters ²²⁹. Although previous studies have attempted to find the optimum composition of transfersomes with some desired properties ²⁰⁴, a new optimisation study was required since both the drug

and sustained release transfersomes have not been reported in the literature to date. Optimisation of properties such as size and entrapment efficiency were essential in order to obtain transfersomes that could produce the required level of anaesthesia without any systemic side effects. Therefore, this chapter aimed to optimise the composition of transfersome using a Taguchi design of experiments (DOE) and lidocaine free-base was chosen as a model LA drug.

Design of experiment is considered a very common method to determine the effect of different parameters on the properties of the delivery system being investigated. DOE approach can vary according to the interacting parameters and all considered factors; there are many DOE approaches such as factorial designs, mixture designs, and Taguchi designs^{230,231}.

Taguchi designs have been proposed to produce a very efficient analysis of mixed parameters using statistical experimental design. It is a combination of mathematical and statistical approaches introduced firstly by Genichi Taguchi²³². It mainly investigates the effect of different parameters on the mean and variance of a process performance property, to define whether the process functions well or not²³³. It is an inexpensive method to examine a large number of variables and parameters but with a reduced number of trials rather than trying all possible combinations of these variables in the case of factorial design. Taguchi design was employed in many studies of dosage forms improvement^{230,231}. To quantify the variation between trials, Taguchi design uses a signal to noise ratio (S/N), in which signal represents the mean value while noise represents the standard deviation. S/N ratio measures the deviation of the response from the desired value^{234,235}. Therefore, applying Taguchi design to optimise

any parameters leads to bring the average quality near to the target value as well as reducing the variation in the quality ^{236,237}.

Thus, the current study optimised the formulation parameters by screening several types of lipid (natural and synthetic), several EAs (surfactants) with different hydrophobic lipophilic balance (HLB) values, and several ratios of lipids to surfactants. Commonly, the more water-soluble lidocaine hydrochloride salt is used for injectable forms, but the free-base is preferable since it exhibits more lipophilic properties. However, in order to use the free-base lidocaine a novel analytical method using high performance liquid chromatography (HPLC) was also developed and validated according to ICH guidelines ²¹⁶ as a reliable and more robust method for quantification of lidocaine in comparison with the usual UV spectrometry method.

3.2 Methods

3.2.1 HPLC Method development and validation

HPLC system was used as reported in section 2.2.4.1, however, to optimise the chromatographic conditions, the effect of several factors was analysed and investigated. These included mobile phase composition, flow rate, and detection wavelength (Table 3.1). The optimised method was then validated according to ICH-guidelines ²¹⁶. A stock solution of lidocaine and a set of diluted standard solutions were prepared. A calibration curve was plotted over the concentration range of 0.1-2 mg/mL. Linearity was evaluated according to the regression value (R^2). Precision was confirmed by proving both repeatability and intermediate precision. Repeatability was assessed using a triplicate sample of 3 different lidocaine concentrations, while the intermediate precision was evaluated over 3 different days. The accuracy was measured by calculating the percent recovery and according to ICH

by proving that the method is precise and linear. The Limit of Detection (LOD) and Limit of Quantification (LOQ) were assessed according to equations (3.1) and (3.2) respectively.

Table 3.1 Parameters used in HPLC method development of lidocaine

Parameters	Value
Mobile phase solution	- 0.01M Phosphate buffer: Acetonitrile (70:30, 50:50, 30:70) - Water: Methanol (30:70,50:50, 70:30) - 0.1M Phosphate buffer: Acetonitrile (30:70)
Detection wavelength	220 - 290 nm
Flow rate	0.5 mL/min, 1 mL/min, 1.5 mL/min

$$LOD = \frac{3.3 \times SD}{S} \quad (3.1)$$

$$LOQ = \frac{10 \times SD}{S} \quad (3.2)$$

Where SD is the standard deviation of the response, and S is the slope of the calibration line.

3.2.2 Design of experiment (DOE)

Taguchi design was employed as a tool to optimise the transfersome formulation parameters. It was used to evaluate the effect of several formulation parameters such as the nature of lipid used (natural or synthetic), the type of surfactant (EA), and the ratio of lipid to surfactant (Table 3.2). The design was constructed using mixed level design (L18 array) with 3 factors, one of them at 2 levels and the other two factors at 3 levels (Table 3.2).

Table 3.2 Taguchi design of experiment including various factors and levels.

Factors (X)	Level		
	1	2	3
Lipid type (X1)	EPC (natural lipid)	DMPC (synthetic lipid)	-
EA (HLB) (X2)	Span 80 (4.3)	Tween 80 (15)	SDC (16)
Lipid:EA (X3)	95:5	75:25	55:45

Minitab® 18.1 software was used to construct the study design, and the selected response variables were studied. The studied variables were transfersome size and entrapment efficiency (%EE). Table 3.3 summarises the composition of Taguchi design transfersome formulations. This design enables identifying and ranking the significant formulation factors that would have an effect on size and %EE.

Table 3.3 . Summary of the composition of each formulation with different types of lipid (SPC, DMPC), EA (Span 80, Tween 80 and SDC) and their ratios (95:5, 75:25 and 55:45 w/w) with each other.

Formulation	X1 (lipid type)	X2 (EA)	X3 (Lipid:EA)
F1	EPC	Span 80	95:5
F2	EPC	Span 80	75:25
F3	EPC	Span 80	55:45
F4	EPC	Tween 80	95:5
F5	EPC	Tween 80	75:25
F6	EPC	Tween 80	55:45
F7	EPC	SDC	95:5
F8	EPC	SDC	75:25
F9	EPC	SDC	55:45
F10	DMPC	Span 80	95:5
F11	DMPC	Span 80	75:25
F12	DMPC	Span 80	55:45
F13	DMPC	Tween 80	95:5
F14	DMPC	Tween 80	75:25
F15	DMPC	Tween 80	55:45
F16	DMPC	SDC	95:5
F17	DMPC	SDC	75:25
F18	DMPC	SDC	55:45

3.2.3 Formulation and characterisation of transfersomes

Preparation of transfersomes was performed as reported in section 2.2.1. Transfersome formulations were prepared using compositions according to Taguchi DOE (Table 3.3). Transfersomes were then characterised as previously mentioned in section 2.2.3.1 for size, PDI, zeta potential, sections 2.2.5 and 2.2.7 for %EE and morphology respectively.

3.3 Results and discussion

3.3.1 HPLC method development

Development of an HPLC method as an accurate method for the analysis of lidocaine free-base was necessary because UV spectrophotometry was the most reported way to quantify the free-base, and all other reported HPLC methods were developed for the analysis of lidocaine HCl²³⁸⁻²⁴². Several methods suggested the use of ACN and PBS as mobile phase components for lidocaine analysis²³⁸⁻²⁴¹. To achieve good peak resolution, the use of a mobile phase with a basic pH has been suggested, while others have proposed the use of MeOH instead of ACN²⁴². Therefore, method optimisation and validation were required in order to improve lidocaine free-base analysis and investigation in formulations. The mobile phase composition, PBS molarity, detection wavelength and flow rate were adjusted to achieve high chromatographic resolution, and short retention time (Rt) of lidocaine free-base. Twenty methods were designed to cover the variables and DAD was used to scan the absorbance over a range of wavelengths (Table 3.4). Upon applying these methods, it was found that some led to chromatograms showing poor peak shapes including broad peaks, fronting and tailing peaks (Table 3.4). Additionally, some methods resulted in a long Rt of lidocaine such as M7, M14 and M16 (11.30, 14.30 and 20.44 min, respectively). Further detection with methods employing slower flow rates (M8, M9, M15, M17, and M18) was not carried out, since a short

run time was the aim of the method development. Among all methods, only three methods (M10, M11, and M12) gave a sharp peak with symmetry more than 0.90 and short retention time of lidocaine. However, M10 with 1.5 mL/min flow rate was excluded as the drug peak occurred immediately after the solvent front. Method M11, employing a mobile phase of 30% PBS (0.01 M) and 70% ACN (% v/v), a flow rate 1 mL/min and a detection wavelength of 255 nm was chosen as it showed the highest peak resolution (Figure 3.1), and absorbance, as well as a reasonable test run time (5 min in total).

3.3.2 HPLC method validation

The validation parameters of the developed method are shown in Table 3.5 and Table 3.6. The data showed good compliance with ICH guidelines ²¹⁶. The analytical method revealed a linear relationship over the concentration range studied (Figure 3.2) and the method was proven to be accurate and precise.

Table 3.4 List of methods tested in the HPLC method development study including different mobile phase composition, flow rate and detection wavelengths, with the obtained results including their *R_t*, symmetry, and shape.

Method	Mobile phase composition (% v/v)	Flow rate (mL/min)	R_t (minutes)	Peak symmetry	Peak shape
M1	Water: MeOH (30:70)	1.5	4.83	0.71	broad and tailing peak
M2	Water: MeOH (30:70)	1	7.23	0.60	broad and tailing peak
M3	Water: MeOH (30:70)	0.5	8.08	0.67	sharp peak
M4	Water: MeOH (50:50)	1.5	8.60	0.43	broad and tailing peak
M5	Water: MeOH (50:50)	1	5.38	0.44	broad and tailing peak
M6	Water: MeOH (50:50)	0.5	3.08	0.58	fronting peak
M7	Water: MeOH (70:30)	1.5	11.30	0.44	broad and tailing peak
M8	Water: MeOH (70:30)	1	-	-	-
M9	Water: MeOH (70:30)	0.5	-	-	-
M10	PBS (0.01M): ACN (30:70)	1.5	1.59	0.90	sharp peak
M11	PBS (0.01M): ACN (30:70)	1	2.84	0.93	sharp peak

Method	Mobile phase composition (% v/v)	Flow rate (mL/min)	Rt (minutes)	Peak symmetry	Peak shape
M12	PBS (0.01M): ACN (30:70)	0.5	4.46	0.95	sharp peak
M13	PBS (0.01M): ACN (50:50)	1.5	3.66	0.71	fronting peak
M14	PBS (0.01M): ACN (50:50)	1	14.30	0.73	fronting peak
M15	PBS (0.01M): ACN (50:50)	0.5	-	-	-
M16	PBS (0.01M): ACN (70:30)	1.5	20.44	0.58	tailing peak
M17	PBS (0.01M): ACN (70:30)	1	-	-	-
M18	PBS (0.01M): ACN (70:30)	0.5	-	-	-
M19	PBS (0.1M): ACN (30:70)	1.5	1.59	0.91	fronting peak
M20	PBS (0.1M): ACN (30:70)	1	2.49	0.79	fronting peak

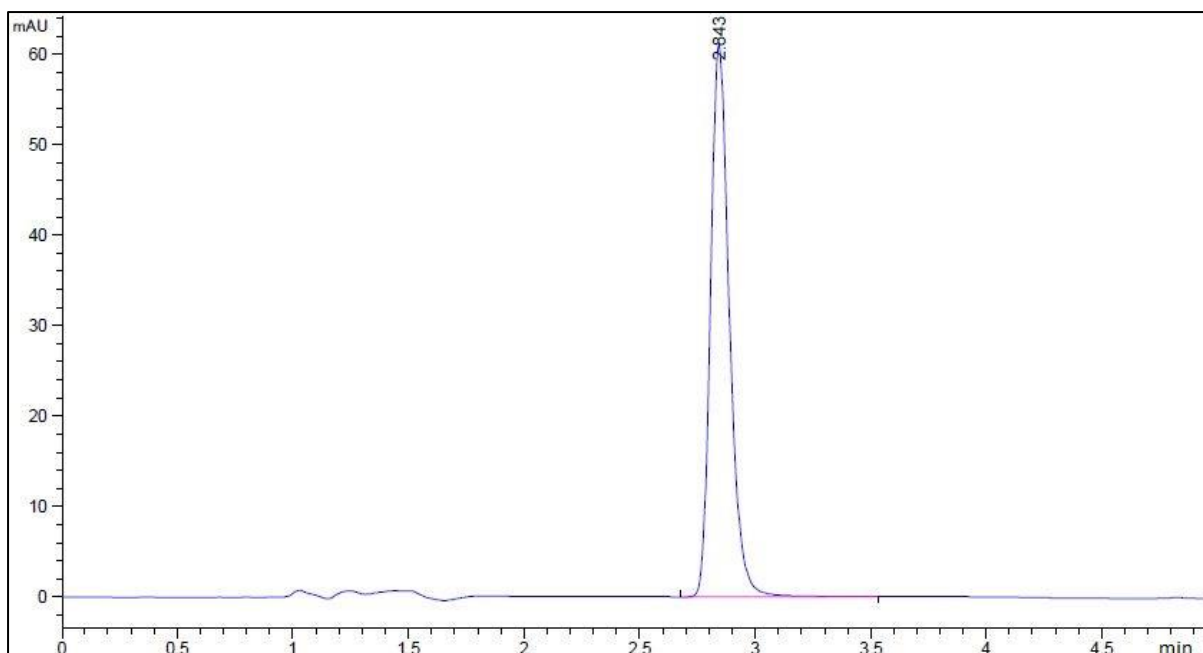


Figure 3.1 Representative lidocaine HPLC chromatogram obtained using method M11.

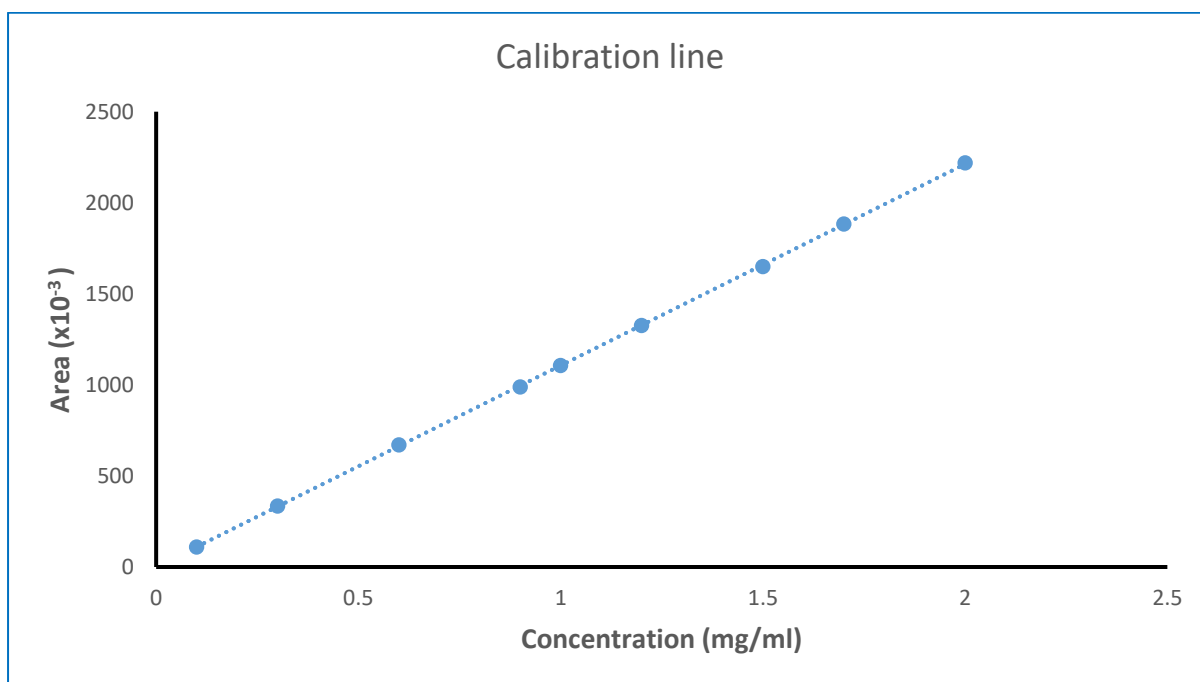


Figure 3.2 HPLC calibration curve over the linear range (0.1-2 mg/ml)

Table 3.5 HPLC method validation parameters of lidocaine free-base.

Parameter	Value
(y= ax ± b)	y= 1106.2x-0.1751
R ²	0.9999
Linearity range	0.1-2 mg/mL
LOD	1.55x10 ⁻⁰⁷ mg/mL
LOQ	4.72x10 ⁻⁰⁷ mg/mL

Table 3.6 Accuracy and precision (intermediate precision and repeatability).

Initial Concentration (mg/mL)	Day 1		Day 2		Day 3	
	Accuracy (%)	RSD (%)	Accuracy (%)	RSD (%)	Accuracy (%)	RSD (%)
0.2	100.43	0.08	97.60	0.06	97.70	0.09
0.4	99.56	0.05	97.95	0.01	96.93	0.09
0.7	100.95	0.10	98.52	0.12	98.48	0.10

3.3.3 Transfersome preparation and characterisation

Taguchi design was used to determine the best formulation combination to achieve transfersomes with the minimum size and the highest %EE. The choice of design parameters was determined by previously reported studies. The type of phospholipids used has been investigated in several studies and has been reported to produce liposomal vesicles with different properties²⁴³. Therefore, natural and synthetic phospholipids (EPC and DMPC) were investigated. Additionally, as introduced in Sections 1.2.2.1 and 1.2.2.2, it was reported that the surfactant type and concentration can also affect transfersome size and %EE²²⁹. It was believed that surfactant at high concentration could cover the surfaces of the transfersomes and therefore prevented them from aggregation^{91,92}. Moreover, higher surfactant

concentration was suggested to enhance the size distribution due to reducing interfacial tension and producing a homogeneous emulsion^{91,92}. However, the effect of surfactant concentration on transfersomes drug entrapment varied as the drug lipophilicity change, because surfactant has a high tendency to interact with the lipid, which could compete with drug loading within the bilayer^{105,110,111}. For example, dexamethasone (a model lipophilic drug) loaded-transfersomes were prepared to evaluate SDC, Tween 80 and Span 80 as edge activators several concentrations⁶⁰. The study revealed that encapsulation efficiency decreased as the concentration of the surfactant increased. On the other hand, few studies have reported that increasing surfactant concentration will increase the number of vesicles formed, which in turn leads to a higher volume of the hydrophobic bilayer domain available to house a hydrophobic drug^{101,112,113}.

For this reason, three surfactants (EA) were used in this DOE in three different percentages (Table 3.2). Lidocaine-loaded transfersomes were prepared according to the designed experiments (Table 3.3). Transfersomes were then characterised and Table 3.7 summarises all the results.

Transfersomes obtained by running the 18 experiments showed sizes below 208.70 ± 4.66 nm with consistent PDI, except two samples (F3 and F18), where transfersome sizes were unexpectedly large (515.35 ± 4.45 nm and 671 ± 15.13 nm respectively). Larger transfersomes may have been formed in these cases due to the high level of surfactant that was used, as it was previously reported that increased liposome size resulted from the presence of surfactant molecules situated within the lipid bilayer in a way that increased its diameter²⁴⁴.

Table 3.7 Transfersome formulation (F1-F18) characterisation results; size, polydispersity index (PDI), zeta potential, and entrapment efficiency (%EE), n=3 ±SD.

Formulation	Size (nm)	PDI	ZP (mV)	EE (%)
F1	188.60 ± 9.33	0.18 ± 0.02	-4.66 ± 1.42	44.26 ± 2.61
F2	208.70 ± 4.66	0.25 ± 0.03	-4.56 ± 0.29	51.73 ± 1.51
F3	515.35 ± 4.45	0.29 ± 0.12	-7.49 ± 0.84	53.87 ± 5.73
F4	181.05 ± 11.66	0.18 ± 0.03	-3.14 ± 0.21	45.82 ± 3.98
F5	146.95 ± 0.63	0.22 ± 0.02	-2.15 ± 1.20	49.83 ± 2.07
F6	121.15 ± 1.34	0.22 ± 0.04	-2.77 ± 0.05	50.19 ± 2.02
F7	195.95 ± 7.28	0.14 ± 0.00	-6.86 ± 1.16	53.05 ± 0.62
F8	98.93 ± 2.07	0.14 ± 0.01	-17.10 ± 0.28	54.55 ± 1.05
F9	134.85 ± 12.51	0.26 ± 0.03	-21.70 ± 0.28	56.97 ± 0.18
F10	188.00 ± 22.06	0.13 ± 0.00	-1.28 ± 1.33	50.76 ± 0.72
F11	200.35 ± 19.02	0.21 ± 0.01	-3.25 ± 0.34	48.93 ± 4.12
F12	194.30 ± 15.41	0.15 ± 0.00	-4.65 ± 0.03	53.07 ± 4.44
F13	171.15 ± 3.18	0.19 ± 0.00	-0.48 ± 0.76	52.96 ± 4.44
F14	96.92 ± 16.37	0.17 ± 0.01	-1.15 ± 1.17	50.67 ± 0.21
F15	116.00 ± 6.64	0.19 ± 0.01	3.94 ± 2.12	50.80 ± 1.22

Formulation	Size (nm)	PDI	ZP (mV)	EE (%)
F16	153.70 ± 28.28	0.15 ± 0.01	-3.60 ± 0.57	50.93 ± 2.07
F17	146.05 ± 0.35	0.30 ± 0.02	-13.20 ± 1.27	52.63 ± 0.12
F18	671.00 ± 15.13	0.59 ± 0.16	-18.65 ± 1.62	55.72 ± 7.33

Additionally, the %EE results obtained from all 18 formulations ranged from 44.26% (F 1) to 56.97% (F 9). Statistical analysis of the obtained data was performed. The %EE results of all 18 formulations showed no significant differences ($P > 0.05$). The low encapsulation efficiency was suggested to be related to the size of transfersome. As the drug has lipophilic properties (Log P of 2.44), it should be entrapped within the lipid bilayer, however, the small size does not offer enough space within the bilayer for large amount of drug to accommodate. Higher entrapment would be expected with micron-sized transfersomes²⁰⁴, however, nanosized transfersomes are preferable for any route of delivery, including buccal^{2,227}, transdermal^{245,246} and parenteral²⁴⁷. It is claimed that both the nanosize (less than 200 nm and consistent PDI in range of 0.1-0.2) and the deformability of transfersomes are the key characteristics for enhanced tissue permeation when administered topically (i.e. buccal)^{245,247,248}. In contrast, statistical analysis of transfersome size showed a considerable variation (Figure 3.3). There was a significant difference in size between most samples that included 5% and 25% EA in comparison to 45%, with P values of either $*P < 0.05$ or $***P < 0.001$ (Figure 3.3 A, B C, E and F). A small but significant difference (with $P < 0.05$) was also noted between samples that included EA of 5% in comparison to samples that had 25% EA (Figure 3.3 A, B, E, and F).

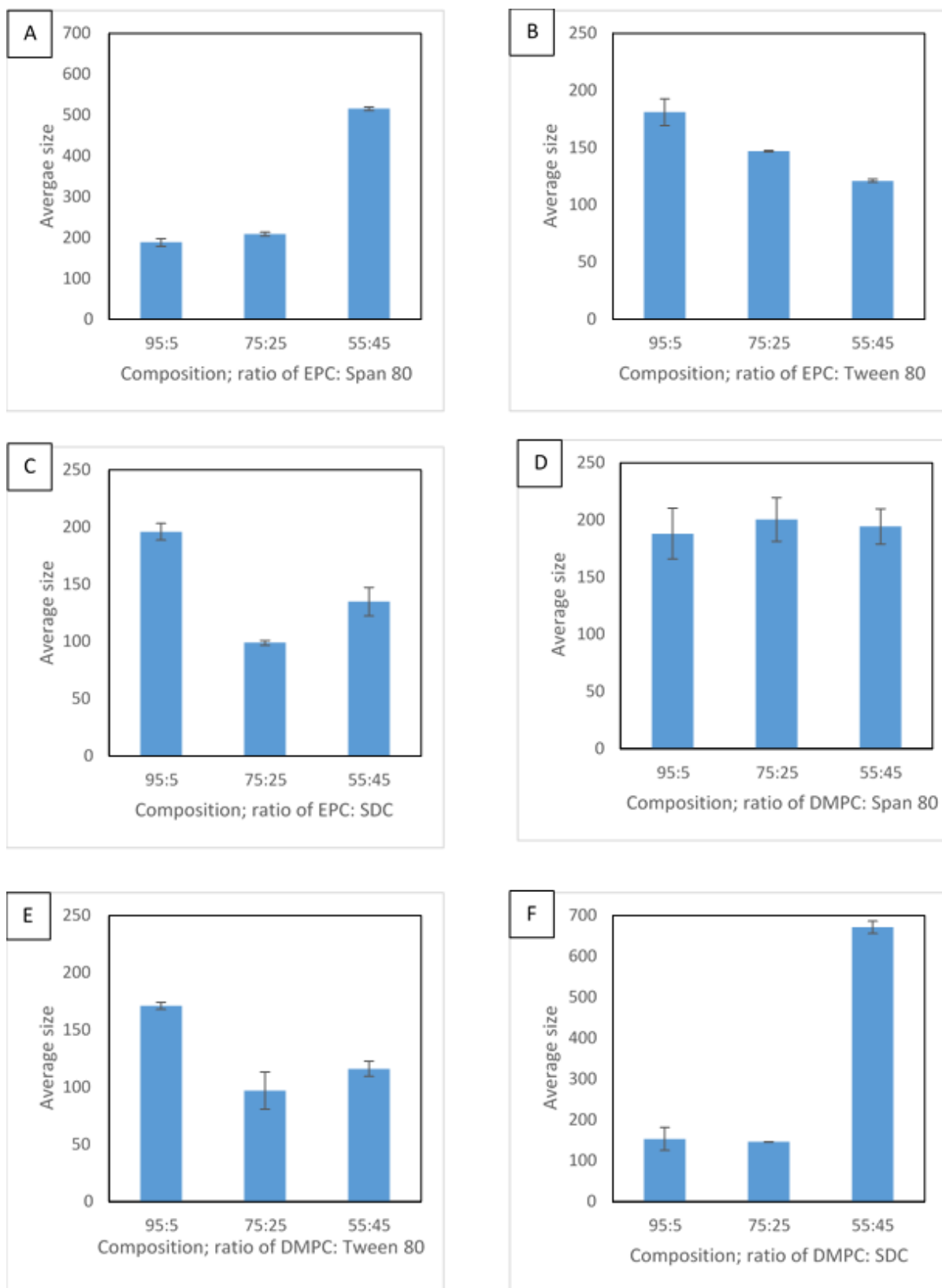


Figure 3.3 Graphical representation of transfersomes size of all 18 formulations, $n=3$, mean values \pm SD.

The results were analysed using Taguchi analysis in Minitab® 18 software, in which the variation of the response was studied using signal to noise (S/N) ratio. S/N ratio is a quality analytical parameter, which is useful to determine the best level of each experimental parameter. The type of S/N ratio is selected depends on the desired characteristic. A larger S/N ratio was considered desirable for the analysis of the %EE results, as a high level of drug entrapment is desirable. However, because there was not a significant difference between the %EE results of the 18 formulations, the Taguchi analysis was carried out considering only transfersome size. In this case, a small S/N ratio was considered desirable for the analysis, as smaller transfersome size is preferable (Table 3.8). The analysis enabled ranking the studied parameters in accordance with the magnitude of their effect on the size of transfersomes. Both the type of surfactant and its concentration were clearly observed to be the most significant factors affecting transfersome sizes (Table 3.8). Additionally, samples that were prepared with Tween 80 showed the smallest size, followed by SDC and Span 80 (Figure 3.4). Furthermore, it was also found that the employed concentration of the EA has a noticeable effect on transfersome size, since increasing the concentration from 5% to 25% clearly resulted in a size reduction. However, further increment of surfactant concentration up to 45% showed a contrasting effect (Figure 3.4). Transfersome sizes were increased in formulations with a high surfactant concentration as a result of the molecular repulsion that possibly occurred between the surfactant and phospholipid molecules within transfersome bilayers ^{229,244}. Additionally, the analysis also showed that the use of either natural or synthetic phospholipids had no significant effect on the size of transfersomes and their ability to entrap drug.

Table 3.8 Response table for Signal to Noise ratios (S/N), showing the rank of the factors X1, X2 and X3 as they affect transfersome size.

Level	X1	X2	X3
1	-45.03	-47.24	-45.07
2	-45.52	-42.74	-43.12
3	-	-45.84	-47.64
Delta	0.49	4.50	4.52
Rank	3	2	1

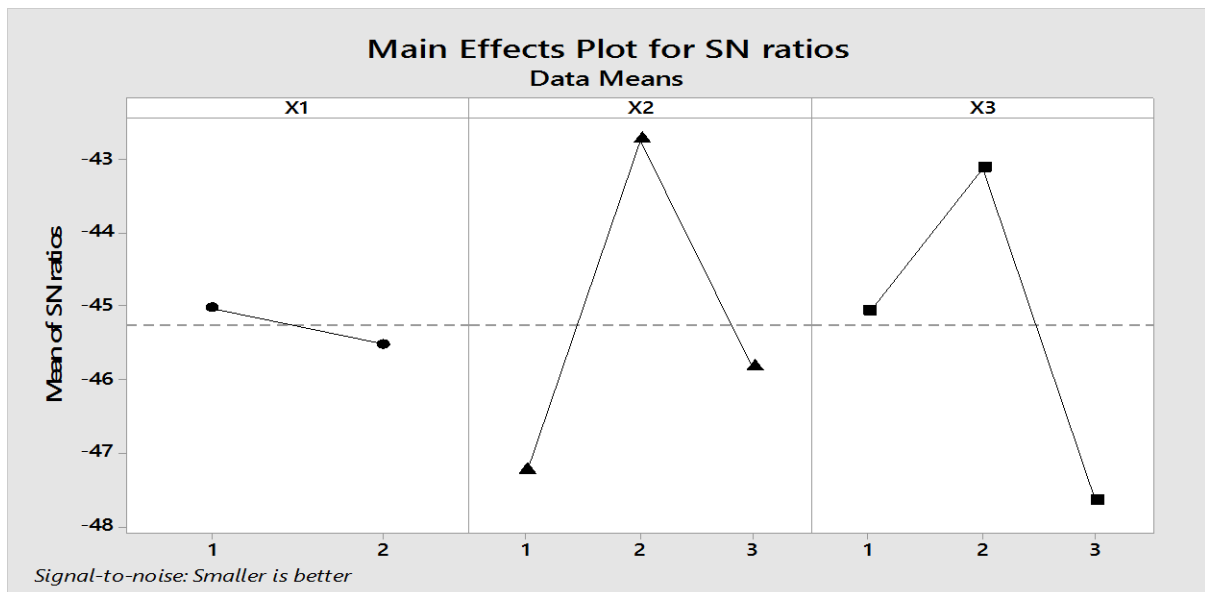


Figure 3.4 Effect of studied parameters using the mean of S/N ratios.

3.3.3.1 Zeta potential

Zeta potential is a parameter that is related to the surface charge, which is a property that any material may acquire in a colloidal solution. Transfersomes (or any particles) have a charge on the surface that will attract a thin layer of counter ions, this layer of ions moves with the particle as they diffuse throughout the solution. Zeta potential is the electrical potential at the boundary of this layer ²⁴⁹. Measuring zeta potential of the obtained transfersomes was crucial to understand if it could induce interactions, toxicity, and since they are intended to be delivered through the buccal cavity that is covered with negatively

charged mucus. Not only that, but measuring the zeta potential of transfersomes is important to assess their surface properties, as it could have a critical effect on their stability by either creating repulsive forces or agglomeration^{94,129}. A large zeta potential value (either positive or negative) usually indicates good physical stability due to electrostatic repulsion of individual particles. On the other hand, a very small value can result in particle aggregation and flocculation due to the development of van der Waals forces. However, zeta potential value will be influenced by many factors such as the material properties, the presence of surfactant and the general suspension chemistry^{249,250}. Therefore, the net charge on transfersome surfaces was suggested to be the combination of both the used phospholipid and surfactant charge. Surfactant type and concentration was reported to greatly affect the transfersomes' zeta potential. For example between several types of surfactant-based transfersomes, cholate-based transfersomes showed the highest negative zeta potential value, and the concentration of the surfactant increased, the net charge of the transfersomes increased as well¹²⁹.

Similarly, the results of Table 3.7 revealed that all prepared transfersomes hold a negative charge, which represents the net surface charge of both the phospholipid and surfactant character²⁵¹. Both EPC and DMPC are zwitterionic compounds with an isoelectric point of 6-7, meaning that at the current experimental conditions (pH = 7.4) they hold a net negative charge. Moreover, samples that were prepared using SDC (F7, F8, F9, F16, F17, and F18) were observed to carry a higher negative charge than Tween 80 and Span 80 based samples. Additionally, the negative charge increased dramatically from -6.86 mV up to -21.70 mV as the SDC concentration increased from 5% (formulation F7) to 45% (F9). Similarly, it increased from -3.60 mV to -18.65 mV in formulations F16 to F18, which was in good agreement with the literature since the surfactant concentration affects the final charge of the lipid vesicles

⁹⁴. However, preparing negatively charged transfersomes was believed to enhance their dispersity and stability, as that would prevent the aggregation and provide long-term stability due to electrostatic repulsion ²⁵²⁻²⁵⁴. Although, possessing a negative charge might repel with the negatively charged mucus, which could be considered a barrier for delivery, but it was reported that negatively charged nanoparticle can form hydrophobic adhesive interactions with mucus network ¹⁵. Surprisingly, it was also reported that negatively charged delivery systems could show enhanced permeability as they won't get entrapped within the mucus networks ²⁵⁵.

3.3.3.2 Transfersome morphology

The morphology of lidocaine loaded transfersomes was observed using TEM and SEM (Figure 3.5). Both TEM and SEM images confirmed that transfersomes displayed a uniform, spherical shape. It was clearly observed with TEM images that transfersomes have an intact bilayer membrane and unilamellar bilayer structure. Transfersomes were effectively achieved and they were found to be approximately 200 nm in size.

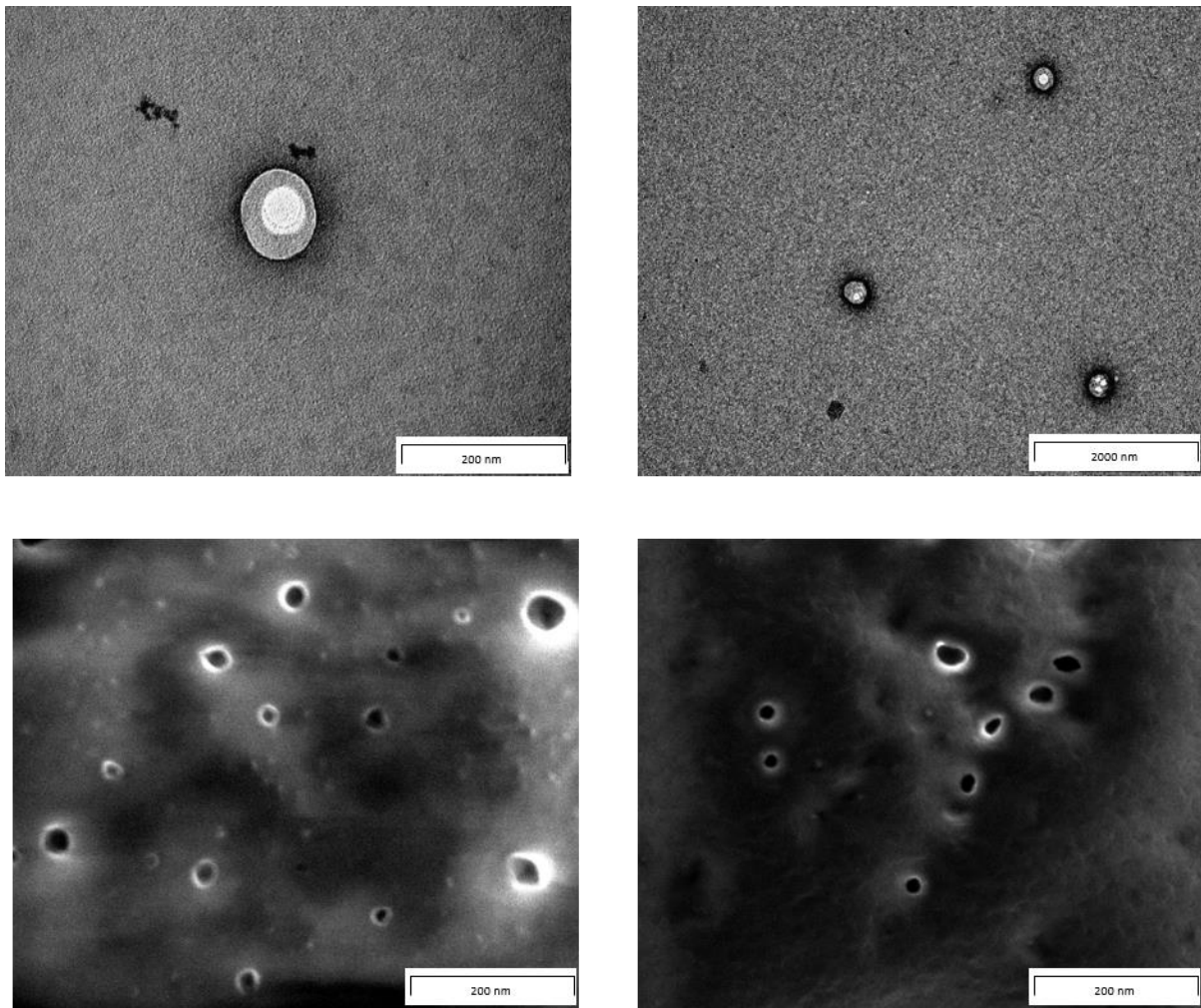


Figure 3.5 Transfersomes morphology, TEM images (top), and SEM images (bottom) of transfersomes.

3.3.3.3 *In vitro* release

According to the optimisation study results, 6 samples were selected for the *in vitro*-release study. As the Lipid: EA ratio had the major effect on the transfersomes properties, the samples were chosen from the ratio that gave the desired properties, which was 75:25 of lipid: EA (Table 3.8). Although the lipid type did not show a significant effect ($p > 0.05$) from the optimisation results. The selected 6 samples were prepared using both lipids; EPC (F2, F5, and F8) and DMPC (F11, F14, and F17) in order to check their effect on the release profile. However, as the EA type was the second important factor to produce the desired transfersomes all 3 EA were considered in the selection of samples (Table 3.7)

The release profile of the 6 samples in addition to a control of free drug was studied over 24 hours. The cumulative amount of drug released was calculated for each formulation. The release profile of the control sample (free drug) revealed that 96% drug amount passed across the dialysis membrane between 1-3 hours, while all 6 transfersome samples showed complete drug release at 24h (Figure 3.6Figure 3.6). Transfersomes samples that were prepared by EPC not only showed sustained release of lidocaine but also a delayed release, with < 2% drug released after 1h (F2, F5, and F8), but subsequently almost 60% after 3h. DMPC-based transfersomes showed between 5-21% drug release after 1h. The release profiles of the six formulations proved that transfersomes were successfully optimised and prepared to sustain the release of lidocaine over 24h. Moreover, it is a promising system to deliver LA with a reduced frequency of administration. That in turn would reduce side effects and enhance the pain management (both acute and chronic) ^{161,256}.

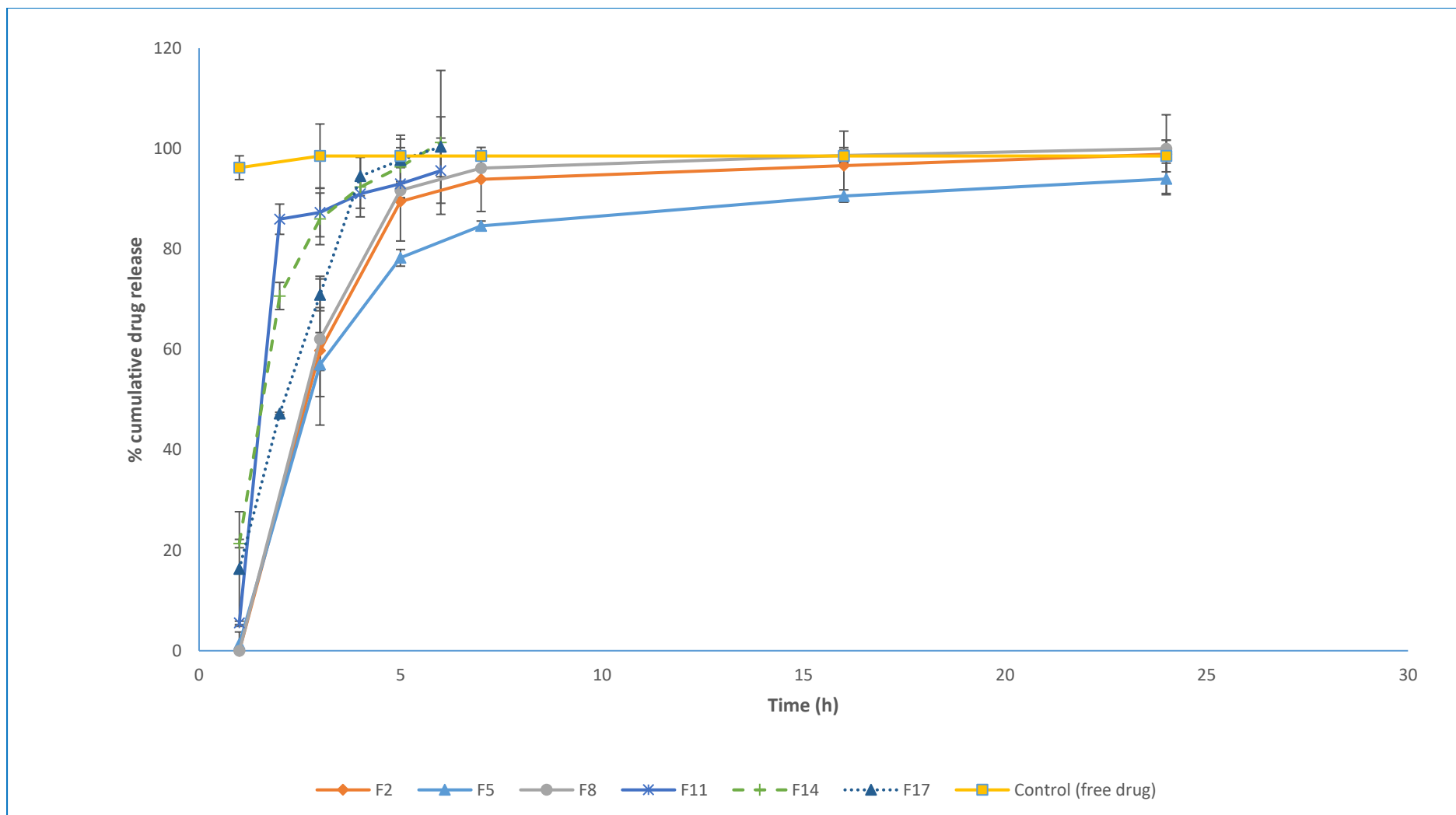


Figure 3.6 Release profile of lidocaine permeated across dialysis bag from 6 different transfersomes formulations versus the free drug (control) over 24h, n=3 ±SD

3.4 Conclusion

In this chapter, transfersomes were optimised to develop a sustained release delivery system of lidocaine. They were formulated using a simple lipid film hydration method. Preparation parameters were optimised using a Taguchi DOE in terms of phospholipid type, type of EA and ratio of phospholipid to EA. Transfersomes were characterised for size, PDI, charge, and %EE. The obtained transfersomes were approximately 200 nm in size with $PDI \leq 0.3$. To determine the entrapment efficiency, a new HPLC method for lidocaine was optimised and validated according to ICH guidelines. The proposed method was validated for linearity, accuracy, sensitivity, intermediate precision and repeatability, and was shown to be valid for the analysis of lidocaine free-base according to ICH guidelines. The calculated %EE varied as the formulation parameters changed, but was generally between 44-56%. Analysing the data obtained by Taguchi DOE showed that the effect of formulation factors on both size and %EE were in the following rank order: lipid: EA ratio >EA type >lipid type. The type of lipid (natural or synthetic) showed no significant effect on transfersome size. Increasing the EA concentration up to 25% resulted in a reduction in transfersomes size; however, with a further increase in EA, transfersome size was seen to increase. Transfersome samples were selected based on the analysis of the optimisation results, and their release profiles were assessed. All 6 samples proved that the optimised transfersomes can be used as a sustained release delivery system of LA as they released lidocaine slowly over 24h in contrast to the free drug that showed complete drug release by 1 hour. These samples were employed for further development and testing, such as ex-vivo release and permeability profile.

**Chapter 4. Transfersomes coating with mucoadhesive
polymer**

4.1 Introduction

The ability to deliver drugs locally into the smooth surface of the buccal mucosa for particular applications such as treatment of oral pain (i.e. by delivering LA or analgesic agents), or treating bacterial infections could be among the advantages compared to other routes of administration. However, among the limitations of local administration to buccal region is the continuous secretion of saliva^{257,258}. Therefore, to overcome this obstacle, many efforts have been made to develop mucoadhesive agents over the years^{41,258}. In this study, a simple approach was adopted to modify transdermal surfaces by coating with mucoadhesive polymer, which could enhance the residence time and improve transdermal stability^{253,259-261}.

Several classes of polymers have been investigated in order to achieve the required mucoadhesive properties. It was suggested that mucoadhesive properties could be achieved by one or a combination of the following methods: adsorption, diffusion, electronic, fracture, and wetting. Although, the mechanism of polymer attachment to the mucosal surface is not fully understood, some theories of mucoadhesion have been reported to explain it. Physical attachments, chemical interaction such as electrostatic, hydrophobic, hydrogen bonding and van der Waal's interactions are all among the theories to explain mucoadhesion^{41,262,263}.

For example, it was suggested that cellulose derivatives such as methylcellulose or hydroxypropylmethylcellulose have been used for their mucoadhesive properties as they exhibit hydrogel forming properties²⁶⁴. While polysaccharide derivatives such as chitosan are believed to have mucoadhesive properties due to its positive charge²⁶⁵⁻²⁶⁷, which could be attracted to the negatively charge mucosa. As the mucosal surface is covered with a mucus

layer, which contains negatively charged mucins as a major component, it holds a negative charge at physiological pH ²⁵⁸.

Furthermore, there are many factors affecting the mucoadhesive properties of the polymers such as its molecular weight, flexibility, charge, concentration and swelling properties ²⁶⁴. It was also suggested that polymers with MW larger than 100,000 exhibit higher mucoadhesive strength ²⁶⁰. Additionally, polymers that contain a substantial degree of flexibility could show better entanglement and greater diffusion into the mucus network ²⁶³. While non-ionic or anionic polymers appear to have low mucoadhesive properties, polymers with cationic charges show superior adhesion in neutral and alkaline environment ^{268,269}. Not only does the polymer ability to swell enhance the mechanical attachment with the mucus mesh, but it was also suggested that polymer swelling could expose the mucoadhesive sites for hydrogen bonding or electrostatic interaction with the mucus network ²⁷⁰. However, it was believed that optimum mucoadhesion could be achieved at a critical degree of polymer swelling ²⁷¹. Another critical factor to consider is the polymer concentration, as it was reported that higher concentrations could result in a longer chain to penetrate through the mucus network and attain better adhesion. Still, for each polymer there is a critical concentration beyond which it will produce a coiled structure and lose its mucoadhesive properties ^{271,272}.

It is believed that incorporation of such mucoadhesive polymers into the delivery system would prolong their residence time at the administration site (i.e. the buccal cavity) ²⁷³. Therefore, coating transfersomes with a mucoadhesive polymer was introduced with the purpose of extending their residence time in the buccal epithelia and overcome the continuous flushing by saliva which was reported to be approximately 0.3-0.4 mL/min ²⁷⁴. The polymers chosen were the most frequently reported to produce good mucoadhesive

properties such as HPMC and chitosan ²⁷⁵⁻²⁷⁷. However, the aim was to develop coated transfersomes that retain the nanosize and good drug encapsulation properties as well as sustained drug release rate. Therefore, several factors such as polymer MW and concentration were considered. Chitosan HCl and two different viscosity grades of HPMC (4000 and 15000) were used individually and 5 different concentrations of these 3 polymers were coated over transfersomes and further characterised.

4.2 Method

Three different water-soluble polymers (HPMC K4M, HPMC K15M or chitosan HCl) were prepared by weighing the required amount of the polymer and dispersing in the required volume of DW in a glass bottle using a magnetic stirrer. All polymers were left to stir until clear solutions were obtained. Five different concentrations were prepared from all tested polymers 0.1, 0.2, 0.3, 0.4, and 0.6% w/v. Transfersome coating was then performed as detailed in section 2.2.2. Coated transfersomes were then subject to further characterisation such as size, PDI, %EE, mucoadhesive and release study sections 2.2.3.1, 2.2.5 and 2.2.6).

4.3 Results and discussion

The selection of the coating polymers was based on their reported mucoadhesive properties ^{278,279}. It was reported that the mechanism of coating of the polymer to lipid-based vesicles, including liposomes or transfersomes, mainly depended on the attraction of the hydrophobic segment of the polymer chain to the lipophilic bilayer of the liposomes ^{207,280}. It was also suggested that some hydrogen bonding may occur between the phospholipid hydrophilic head groups and the polysaccharide ²⁸¹.

4.3.1 Coated transfersomes characterisation

4.3.1.1 Size and PDI of the coated formulations

All prepared samples were characterised after coating with different polymers for their size and PDI. Coated transfersomes showed significant increase in the size and PDI in comparison with the original size of the uncoated transfersomes (Table 4.1, Table 4.2 and Table 4.3) and (Figure 4.1, Figure 4.2 and Figure 4.3). The substantial increase in the transfersomes size confirms the successful coating of transfersomes with the three different polymers. The size of transfersomes coated with HPMC K4M sharply increased in almost all samples (Table 4.1); the size of transfersomes increased significantly with increasing concentration of the polymeric solution. For instance, transfersomes size of formulation F5, F8, and F11 increased gradually with increasing HPMC K4M concentration from 0.1% to 0.6%, The PDI also showed unimodal distribution with a dramatic increment from 0.2 to 0.9 after coating with concentrations of 0.1% and 0.6% respectively. This could confirm the ability to form coating layers that may increase in thickness with increasing polymeric solution concentration. Additionally, coating with higher concentration of the polymeric solution (i.e. higher viscosity) resulted in PDI \sim 0.9 in all formulations. Similarly It was noted that the transfersomes size of formulation F2 jumped from 208 nm when uncoated to micron sized (with PDI \sim 0.7) after coating with 0.1% solution, with a further increase to more than 5 μ m (PDI \sim 0.9) after coating with 0.6% solution. This could be explained by not only the formation of thick coating layers but also due to particle aggregation that could occur between the coated transfersomes as a result of electrostatic adhesion ²⁸².

Table 4.1 Results of HPMC K4M coated transfersomes characterisation for size, PDI, and %EE, n=3, mean values \pm SD, stars are to flag levels of significant differences compared to uncoated (*, ** and *** represents $P<0.05$, $P<0.01$ and $P<0.001$ respectively).

Sample	Uncoated		0.1% w/v		0.2% w/v		0.3% w/v		0.4% w/v		0.6% w/v	
	Size (nm)	PDI	Size (nm)	PDI	Size (nm)	PDI	Size (nm)	PDI	Size (nm)	PDI	Size (nm)	PDI
F2	208.7 ± 4.66	0.25 ± 0.03	1012.23 ± 0.69 ***	0.75 ± 0.06	3862.91 ± 16.10 ***	0.98 ± 0.01	3623.90 ± 59.15 ***	0.98 ± 0.02	3862.65 ± 15.30 ***	0.98 ± 0.02	5852.38 ± 43.21 ***	0.83 ± 0.07
F5	146.95 ± 0.63	0.22 ± 0.02	162.7 ± 2.35 ***	0.22 ± 0.05	206.71 ± 1.80 ***	0.24 ± 0.04	225.74 ± 4.31 ***	0.36 ± 0.02	224.74 ± 4.49 ***	0.27 ± 0.01	382.03 ± 2.85 ***	0.99 ± 0.00
F8	98.93 ± 2.07	0.14 ± 0.01	135.84 ± 0.47 ***	0.32 ± 0.03	161.18 ± 1.76 ***	0.31 ± 0.00	330.48 ± 22.50 ***	0.65 ± 0.04	371.55 ± 7.00 ***	0.38 ± 0.01	466.97 ± 1.19 ***	0.93 ± 0.05
F11	200.35 ± 19.02	0.21 ± 0.01	195.23 ± 3.00 ns	0.22 ± 0.01	207.58 ± 1.51 ns	0.22 ± 0.01	262.72 ± 4.05 ***	0.42 ± 0.01	331.71 ± 4.11 ***	0.84 ± 0.03	565.78 ± 7.08 ***	0.98 ± 0.01
F14	96.92 ± 16.37	0.17 ± 0.01	707.02 ± 0.83 ***	0.98 ± 0.02	1340.25 ± 16.13 ***	0.97 ± 0.03	2776.22 ± 14.44 ***	0.95 ± 0.04	9679.08 ± 27.36 ***	0.99 ± 0.01	8567.61 ± 11.81 ***	0.89 ± 0.04
F17	146.05 ± 0.35	0.3 ± 0.02	634.31 ± 10.59 ***	0.90 ± 0.05	667.94 ± 11.82 ***	0.52 ± 0.03	2560.40 ± 37.32 ***	0.27 ± 0.00	9368.38 ± 25.65 ***	0.67 ± 0.01	784.80 ± 6.90 ***	0.93 ± 0.04

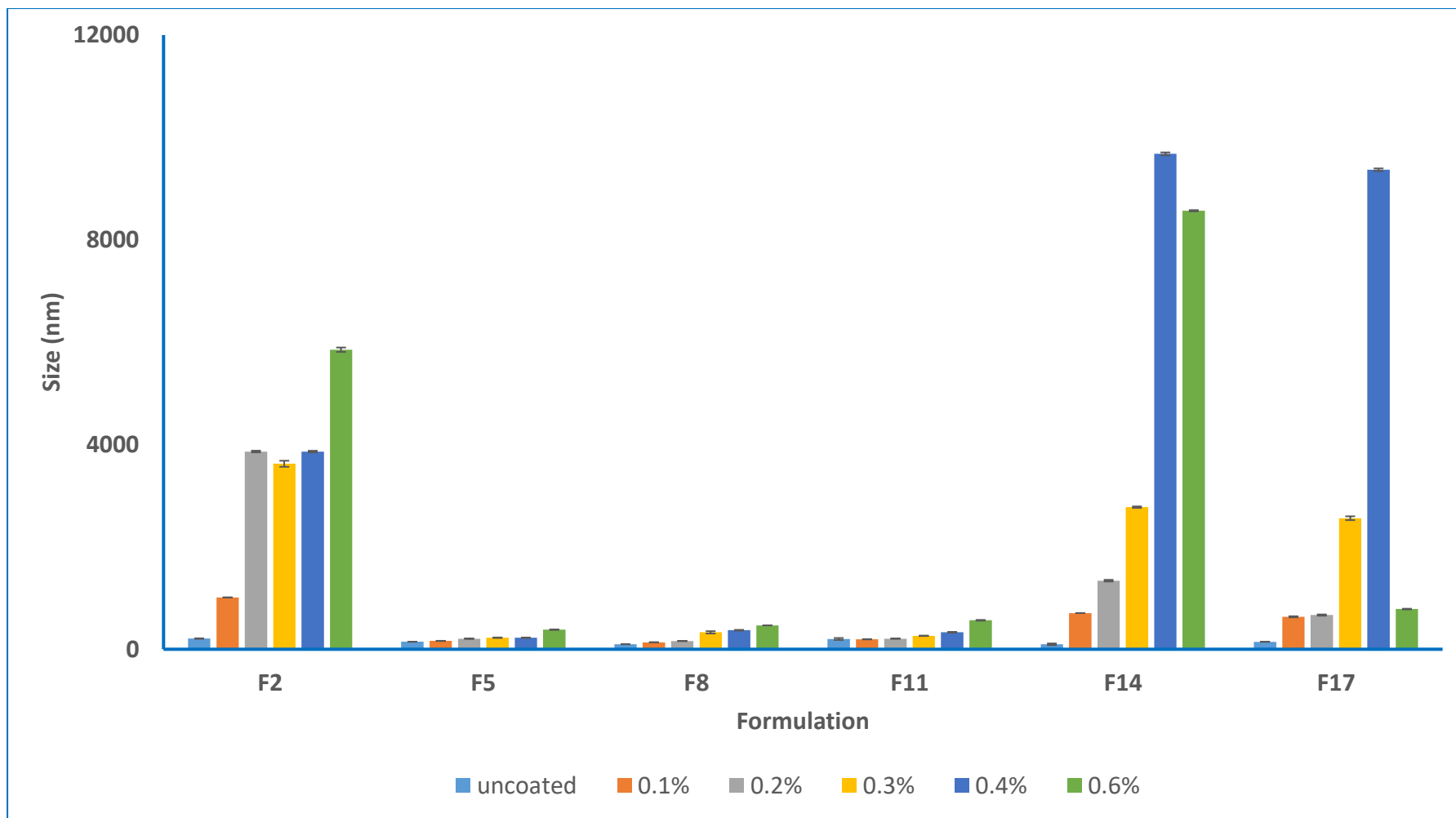


Figure 4.1 Results of HPMC K4M coated transfersomes characterisation for size, n=3, mean values \pm SD.

Table 4.2 Results of HPMC K15M coated transfersomes characterisation for size, PDI, and %EE n=3, mean values \pm SD, stars are to flag levels of significant differences compared to uncoated (*, ** and *** represents $P<0.05$, $P<0.01$ and $P<0.001$ respectively).

Sample	Uncoated		0.1% w/v		0.2% w/v		0.3% w/v		0.4% w/v		0.6% w/v	
	Size (nm)	PDI	Size (nm)	PDI	Size (nm)	PDI	Size (nm)	PDI	Size (nm)	PDI	Size (nm)	PDI
F2	208.7 ± 4.66	0.25 ± 0.03	1727.75 ± 5.44 ***	0.99 ± 0.01	2122.18 ± 5.72 ***	0.99 ± 0.01	3645.42 ± 7.80 ***	0.99 ± 0.01	2656.1 ± 3.67 ***	0.99 ± 0.01	3563.36 ± 5.12 ***	0.98 ± 0.01
F5	146.95 ± 0.63	0.22 ± 0.02	161.31 ± 4.47 **	0.26 ± 0.04	269.94 ± 4.23 ***	0.37 ± 0.01	267.31 ± 2.40 ***	0.56 ± 0.01	226.54 ± 3.37 ***	0.45 ± 0.01	287.11 ± 2.66 ***	0.94 ± 0.04
F8	98.93 ± 2.07	0.14 ± 0.01	205.59 ± 3.40 ***	0.48 ± 0.01	172.86 ± 6.90 ***	0.43 ± 0.04	199.92 ± 1.37 ***	0.44 ± 0.03	193.36 ± 5.13 ***	0.45 ± 0.03	479.89 ± 1.69 ***	0.65 ± 0.03
F11	200.35 ± 19.02	0.21 ± 0.01	191.81 ± 5.76 ns	0.17 ± 0.00	233.75 ± 4.96 ***	0.28 ± 0.01	360.69 ± 1.31 ***	0.55 ± 0.03	514.45 ± 2.35 ***	0.93 ± 0.04	931.97 ± 3.11 ***	0.93 ± 0.04
F14	96.92 ± 16.37	0.17 ± 0.01	402.98 ± 5.12 ***	0.28 ± 0.00	494.71 ± 7.06 ***	0.96 ± 0.05	1141.22 ± 5.45 ***	0.91 ± 0.03	2356.26 ± 6.39 ***	0.99 ± 0.00	6988.23 ± 2.80 ***	0.98 ± 0.02
F17	146.05 ± 0.35	0.3 \pm 0.02	1643.68 ± 10.33 ***	0.98 ± 0.01	2076.22 ± 4.91 ***	0.85 ± 0.05	2264.83 ± 3.65 ***	0.99 ± 0.01	2696.75 ± 6.51 ***	0.96 ± 0.06	3051.56 ± 14.24 ***	0.98 ± 0.01

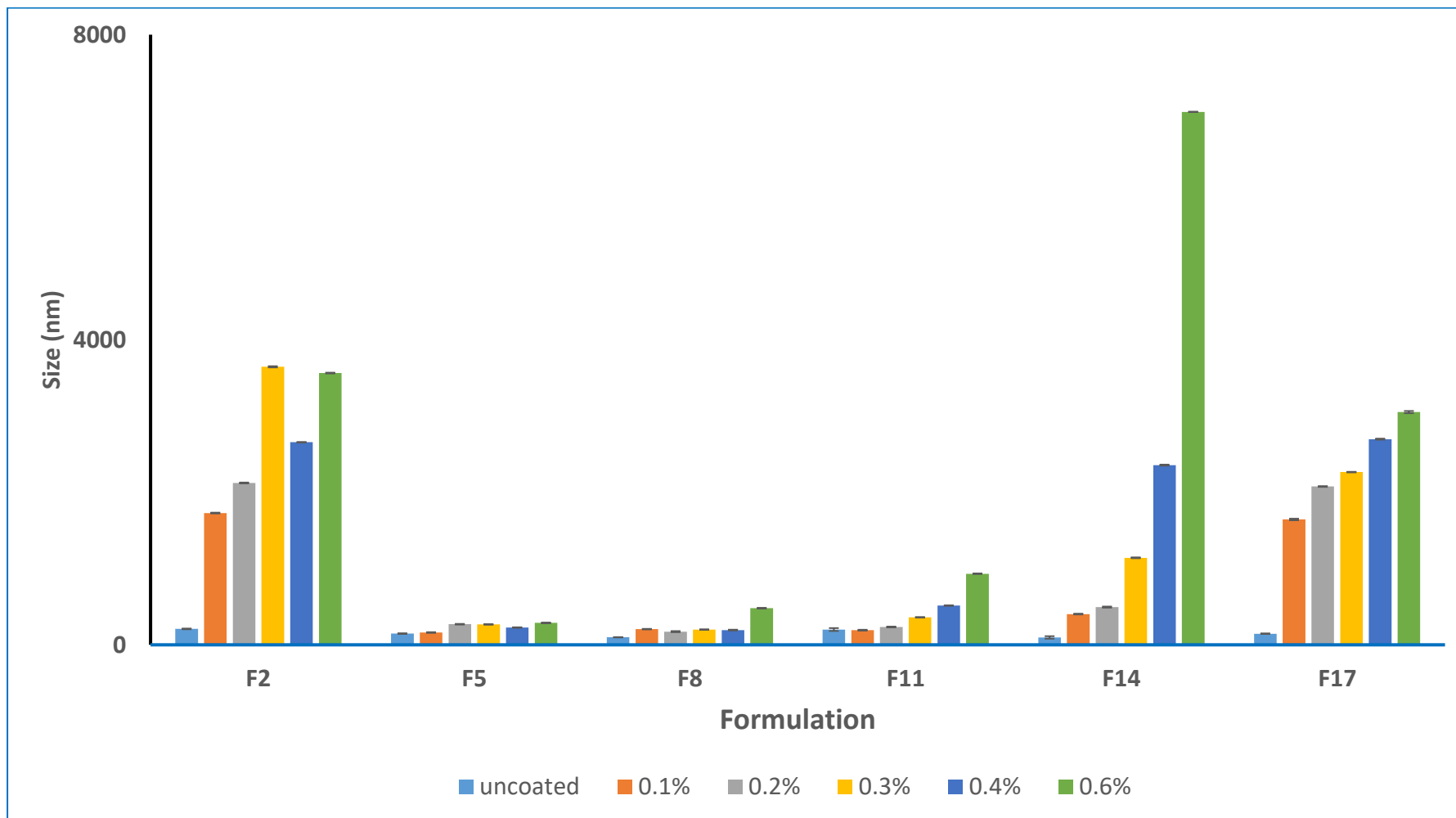


Figure 4.2 Results of HPMC K15M coated microspheres characterisation for size, $n=3$, mean values \pm SD.

Table 4.3 Results of chitosan coated transferrinsomes characterisation for size, PDI, and %EE, n=3, mean values \pm SD, stars are to flag levels of significant differences compared to uncoated (*, ** and *** represents $P<0.05$, $P<0.01$ and $P<0.001$ respectively).

Sample	Uncoated		0.1% w/v		0.2% w/v		0.3% w/v		0.4% w/v		0.6% w/v	
	Size (nm)	PDI	Size (nm)	PDI	Size (nm)	PDI	Size (nm)	PDI	Size (nm)	PDI	Size (nm)	PDI
F2	208.7 ± 4.66	0.25 ± 0.03	466.37 ± 2.36 ***	0.65 ± 0.03	474.86 ± 3.61 ***	0.75 ± 0.04	526.56 ± 3.70 ***	0.47 ± 0.04	634.67 ± 4.12 ***	0.74 ± 0.03	726.00 ± 2.91 ***	0.84 ± 0.01
F5	146.95 ± 0.63	0.22 ± 0.02	153.43 ± 5.66 ns	0.22 ± 0.02	156.25 ± 1.82 ns	0.27 ± 0.03	166.08 ± 4.40 ***	0.28 ± 0.01	165.03 ± 2.75 ***	0.27 ± 0.03	155.76 ± 3.02 ns	0.23 ± 0.01
F8	98.93 ± 2.07	0.14 ± 0.01	129.47 ± 3.98 ***	0.29 ± 0.01	129.14 ± 1.62 ***	0.38 ± 0.01	124.64 ± 4.55 ***	0.35 ± 0.02	143.99 ± 2.64 ***	0.40 ± 0.02	127.89 ± 1.46 ***	0.38 ± 0.01
F11	200.35 ± 19.02	0.21 ± 0.01	164.93 ± 1.91 ***	0.15 ± 0.02	167.48 ± 2.38 ***	0.18 ± 0.04	170.40 ± 0.86 ***	0.18 ± 0.01	176.93 ± 3.00 ***	0.17 ± 0.01	176.29 ± 2.50 ***	0.20 ± 0.01
F14	96.92 ± 16.37	0.17 ± 0.01	315.14 ± 3.00 ***	0.35 ± 0.00	485.57 ± 4.06 ***	0.57 ± 0.03	562.8 ± 2.95 ***	0.86 ± 0.04	737.26 ± 4.42 ***	0.92 ± 0.03	958.71 ± 2.18 ***	0.73 ± 0.02
F17	146.05 ± 0.35	0.3 ± 0.02	648.12 ± 2.24 ***	0.57 ± 0.02	747.07 ± 1.68 ***	0.65 ± 0.04	1104.44 ± 5.24 ***	0.85 ± 0.04	1000.19 ± 7.35 ***	0.96 ± 0.02	1091.90 ± 3.82 ***	0.55 ± 0.03

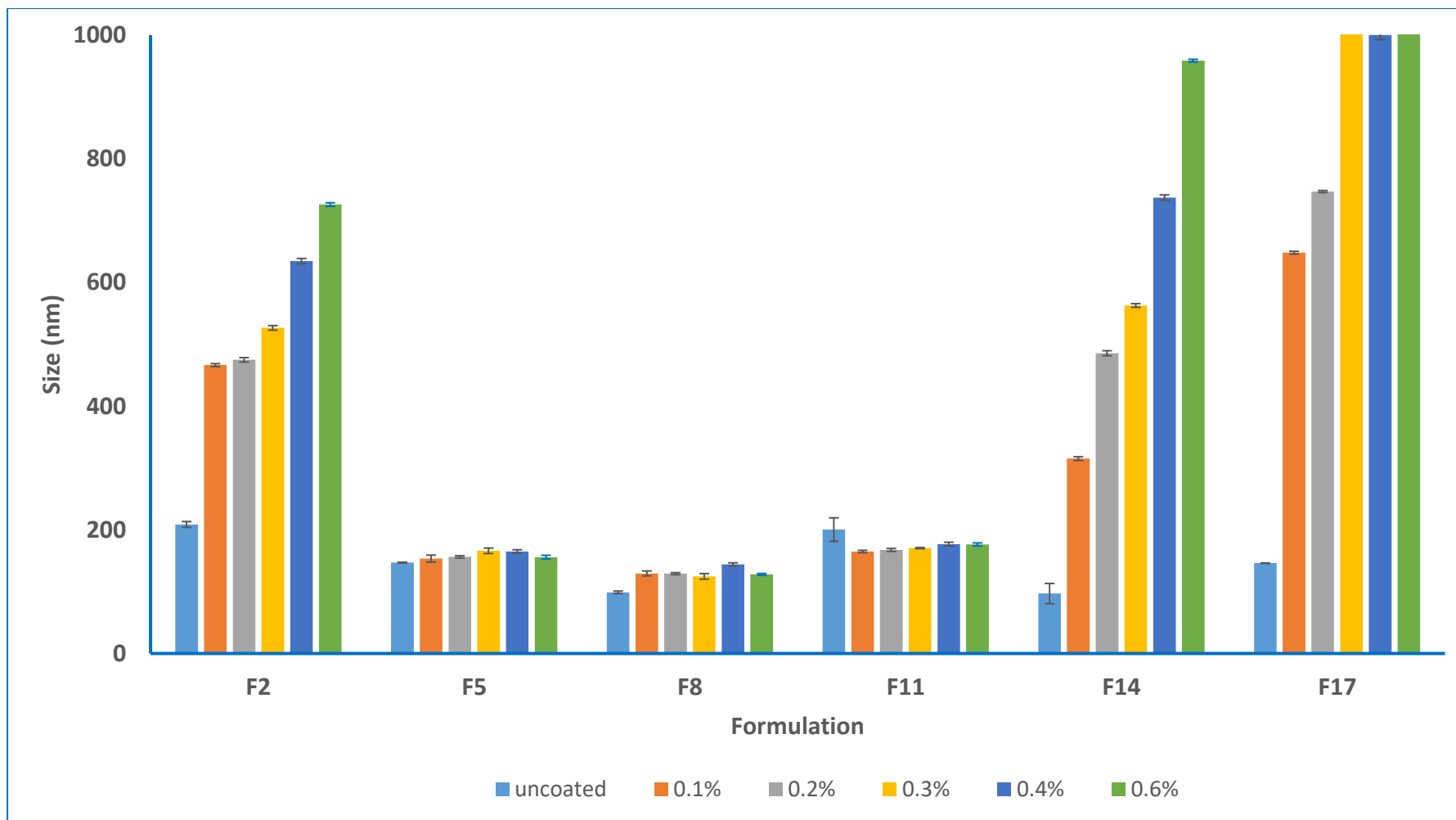


Figure 4.3 Results of chitosan coated transferrinosomes characterisation for size, $n=3$, mean values \pm SD.

It was also reported that both the molecular weight and the viscosity of the polymeric solution might have an effect on the thickness of the coat and the subsequent transfersomes size ²²⁴. That was clearly noted by comparing the size of both HPMC K4M and K15M coated transfersomes (Table 4.1 and Table 4.2). Although there were some variations at certain concentrations where HPMC K4M coated samples were larger in size than the corresponding HPMC K15 ones, this could be because of the aggregation of the particles rather than the coat thickness itself. Still, most transfersome samples (F2, F5, F8, F11, F14, and F17) that were coated with HPMC K15M (i.e. MW of 750 kDa) showed significantly larger size than the lower MW HPMC K4M ones (i.e. MW of 500 kDa). In general, it was suggested that higher molecular weight polymer could show higher number of binding sites between polymer and transfersomes bilayer leading to a thicker polymeric coat, which may explain the greater size after coating with HPMC K15M in comparison with HPMC K4M ²²⁴.

The same trend was obtained for chitosan-coated transfersomes (Table 4.3) which also proves the formation of coating layers that increased in thickness by increasing the concentration of chitosan solution. With increasing chitosan concentration, the size of the coated transfersomes increased significantly in all formulations in comparison to the uncoated sample, except formulation F5 that showed a slight increase (non-significant, $P > 0.05$) in size after coating with 0.1% and 0.2% concentrations of chitosan solutions and preserved a PDI \sim 0.2. Overall, the results obtained with chitosan coating were in agreement with previous reported literature. When low molecular weight chitosan was used by Li et al, they concluded that concentrations up to 0.25% were the best to obtain a good coating layer with a slight increase in the size compared to uncoated ones ²⁸².

4.3.1.2 The %EE of the coated Transfersomes

Characterising the encapsulation efficiency after the coating process was crucial not only to check if it would be enhanced by coating but also to ensure that the coating process did not affect the integrity of the transfersomes bilayer or composition. Although the aim was to produce nanosized transfersomes, and some formulations reached micron size after coating with some polymers, the %EE was evaluated for all coated formulations at all concentrations. A comparison before and after the coating process was performed and bar charts of the results were plotted (Figure 4.4, Figure 4.5 and Figure 4.6). The %EE varied between formulations after coating and inconsistent increase was found as compared to uncoated transfersomes, the increase in the %EE is critical to consider since the coating process was conducted on the total formulation that includes both intact transfersomes as well as the free untrapped drug. However, the general method of measuring %EE is usually conducted by separating the free drug from transfersomes using Amicon® centrifugal filter tubes as reported in section 2.2.5. But to check if the coating would enhance the encapsulation and drug loading of transfersomes, the free drug was left with the loaded transfersomes while the coating solution was added as described in section 2.2.2.

After coating with HPMC K4M (Figure 4.4), the first three formulations F2, F5, and F8 (i.e. EPC-based formulations), showed a significant increase in the %EE with $p < 0.01$ but increasing the polymer concentration beyond 0.2% did not significantly increase the %EE. However, DMPC-based formulations, especially F11 and F14, showed the opposite trend with a significant reduction in the %EE ($P < 0.001$) after coating with the five different concentrations (Figure 4.4). The reduction in entrapment of the coated transfersomes indicates that some drug escaped the bilayer during the coating process, which was similar to

the report by Refai et al. during the development of mucoadhesive coated liposomes²²⁴. On the other hand, EPC-based vesicles were believed to have better drug carrying ability, and the leakage rate of the entrapped drug was reported to be lower than other lipids²⁸³, which could be the reason behind preserving the good entrapment of EPC-based formulations even after coating.

The drug entrapment varied after HPMC K15M coating where most of the formulations preserved the same entrapment efficiency, while some showed a slight increase. However, the slight increase in the %EE was mainly observed with transfersome formulations that showed larger size after coating. The presence of a thick mucoadhesive coating layer may attach some free drug during the coating process and it was suggested that %EE would be enhanced by coating and it may further increase with increasing the coating polymer concentration²⁸⁴. Transfersomes coated with chitosan HCl, demonstrated the same general trend of increasing the %EE as shown in Figure 4.6. However, a remarkable increase in the %EE was attained after coating formulation F5 with chitosan HCl with concentration of 0.1% and 0.2%, with a very significant difference ($P < 0.001$) in comparison with the corresponding uncoated sample (Figure 4.6).

4.3.1.3 Coated sample selection

Overall, a selection for the best formulation is crucial for further development of the delivery system, that could be achieved by gathering all characterisation results of the polymer-coated formulations in term of size, PDI, and %EE. In general, both grades of HPMC polymers showed a larger size and inconsistent PDI, which was in contrast to the aim of forming nanosized particles. Only sample F11 did not show a significant increase in size after coating with HPMC K4M and K15M at 0.1% concentration. Similarly, formulation F5 showed a slight, but

insignificant increase in size. However, in contrast to formulation F11 that produced a 27.42% decrease in %EE after coating with HPMC K4M and no difference after coating with HPMC K15M, formulation F5 showed a remarkable and significant enhancement in the drug entrapment after chitosan coating. Therefore, F5 coated with chitosan HCl at 0.1% and 0.2% were selected for demonstrating high %EE of 84.29% and 81.59% respectively. Nevertheless, as there was not a significant difference in the outcome after coating with 0.1% or 0.2%, F5 coated with 0.1% chitosan HCl (F5-CH) was the formulation of choice and was subject to further characterisation such as in vitro release and mucoadhesive properties.

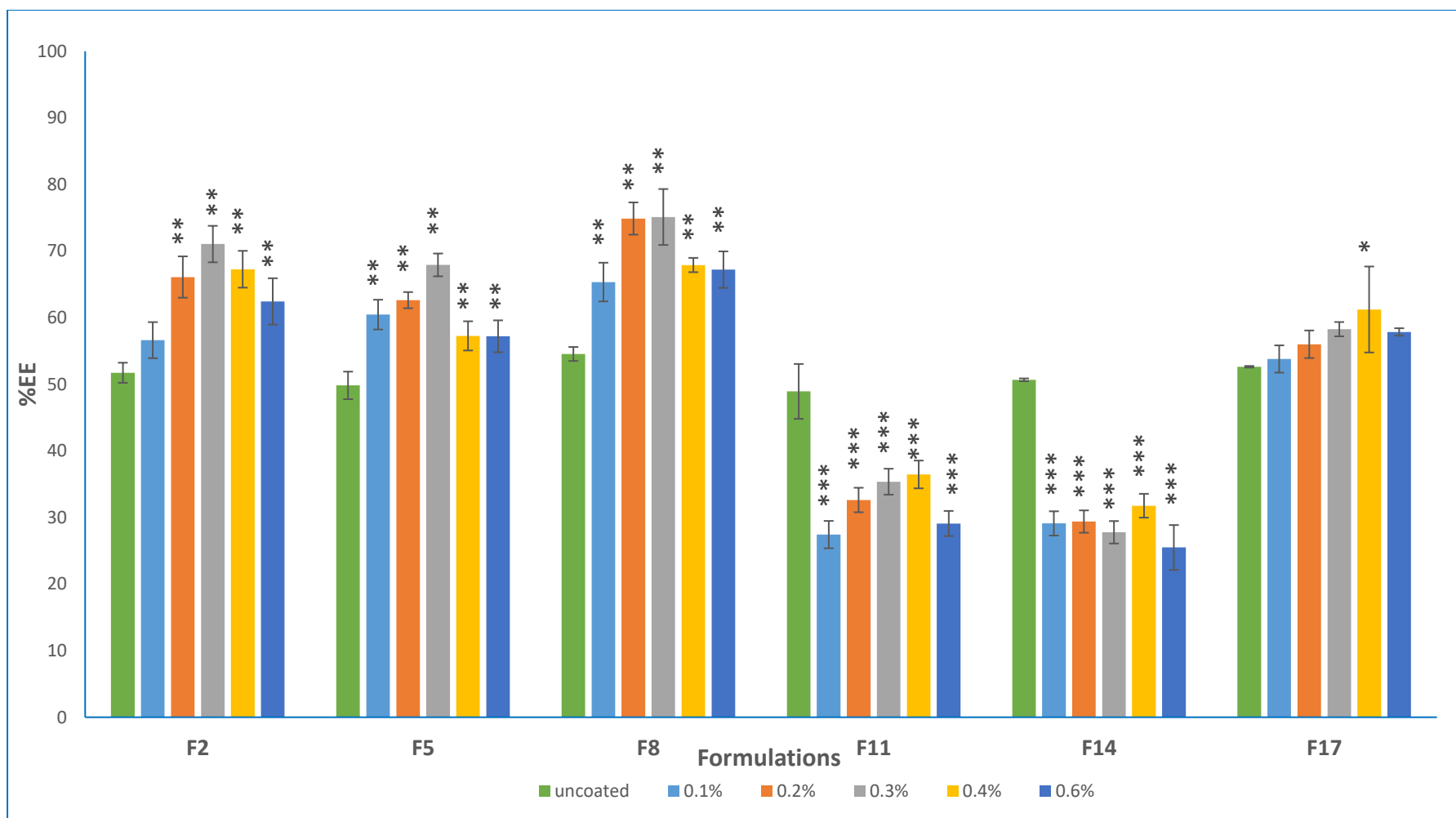


Figure 4.4 %EE for Formulations (F2, F5, F8, F11, F14, and F17) after coating with HPMC K4M with concentrations 0.1, 0.2, 0.3, 0.4 and 0.6 % w/v, stars are to flag levels of significant differences compared to uncoated (*, ** and *** represents $P < 0.05$, $P < 0.01$ and $P < 0.001$ respectively), $n=3$, mean values \pm SD.

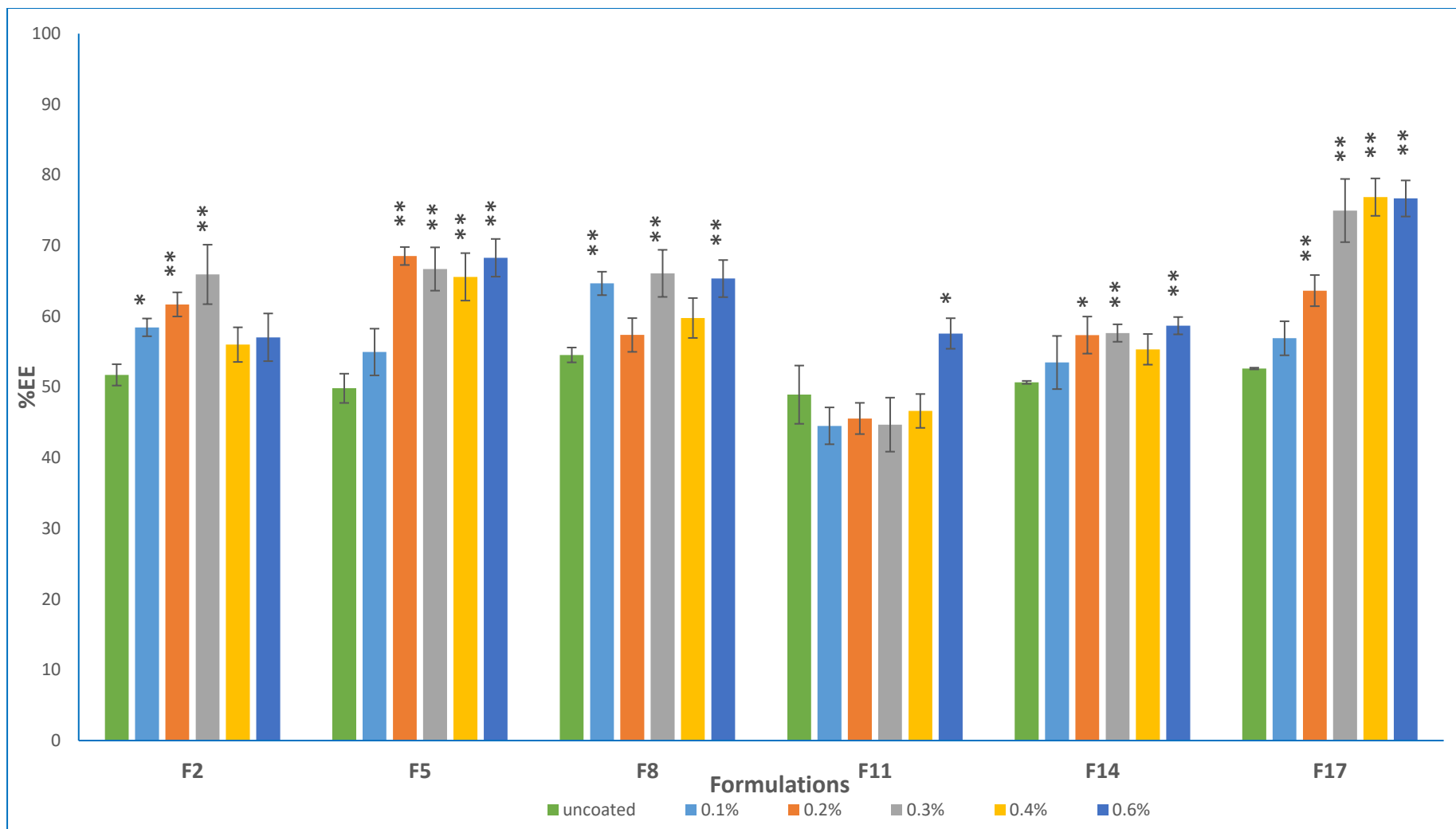


Figure 4.5 %EE for Formulations (F2, F5, F8, F11, F14, and F17) after coating with HPMC K15M with concentrations 0.1, 0.2, 0.3, 0.4 and 0.6 % w/v, stars are to flag levels of significant differences compared to uncoated (*, ** and *** represent $P<0.05$, $P<0.01$ and $P<0.001$ respectively), $n=3$, mean values \pm SD.

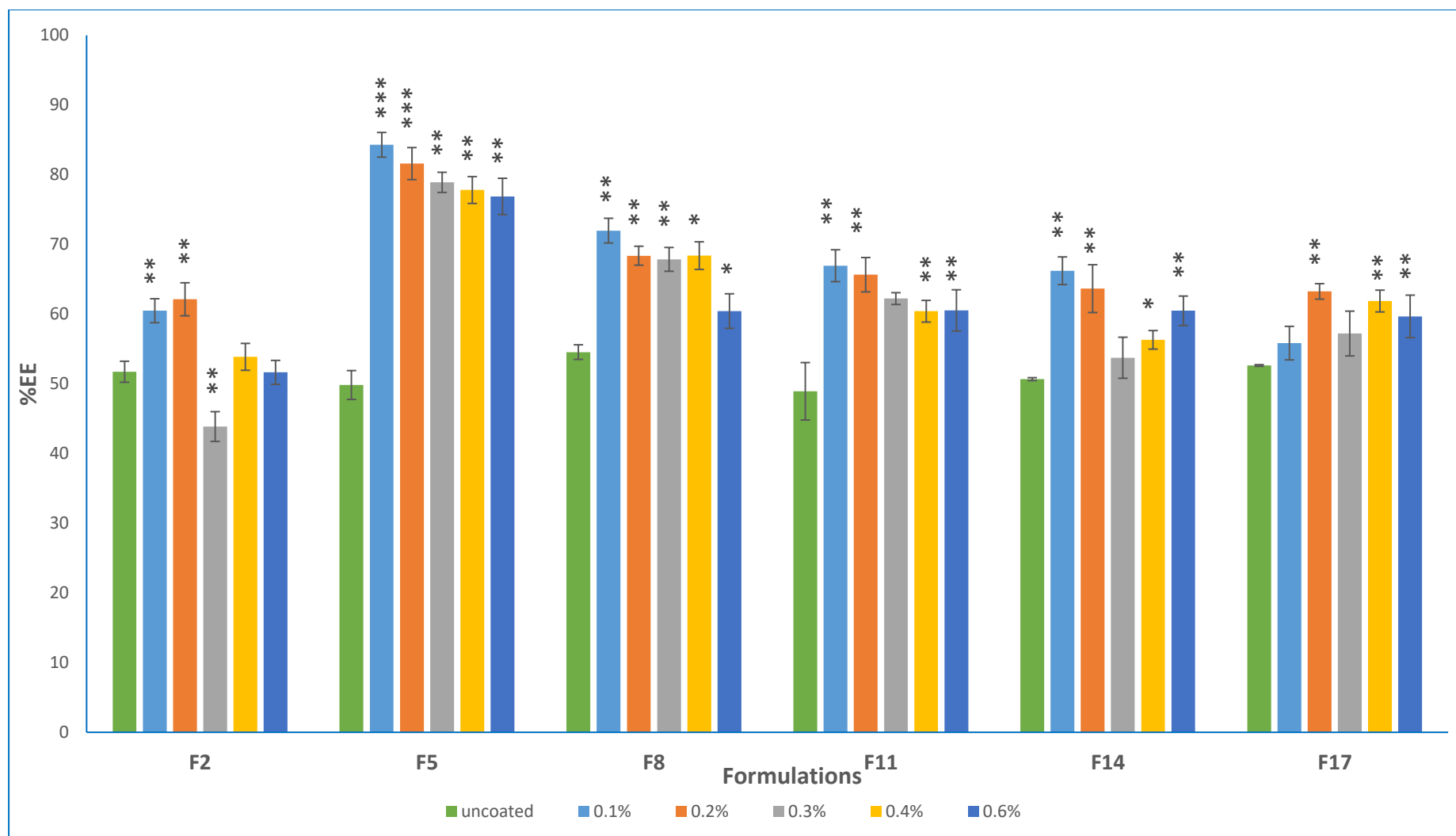


Figure 4.6 %EE for Formulations (F2, F5, F8, F11, F14, and F17) after coating with Chitosan HCl with concentrations 0.1, 0.2, 0.3, 0.4 and 0.6 % w/v, stars are to flag levels of significant differences compared to uncoated (*, ** and *** represents $P < 0.05$, $P < 0.01$ and $P < 0.001$ respectively), $n=3$, mean values \pm SD.

4.3.1.4 Coated transfersome morphology

SEM was used to screen the morphology of the coated transfersome (F5-CH sample). The SEM stub was prepared as mentioned in section 2.2.7.4. Chitosan coated transfersomes preserved the spherical shape as shown in Figure 4.7. SEM images revealed that transfersomes still maintain a relatively uniform size and shape even after chitosan coating, however, clear images to show the surface details of the coating layer were not obtainable on the nanoscale level.

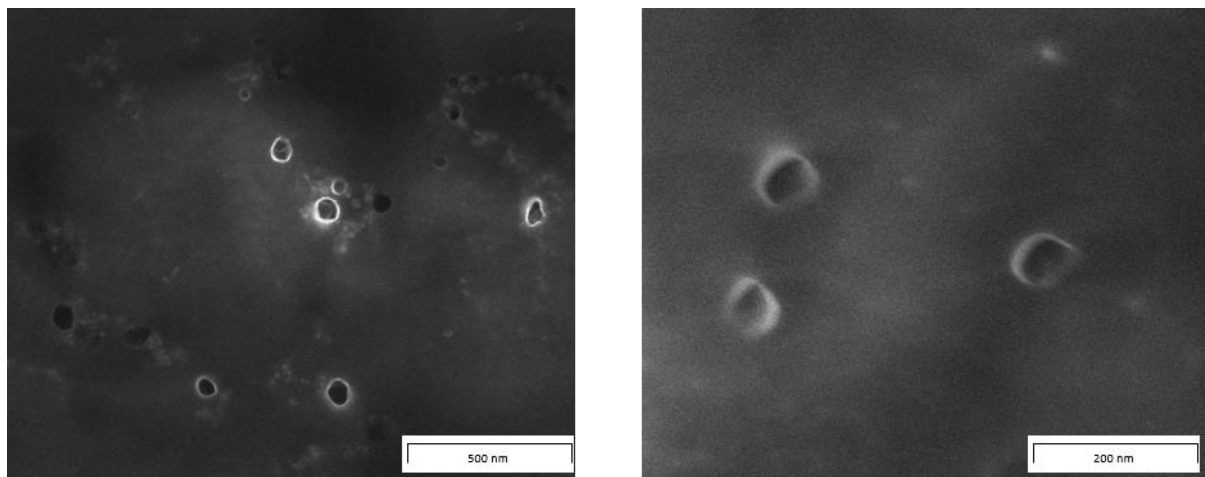


Figure 4.7 SEM images of chitosan coated transfersomes (F5-CH)

Furthermore, SEM imaging was also employed to prove the concept of mucoadhesive properties of the coated transfersomes. SEM imaging of both untreated and treated epithelium was conducted as shown in Figure 4.8. SEM images of untreated tissue showed continuous and smooth surfaces in comparison to the rough and porous surface that was observed from the treated tissue. However, some intact transfersomes were still seen on the surface of the treated tissue, marked with red arrows in Figure 4.8. Additionally, some spherical bulbs were also observed fused on the surface of the treated tissue while the untreated tissue was completely free from any similar observations. These fused bulbs were also believed to be transfersomes (marked with green arrows in Figure 4.8). As coated

transfersomes have been observed after the harsh processing of washing, vacuum drying and coating; this supports the claim of the chitosan coated transfersomes possessing a mucoadhesive property which was widely reported in the literature ²⁸².

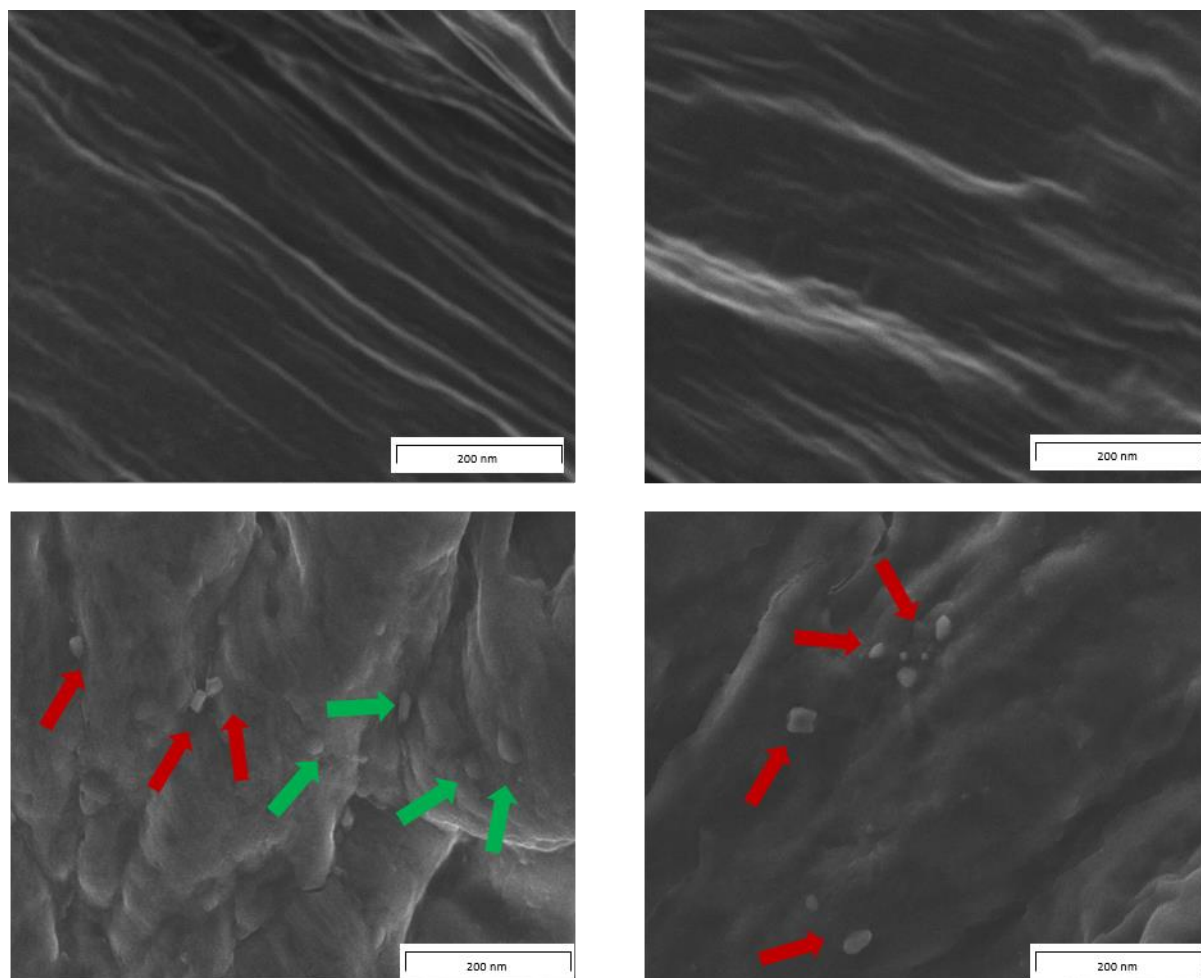


Figure 4.8 SEM images of untreated tissue (top) and after tissue after treating with F5-CH (bottom).

4.3.2 In vitro release of F5-CH formulation

The release profile of F5-CH formulation was studied over 24 hours and the cumulative amount of drug released was calculated as shown in Figure 4.9. In comparison with free lidocaine, F5-CH formulation sustained the lidocaine and the amount released reached the maximum (i.e. 100% drug release) at 16 h.

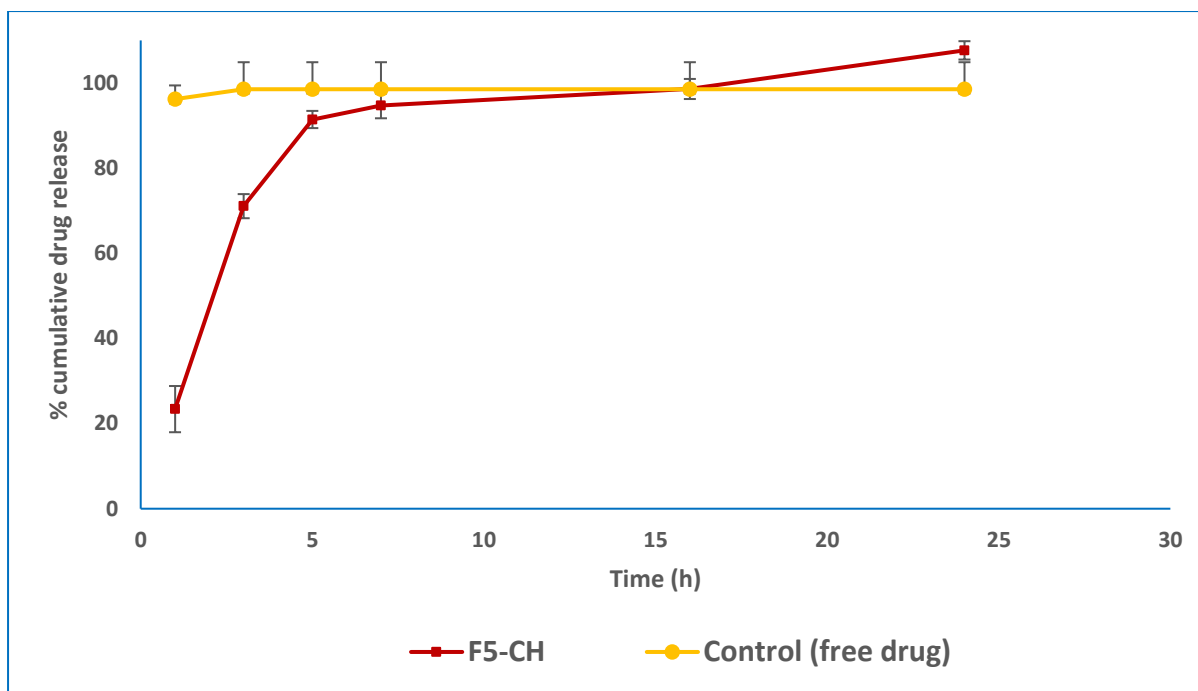


Figure 4.9 Release profile of lidocaine permeated across dialysis bag from chitosan coated formulation (F5-CH) versus the free drug (control) over 24h, n=3, mean values \pm SD.

The uncoated formulation (F5) not only showed sustained release of lidocaine but also a delayed release with only 1.37% drug released after 1 h as mentioned in section 3.3.3.3. In contrast, chitosan coated formulation (F5-CH) showed a release with 23.4% during the first hour (Figure 4.9 and Figure 4.10). It was suggested that the drug could be completely entrapped in the transfersomes without any free drug adsorbed on the transfersomes surface, which may explain the delayed release from the uncoated formulation. Moreover, there was a significant increase in the release profile from F5-CH in comparison to the release from the uncoated one, but the general pattern was similar. Both F5-CH and F5 formulations exhibited a sustained release profile with complete drug release between 16h and 24h respectively. Chitosan HCl has relatively good solubility in water²⁸⁵, which may cause a high corrosion rate of the coating layer and consequently releasing the adsorbed drug within the coating layer in an immediate and quicker rate²⁸⁶. While the rest of the sustained lidocaine release could be mainly driven by the slow erosion of the transfersome lipid bilayer. In

general, although F5-CH formulation showed higher release rate than the uncoated one, the coated transfersomes were still able to sustain the drug release over 24 h. In addition, the higher release rate from the coated transfersomes could be related to the increased of the amount of drug encapsulated within the coat layer (84.29%), compared to the uncoated samples (49.83%).

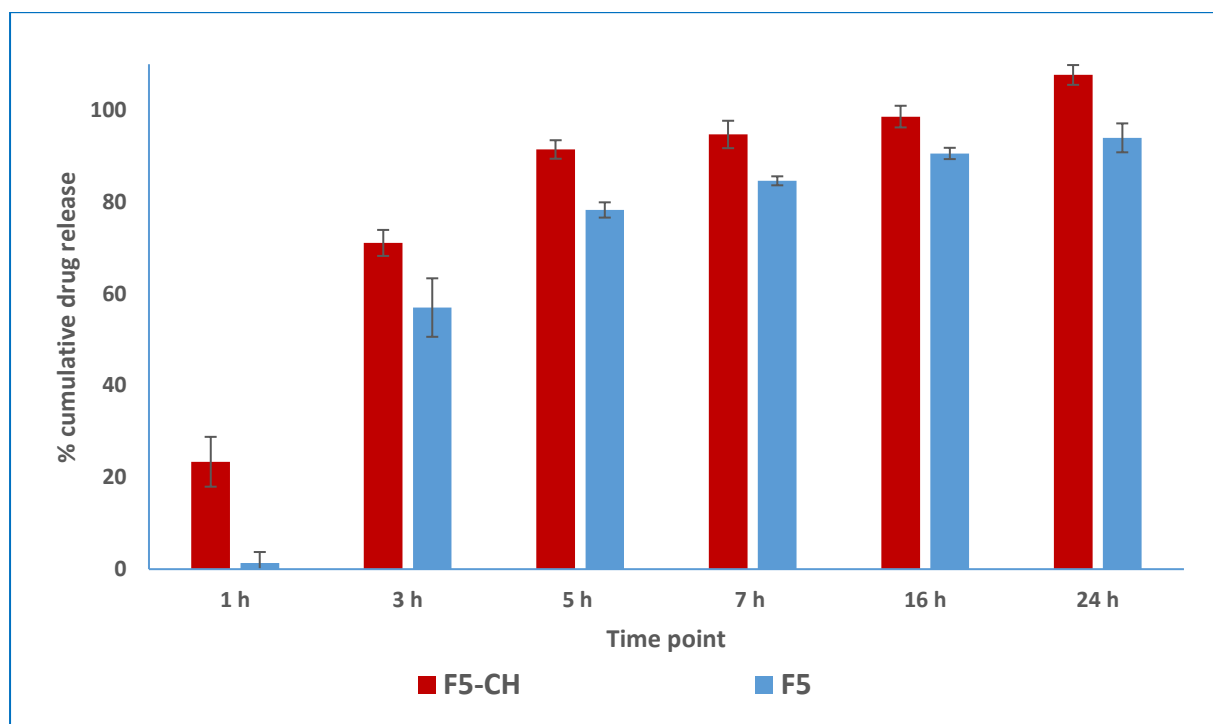


Figure 4.10 Percentage cumulative drug release permeated across dialysis membrane from chitosan coated formulation (F5-CH) versus the uncoated transfersome (F5) over 24h, n=3, mean values \pm SD.

To ease the release study method the total formulation (including both the coated transfersomes and the left untrapped drug), however, the amount of free drug was subtracted at each time point, so the release profile is completely representing the release of the drug from the coated transfersomes. In addition, the most common method for purifying loaded transfersomes (coated or not) from the free drug is conducted by applying high centrifugal forces mainly by ultracentrifuge, however, that may cause transfersomes rupture and drug loss leading to inaccurate measurement of %EE ²⁸⁷.

Therefore, the purification of transfersomes was believed to be one of the main limitations in their manufacturing process that requires applying effective methods to remove the free drug not entrapped in the transfersomes. Several purification methods have been reported in literature such as centrifugation, column chromatographic separation, dialysis, cation-exchange resin, and ultrafiltration ²⁸⁷. Each of these method has its own advantages and disadvantages, so a suitable method should be carefully chosen, and more efforts need to be exerted into this field to improve the manufacturing process of transfersomes. Although in this research a few methods were screened to find the effective way to purify transfersomes from the free drug, due to time limitation this was out of the scope of this research. The main outcome was concluding that centrifuging transfersomes at high forces would lead to massive loss from their entrapped drug, therefore the full formulation was used in all test but with subtracting the free drug fraction at each time point.

4.4 Conclusion

In this chapter, three different polymers (HPMC K4M, HPMC K15M, and chitosan HCl) with reported mucoadhesive properties were screened for forming a continuous coating layer. The resultant formulations were characterised for size, PDI and %EE, aiming to preserve the uniform nanosize of transfersomes as well as enhancing the %EE. There was clear evidence of forming the coating layer as all formulations showed an increased size after the coating. However, transfersomes coated with HPMC K4M and K15M significantly failed to keep the nanosize or homogenous distribution that obtained with the uncoated ones. Chitosan HCl coated transfersomes showed a slight increment in the size as well, except formulation F5 at low chitosan HCl concentrations (i.e. 0.1 and 0.2 % w/v). Not only did formulation F5 show a non-significant difference in size after coating with chitosan HCl but it also had a higher drug

entrapment (84%) compared to the uncoated sample (49%). Therefore, the chitosan coated formulation (F5-CH) was selected and tested for mucoadhesion and drug release properties. F5-CH exhibited a sustained release profile over 24 h with an immediate release of 23.4% during the first hour, which could guarantee the immediate effect of LA. These findings proposed a novel buccal drug delivery system utilising chitosan HCl coated transfersomes, whose toxicity profile and permeability through *in vitro* and *ex vivo* models will be further investigated in the following chapter.

**Chapter 5. *In vitro* and *ex vivo* evaluation of LA loaded
transfersomes**

5.1 Introduction

Several preparations have been developed for drug delivery through buccal administration. Regardless of the type of the preparation, all efforts were utilised to ensure the quality of the produced dosage form along the journey of formulation development. *In vitro* and *ex vivo* studies have been extensively employed for the assessment during the formulation development as well as the routine quality control tests of the final dosage form in advance of the more expensive, time-consuming *in vivo* studies or clinical trials that apparently require lots of ethical considerations. Permeability testing is among these employed studies, as the permeability through the buccal mucosa of the drug or the complete delivery system is crucial to achieving the therapeutic need.

The most used model to predict the permeability of a drug through the buccal mucosa is the *ex vivo* model (also called *in vitro* animal model) ²⁸⁸. The *ex vivo* animal model proved to be suitable for showing high similarity to human buccal mucosa, in addition to offering a substantial lower cost in comparison with *in vivo* animal studies. Simply isolated animal buccal mucosa mounted between two diffusion chambers (donor and receiver chambers) represents the *ex vivo* model, and the drug mobility through the tissue could be assessed by sampling from the receiver chamber over certain time intervals. Buccal mucosa from several animals such as rats, hamsters, dogs, monkeys and pigs have been investigated for the feasibility of being used as an *ex vivo* model ²⁸⁸. Unlike human buccal mucosa, both hamsters and rats buccal mucosa are keratinised, which makes it unsuitable for being used as an *ex vivo* model ^{289,290}. Non-keratinised mucosa could be obtained from dogs, monkeys and pigs. However, buccal mucosa of dogs and monkeys is found to be thinner than human buccal mucosa, meaning the former is more permeable; therefore, they have limited use ^{291,292}. The pig buccal

mucosa is the most suitable one, being the most representative of human buccal mucosa in term of thickness and constituents. It is cheap as well as feasibly obtained fresh from any slaughterhouse and it does not impose any ethical considerations in comparison to dogs and monkeys^{288,293}.

Substantial efforts have been applied to overcome the limitations associated with getting and using animal buccal mucosa. In this regard, cell-based *in vitro* models have shown an increasing trend to substitute the *ex vivo* ones. Several cell-based models have been developed using both primary and continuous cell lines from mammalian, including human origins. Some of these *in vitro* models were prepared using transwell systems where the cells are co-cultured on filters. The cell-based model has been developed using the continuous TR146 cells which are similar to human buccal mucosa due to their stratified epithelial like cells, and it has been extensively used for studying drug permeability. A commercial version of three dimensional (3D) multilayer epithelium based on TR146 cells is available in the market, from SkinEthic (EPISKIN, France), and it has been extensively employed to test drug toxicity and permeability^{294,295}. However, TR146 cells are derived from cancerous origin as they were obtained from human neck node metastasis, which originated from buccal squamous carcinoma, making them to behave differently than normal healthy cells, as they are not fully differentiated.

Thus, to overcome the limitations of TR146 cell-based model, there is a real need to develop an *in vitro* cell-based model using a normal cell line that resemble the human buccal mucosa. Nevertheless, to validate the developed model, the results should be compared to a well-known model such as the *ex vivo* ones. In this chapter, initially the safety profile of transfersomes as whole formulation as well as each ingredient employed were screened. This

was followed by a cell-based model that was developed using NOK cells. In order to draw a full profile of transfersomes permeability, the results from the cell-based model were compared with those obtained through an *ex vivo* model that used porcine oesophagus epithelium.

5.2 Method

The toxicity profiles of all transfersome ingredients as well as the transfersome formulations were assessed using AB viability test as detailed in section 2.2.8. The permeability profile was studied using an *ex vivo* model as described in section 2.2.9 and NOK cell-based model was developed and used for permeability testing as mentioned in section 2.2.10.

5.3 Results and discussion

5.3.1 Cell viability and transfersomes toxicity

The cytotoxicity profiles of both the ingredients and the transfersomes were evaluated using Alamarblue (AB) assay 24 h post exposure to treatment. AB assay is one of the most used cytotoxicity assays and is based on monitoring the reducing environment of the living cell. The basis for the use of AB is the fact that cells maintain a reducing environment within their cytosol when they are metabolising, which can be spectrophotometrically detected through the conversion of fluorometric indicators. AB measures the reducing environment of the viable cells through the conversion of resazurin (oxidised form, which is blue and non-fluorescent) to resorufin (reduced form, which is red and highly fluorescent), which represents an indirect method for measuring the cell viability. However, the main disadvantage of AB is that, as it is not a direct cell counting technique, the measured fluorescence can be affected by the change of cell number as well as cell metabolism²⁹⁶.

As cell viability test was carried out in parallel with studies reported in Chapter 4, the toxicity profiles of all ingredients of the optimised 6 samples that were obtained by the DOE data analysis (F2, F5, F8, F11, F14, and F17) were evaluated over 24 h in the MRC5 and MRC5-SV2 cell lines. All ingredients (including, EPC, DMPC, Tween 80, Span 80, SDC, and lidocaine) were assessed over a range of 3 different concentrations (see Table 2.1 for concentrations) (Figure 5.1 and Figure 5.2).

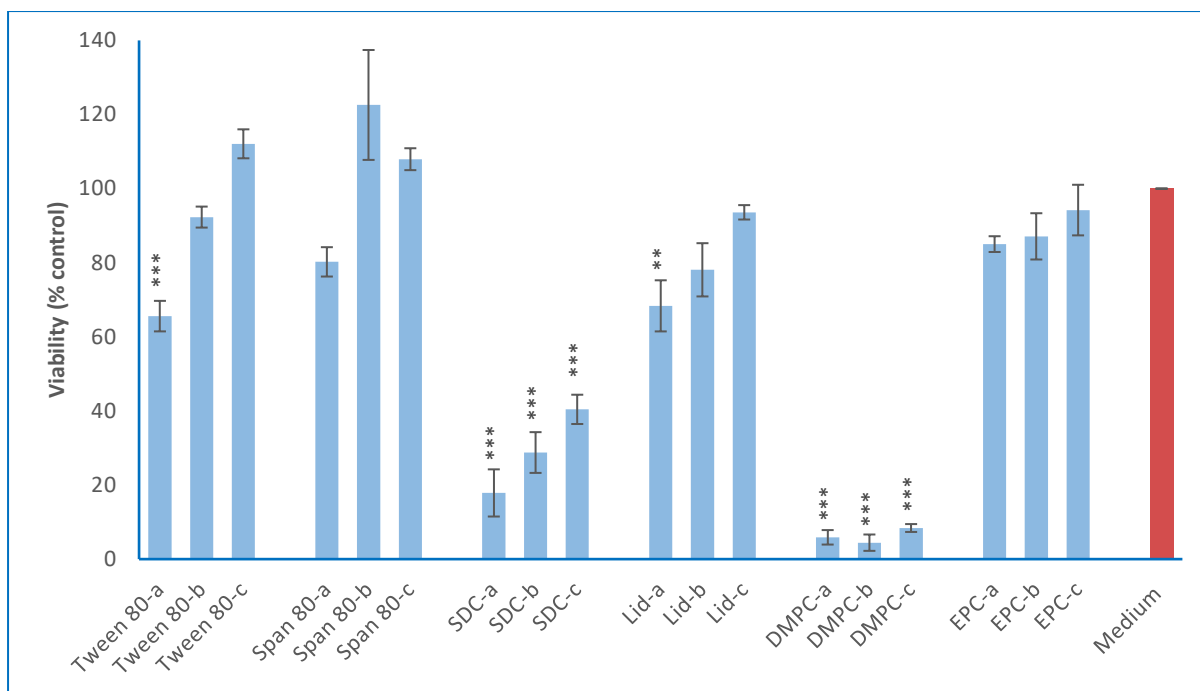


Figure 5.1 MRC5 cell viability measured by AB assay after 24 h exposure to the ingredients, data represent mean \pm SD, n=3. Stars are to flag levels of significant differences compared to control (*, ** and *** represents $P < 0.05$, $P < 0.01$ and $P < 0.001$, respectively).

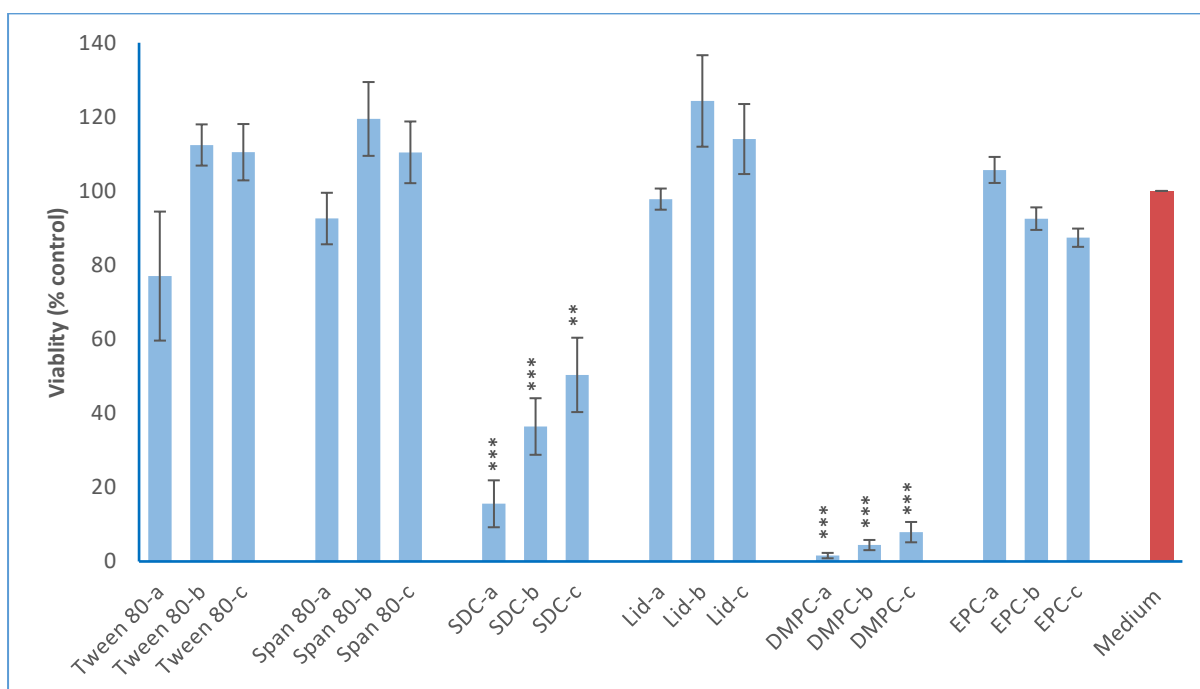


Figure 5.2 MRC5-SV2 cell viability measured by AB assay after 24 h exposure to the ingredients, data represent mean \pm SD, n=3. Stars are to flag levels of significant differences compared to control (*, ** and *** represents $P < 0.05$, $P < 0.01$ and $P < 0.001$, respectively).

The results revealed that DMPC lipid was significantly toxic to both the MRC5 and MRC5-SV2 cells. Both MRC5 and MRC5-SV2 cells showed less than 10% viability after DMPC treatment at its three different concentrations, while the natural lipid EPC appeared to be well tolerated by both cell lines. After EPC treatment, MRC5 cell viability ranged between 85-94% and MRC5-SV2 between 87-105% (Figure 5.1 and Figure 5.2). These results confirming that DMPC is more toxic than EPC are consistent with the literature, where it was reported that the toxicity of lipid is related to a few factors such as the type of the lipid, the charge and the phospholipid chain lengths ²⁹⁷. It has been suggested that liposomes based on saturated lipids (such as DMPC) seem to be more toxic than liposomes based on unsaturated lipids (i.e. EPC) ²⁹⁸. Although some EPC-based liposomes were reported to show high toxicity, which was explained to be due to the high positive charge the liposome carried and not because of the lipid itself. Additionally, it was previously reported that DMPC showed higher toxicity than lipids containing longer phospholipid chain lengths ^{297,298}.

Edge activators (surfactants) such as Tween 80 and Span 80 showed that they were completely safe to the cells. The cell viability values each approached 100% for both MRC5 and MRC5-SV2 cells, with no significant difference ($p > 0.05$) compared to the control for all studied concentrations, except for the treatment of MRC5 cell with the highest concentration of Tween 80, which resulted in a viability of 65.6% that was significantly lower than the control ($P < 0.001$). On the other hand, SDC showed significant toxicity even at the lowest concentration, with a maximum viability of 40% and 50% for both MRC5 and MRC5-SV2 respectively (Figure 5.1 and Figure 5.2).

Generally, in literature many studies have been conducted to compare the cytotoxicity of several surfactants on different cell lines; since it was believed that each cell line will behave

differently after being treated with tested formulation. For example, it was found that most of the ionic surfactants showed high toxicity to a variety of cell lines at different concentrations, whether they were cationic, anionic or zwitterionic^{299,300}. Additionally, it was suggested that surfactant toxicity mainly depends upon the ability to partition into the cell membrane, changing the cell membrane permeability, and subsequently entering the cytoplasm³⁰¹.

Therefore, the results obtained in this research are in agreement with several previous reports, despite the differences in the cell lines used or concentrations tested. Both Tween 80 and Span 80 were reported to interact the least with the biological membrane (at several concentrations) and subsequently had the least toxic effect^{299,301,302}. Similarly, the low viability that was obtained after SDC treatment was also consistent with the literature, as many studies have demonstrated its high cytotoxicity, even at very low concentrations^{303,304}, and it is believed that SDC could induce a nonspecific lysis of cell membranes³⁰⁵.

Lidocaine was well tolerated by both MRC5 and MRC5-SV2 cells after 24 h exposure to three different concentrations (Lid-a= 33.28 mM, Lid-b= 8.53 mM, and Lid-c= 4.26 mM), with almost 100% viability retention for the MRC5-SV2 cells. MRC5 viability values were 78% and 93% after treatment with 8.53 mM and 4.26 mM of lidocaine, respectively, which were not significantly different from the control. However, MRC5 viability was reduced significantly to 68.35% ($P < 0.01$) following treatment with the highest lidocaine concentration (Lid-a = 33.28 mM). The maximal lidocaine concentration tested (33.28 mM) which was slightly toxic, was only tested because it had been used in previous *in vitro* studies, but the actual concentration to be loaded onto the final delivery system will not exceed 8.53 mM, a concentration that proved to be completely non-toxic over the 24 h exposure time and, thus, safe.

A few studies have reported the cytotoxicity of lidocaine on several cell lines and the toxicity seemed to be related to both lidocaine concentration and the cell type. For example, it was revealed that it reduced the viability of lung fibroblast at only 0.2 mM³⁰⁶. In other studies, it was found to be toxic at very high concentrations of 73 mM and 184mM to corneal epithelium and neuronal cell lines, respectively, even with a very short exposure time of a maximum of 10 minutes^{307,308}. On the other hand, another study found that it decreased the viability of muscle-derived progenitor (MDC) cells to 70.4% at 1 mM³⁰⁹.

Overall, as both DMPC lipid and SDC surfactant were shown to be highly toxic, both were eliminated from being included further in transfersome formulations. Therefore, EPC-based transfersomes with Span 80 and Tween 80 (i.e. F2 and F5) were assessed for toxicity as a whole carrier, with and without drug. However, in order to ascertain the safety of the formulations in the tested MRC5 and MRC5-SV2 cells as well as in a cell type that is more representative of the buccal epithelium, a third cell line, the NOK cell line, was included in the toxicity study.

The potential effects on cell viability of blank and drug-loaded formulations (F2 and F5) were evaluated at their concentrations that would be used in the final dosage form, which also matched the safe concentrations of their ingredients. Both blank and loaded transfersomes (F2 and F5) did not show any toxicity and, therefore, could be considered safe (Figure 5.3). All the three cell lines (NOK, MRC5, and MRC5-SV2) were fully viable after 24 h exposure to the formulations with $\geq 100\%$ viability and showed no significant difference in viability to untreated cells (i.e. control). Particularly, there was no significant difference in NOK cell viability when the cells were treated with blank or loaded transfersomes of either F2 or F5 ($p > 0.05$), demonstrating that both F2 and F5 are non-toxic and should be safe at the delivered

concentration. While a comparative study of anticancer drug-loaded vesicles found transfersomes to be more toxic than liposomes and niosomes, which could be related to their synergistic toxicity with the drug ³¹⁰, another study demonstrated a safe and non-toxic profile for vaccine-loaded transfersomes ³¹¹. This was what prompted in our study the toxicity screening of ingredients at several concentrations, using different cell lines. We conclude that F2 and F5 transfersomes are certainly safe because each of their ingredients was screened separately for non-toxicity and the full formulations were also tested as blank and loaded forms, using three cell lines, and none of these entities was toxic.

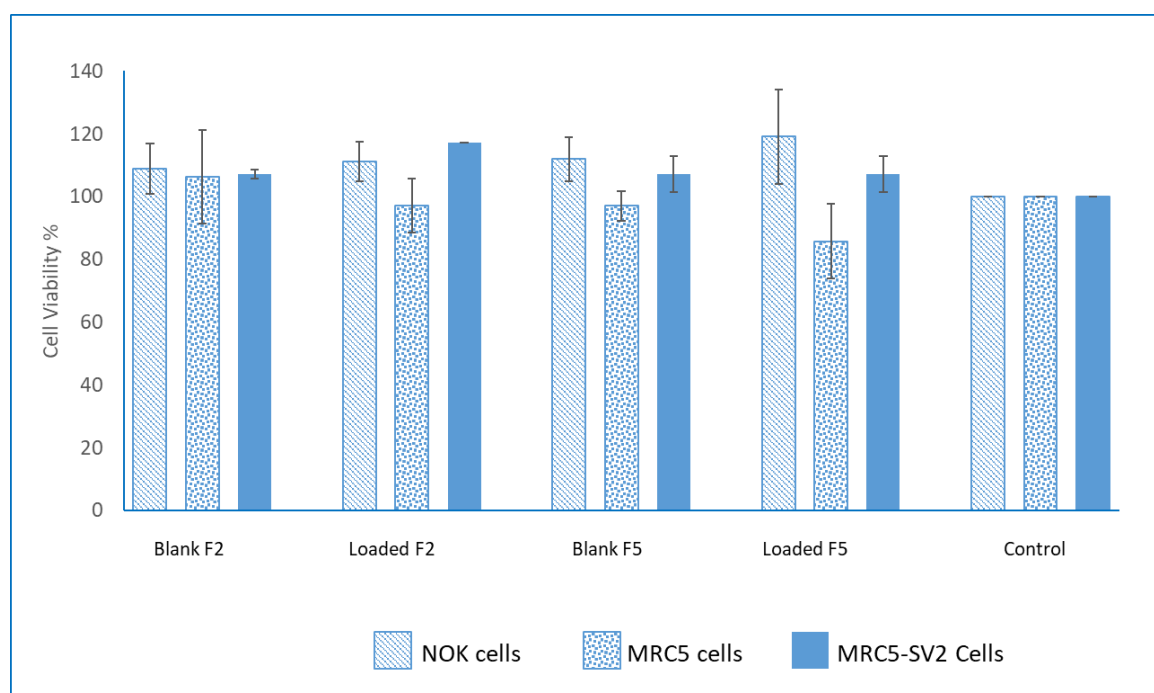


Figure 5.3 Cell viability measured by AB assay after 24 h exposure to blank and loaded transfersomes F2, and F5. Data represent mean \pm SD, n=3. The level of significant differences compared to control or for the comparison of each pair of formulations for the same

In spite of the safety profile of formulations F2 and F5, only formulation F5 was the selected formulation after the coating trials (section 4.4) as it showed the smallest size and enhanced drug entrapment, therefore, F5-CH was further characterised and loaded into the final dosage

form. As chitosan of 0.1% w/v was selected to be the coating polymer, AB test was conducted to check chitosan safety using the three cell lines (i.e. NOK, MRC5, and MRC5-SV2).

Chitosan was demonstrated to have a completely non-toxic profile in all the three cell lines, with cell viability values of $92.16 \pm 2.51\%$, $87.66 \pm 1\%$, and $104.63 \pm 0.72\%$ for NOK, MRC5, and MRC5-SV2 cells, respectively. Chitosan has been employed extensively in nanoparticle formulations over the last few decades due to its high safety profile. Its toxicity was widely assessed in several studies using a variety of cell lines, such as airway-based cells (e.g. bronchial Calu-3 and alveolar 549 cells) and buccal cells (e.g. TR146), in all of which chitosan was shown to be generally non-toxic and well-tolerated³¹²⁻³¹⁴. Therefore, the cell viability results for chitosan in this study are consistent with reports in the literature.

5.3.2 *Ex-vivo* permeability

The permeability of F5 and F5-CH transfersomes through an *ex vivo* tissue model was assessed to complement data from the *in vitro* release studies (sections 3.3.3.3 and 4.3.2) and thus make our findings more reliable, taking into consideration that the tissue is more representative than the synthetic cellulose membrane. The *ex vivo* assay was performed using pig oesophagus epithelium instead of the buccal epithelium. The main reason behind that was to overcome the limitations of using the buccal epithelium, but the use of pig oesophagus epithelium has also been demonstrated to be an equivalent barrier to the buccal one, since both have similar histological characteristics and compositions. Furthermore, it shows more advantages than buccal epithelium, as it offers larger surface area with less damage to the dissected part as a consequence of the easy separation and preparation^{315,316}.

All pieces of the separated oesophagus epithelium were checked for thickness to reduce potential variability. The epithelium thickness was in the range 420 - 500 μm , which is

illustrative of the buccal epithelium that has a mean thickness of 300-500 μm ^{317,318}. The integrity of the epithelium was checked visually before and after it was mounted into Franz cells and then at the end of the study, to ensure that the permeability was not caused by any damage to the epithelium (Figure 5.4).

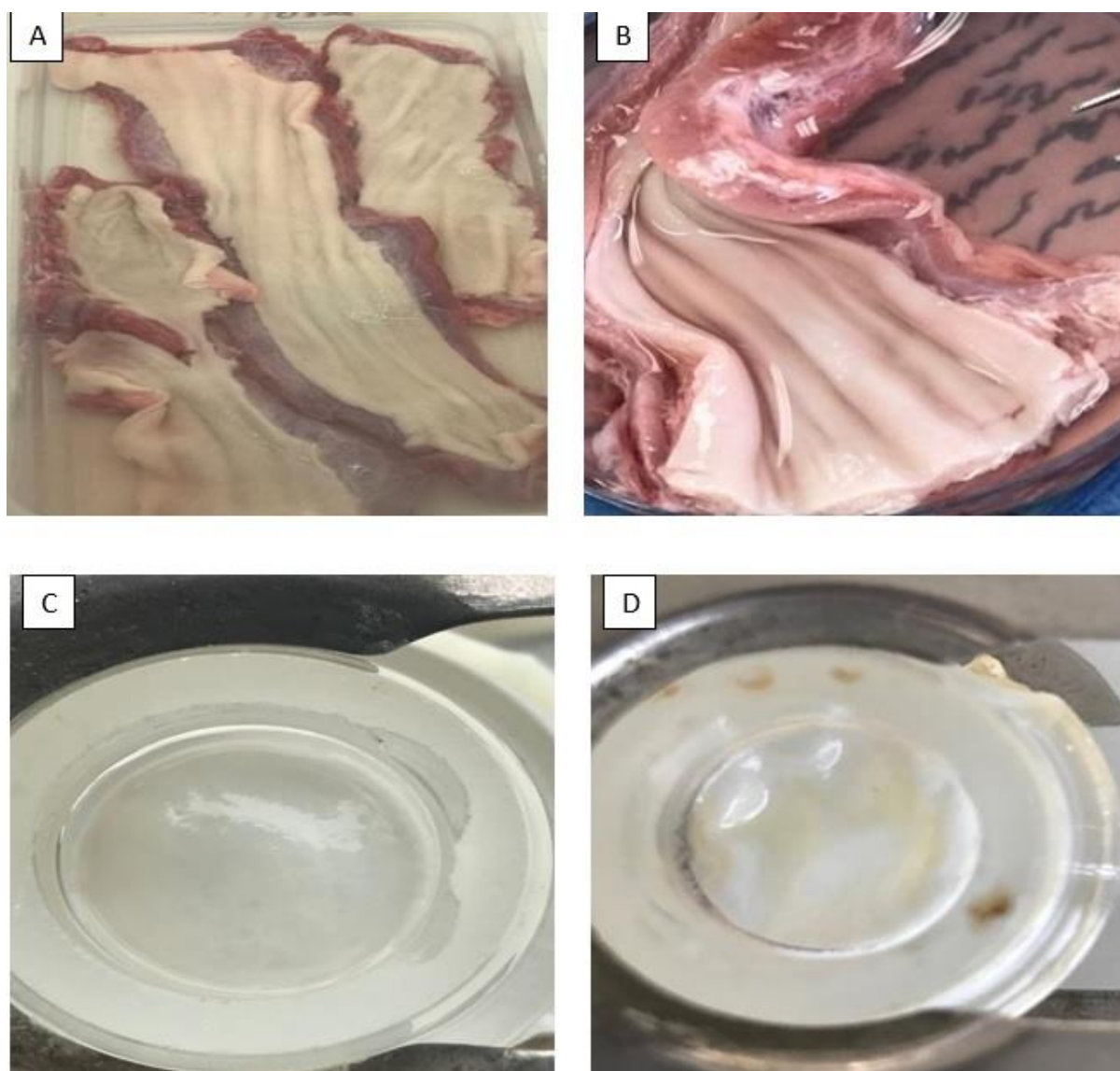


Figure 5.4 A and B- images of fresh oesophagus tissue; C and D- images of epithelium mounted onto Franz diffusion cells before and after permeability study, respectively.

The permeability profiles of F5 and F5-CH showed the same trend as the *in vitro* release profiles but with slower rates. Both F5 and F5-CH demonstrated very slow permeation during the first few hours, with an accumulative concentration of only 15.33% and 14.90%,

respectively, after 3 h (Figure 5.5). Permeation of 94% of drug from uncoated transfersomes F5 was gained after 24 h, while chitosan-coated transfersomes (i.e. F5-CH) showed more sustained release, slower permeation and a maximum of 80% detected after 24 h, with highly significant difference ($p < 0.001$) in comparison to F5. Similarly, about 90% permeation was observed in the *in vitro* assessment, but only after 7 h (section 4.3.2). Thus, except for differences in release timescales, which could be attributable to the higher complexity of the tissue organisation, results from both *in vitro* and tissue permeability studies were consistent with each other.

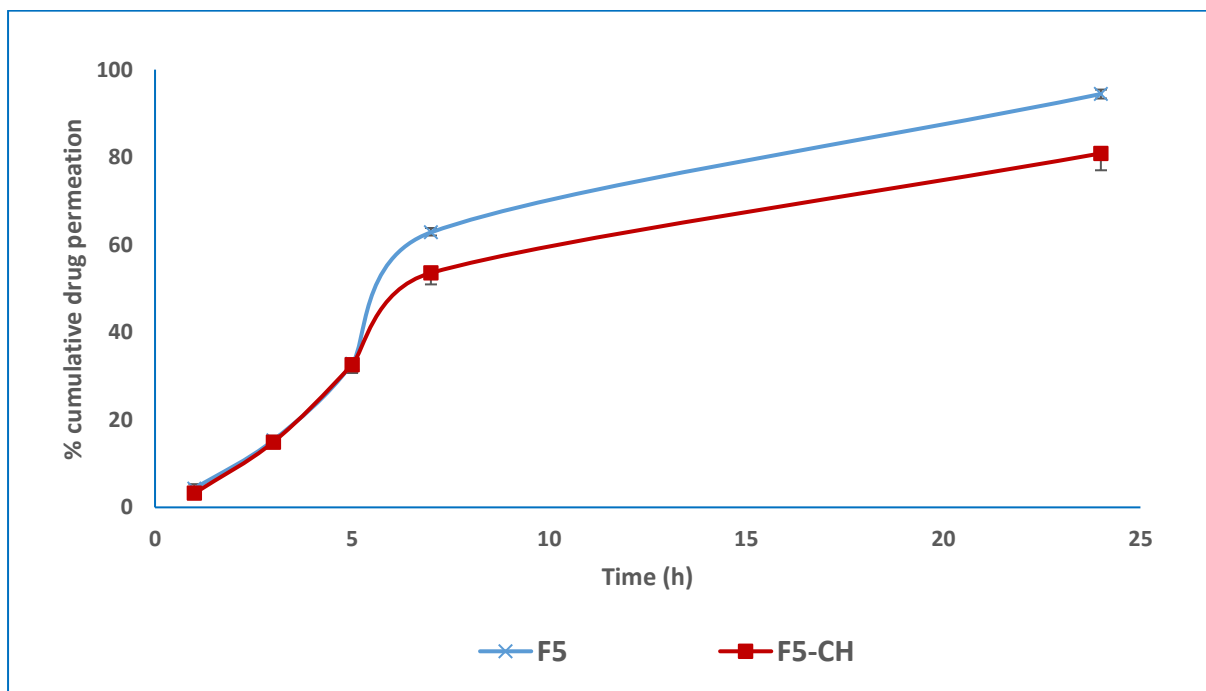


Figure 5.5 Permeation profiles (up to 24 h) of F5 and F5-CH formulations using pig oesophagus epithelium as an *ex vivo* model, Values are mean \pm SD for $n=3$ independent experiments.

5.3.3 Cell-based model development and permeability test

The cell-based model was prepared using NOK cells and the cells were cultured over 28 days to ensure complete confluency followed by the development of a few layers of cells in order to mimic the buccal epithelium. The model development was challenging because it required many optimisation steps such as determining the optimal cell density, ensuring the wettability

of the transwell membrane before cell seeding, the daily monitoring of confluency and refreshing the medium every other day without damaging the confluency (Figure 5.6).

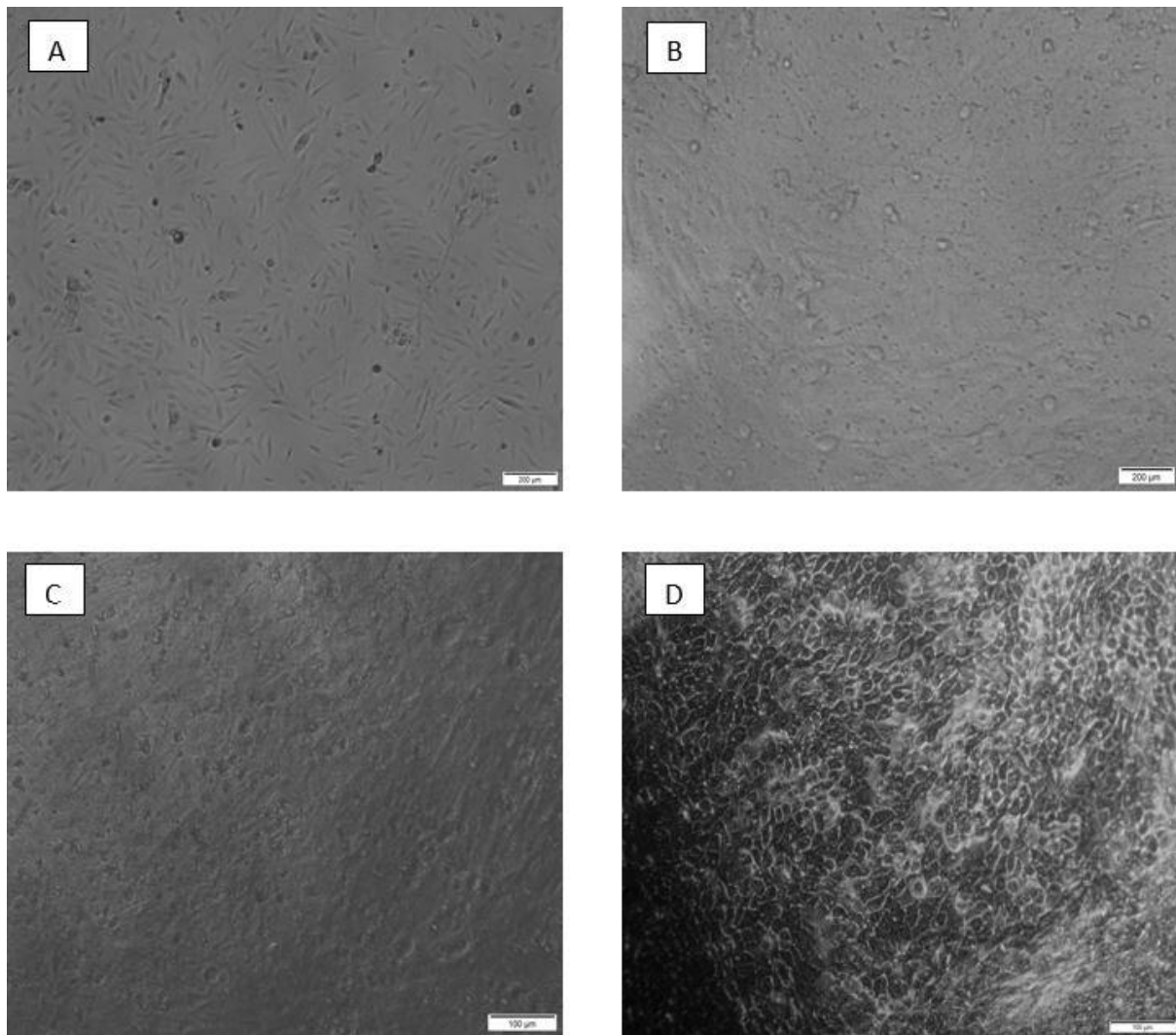


Figure 5.6 Optical microscope (bright-field) images of NOK cells acquired during the development of the cell-based model. A) Cultures in an open well, B) Cultures in a transwell 24 h after seeding, C) Cultures in a transwell after 28 days from seeding, and D) fixed cells in cell-based model after 24 h of treatment.

Drug permeability through a blank transwell was determined under the same conditions, except no cells were seeded. After 24 h, a sample withdrawn from the basolateral chamber showed 87% recovery of lidocaine, which indicates that both the filter and the study conditions did not affect the drug transport from the apical side to the basolateral one.

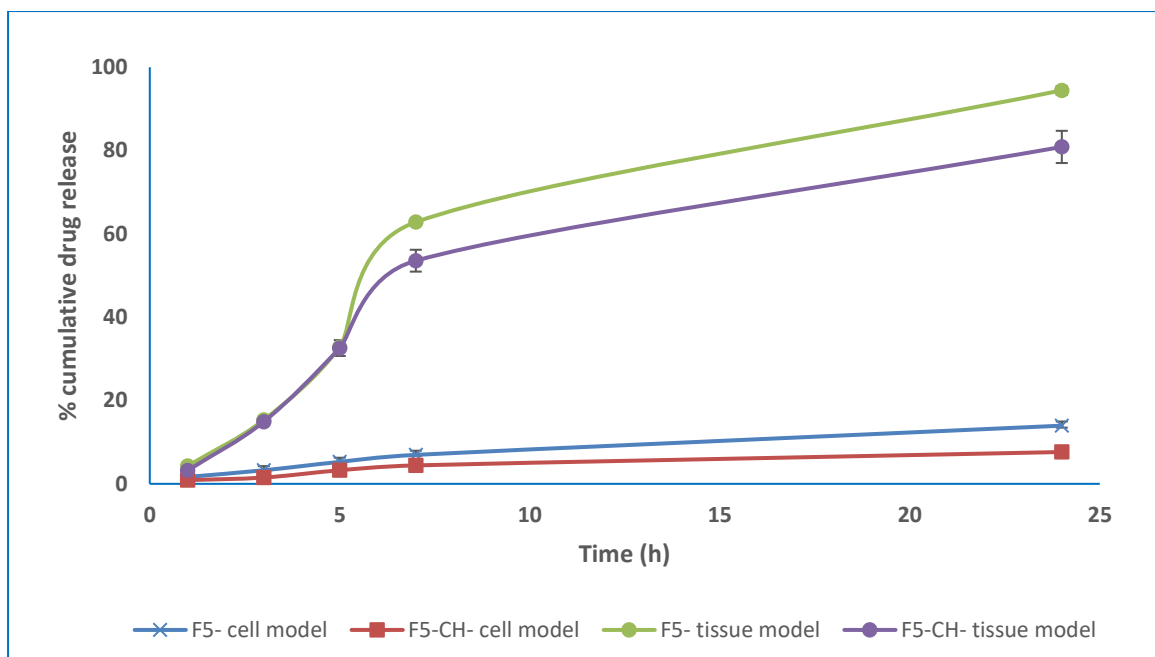


Figure 5.7 Permeation profiles (over 24 h) of F5 and F5-CH formulations using a cell-based model in comparison to the release profile from the ex vivo (tissue) model. Values are mean \pm SD for n=3 independent experiments.

Drug release from formulations (F5, F5-CH) and permeation through the cell-based model showed a similar trend to the permeation of drug through the ex vivo model (section 5.3.2). Additionally, chitosan-coated transfersomes F5-CH showed slower release than the uncoated one, with a slight but significant difference ($p < 0.05$) (Figure 5.7). Despite that, the percentage of accumulative drug permeation after 24 h was demonstrated to be 13.96% and 7.63% from formulations F5 and F5-CH, respectively.

Samples from the apical part (the top medium above cells) were also checked to explore any drug remaining on the top. An average percentage of only 2.63% and 8.28% of the drug was found remaining in the apical chamber of the cell-based model after 24 h treatment with F5 and F5-CH, respectively ($p < 0.05$).

With the total percentage of drug obtained from both apical and basolateral chambers after 24 h not exceeding 16.59% from F5 and 15.91% from F5-CH, about 85% of the drug (from

both F5 and F5-CH) probably remained trapped within the cell multilayers. Confirming this requires further investigations, such as tagging the transfersomes with a fluorescent dye to determine their exact place within the cell model. Developing similar models using other cell lines and checking the transport profile of the transfersomes through them could be another way to confirm the results are independent of the cell type used. While such further investigations would be desirable, our results clearly demonstrated the fulfilment of our aim of designing a transfersome formulation that would cross into the epithelia and remain there to release the drug slowly in eliciting its therapeutic effect.

Additionally, chitosan coating demonstrated that it would retard the transfersomes transportation through the epithelium cell layers, which could be related to its mucoadhesive properties, unlike other studies where chitosan was shown to enhance the transport of some small molecules through various barriers such as nasal and intestinal mucosa^{319,320}. It was believed that chitosan could have a permeation-enhancing effect as it works on tight junctions, but that might not be the case in buccal permeation due to the lack of tight junctions in the buccal mucosa³²¹.

Here, it is also worth mentioning that cell-based study provides a live model (living and growing cells in culture), which is not the case in the *ex vivo* model. Although the oesophagus tissue was freshly obtained from the slaughterhouse and was used within few hours, it could have been affected by the heat application during the epithelium separation. Additionally, although the *ex vivo* model for permeability testing looks simple and straightforward, it has a few limitations. The excision procedure of the tissue is the main drawback in using the *ex vivo* model, as it is a challenging and time-consuming process that requires developing good skills in order to avoid damaging the tissue during the separation and handling. Not only the

integrity of the dissected tissue but also the limited surface area which can be obtained from the buccal region, and the high individual variations were all among the limitations of using animal buccal mucosa as an *ex vivo* model for testing drug permeability^{288,293}.

On the other hand, some researchers believed that cell culture models cannot replace the *ex vivo* or *in vivo* tests due to the anatomical and physiological complexity of the human buccal tissue. For example, some studies revealed that certain APIs could permeate through the some cell culture model ten times faster than in human buccal mucosa, hence they suggested using more than one cell line to assess their permeability²⁹¹.

Therefore, to study the permeability behaviour of APIs or delivery system in general and to overcome the limitations of both methods, it is recommended to combine two different models (i.e. cell-based model and animal tissue-based model) to achieve better understanding and obtain results that are more reliable.

5.4 Conclusion

This chapter aimed to use an *ex vivo* model to draw a better understanding of the permeability of the optimised formulations, in addition to developing a cell-based model that avoids the limitations associated with the *ex vivo* study. The *ex vivo* model using the porcine oesophagus epithelium demonstrated slow permeation of both F5 and F5-CH and a sustained drug release, with cumulative percentages of 94% and 80%, respectively. Similar trends were obtained in the cell-based model, which led to the conclusion that chitosan-coated transfersomes (F5-CH) could slow the permeation and retard the drug release more than the uncoated transfersomes. The cell-based model was successfully developed using NOK cells, and it was employed to study the permeability of the formulations, but more characterisation and further investigations are needed to explain the entrapment of the formulations within

the cell layers. The developed NOK cell model is a credible starting point for future drug development.

Chapter 6. Buccal film preparation

6.1 Introduction

Following the optimisation and characterisation in the previous chapters, loading the successful coated transfersomes into a feasible and convenient dosage form is considered in this chapter. Mucoadhesive films loaded with LA are flexible, easy to use and superior to injections that induce pain, injuries and require a skilled professional to be administered.

Mucoadhesive films can be formulated as multilayer films (i.e. oral patches), usually designed with a non-dissolvable backing layer, which then need to be removed manually³²². Otherwise, they can be formulated as single-layer film that can be left in place while it erodes with time. However, single-layer films designed from a mixture of polymers have been shown to exhibit superior mucoadhesive properties to the films that were produced of single polymer³²³.

Polymers such as HPMC of several grades are commonly employed for film formation. HPMC which is a propylene glycol ether of methylcellulose, It is one of the most frequently used polymers in pharmaceutical product development, having many applications including; modified release matrix tablets, binder in granulation processes, viscosity enhancing in suspension products and as a film forming agent. In addition, it is known to be from the first generation of mucoadhesive polymers³²⁴. It is a hydrophilic polymer, soluble in water with rapid swelling properties allowing it to interact quickly with the mucus network^{325,326}. An aqueous solution of 2% w/v Metolose 603 (HPMC 300) or Metolose 606 (HPMC 600) has a viscosity of 3 cP and 6 cP respectively at room temperature.

Similarly, HPC polymer is widely employed for buccal film formation; it is non-ionic synthetic cellulose derivative, and it has aqueous solubility at temperature $>38^{\circ}\text{C}$ ^{324,327}. It is available in a range of molecular weights, viscosities and particle sizes. Klucel EXF (a commercial

available grad of HPC) has mw of 80000 and it shows viscosity of 300 -600 cP for a solution of 10% w/v. PVA is another polymer that is extensively used in film manufacturing due to its potential to form hydrogen bonds with mucin, giving the highest mucoadhesion residence time ^{324,328}.

Therefore, a mixture of polymers that demonstrated superior mucoadhesive properties in literature are usually employed to avoid the disadvantage of using buccal films that could be washed away by the saliva ^{323,324}. Some of these polymers are investigated in this research chapter and loaded with the chitosan coated transfersomes (F5-CH), aiming to reduce that risk and allow transfersomes (and drug) to pass into the buccal mucosa.

6.2 Method

The films were prepared by applying a solvent casting method as mentioned in section 2.2.11. Mixtures of polymeric solutions were cast in several combinations and ratios (Table 6.1), the polymers were selected randomly based on their reported mucoadhesive and robustness properties in film formation ³²⁴.

Table 6.1 Mixture of polymeric solutions screened for film preparation

Code	Mixture components	Ratio
BF1	HPMC 300	only
BF2	HMPC 600	only
BF3	HPMC 600 and glycerine	1:0.01
BF4	HPMC 600 and HPC	1:1
BF5	HPMC 600, HPC and glycerine	1:1:0.01
BF6	HPC	only
BF7	HPC and glycerine	1:0.01
BF8	HPC, and low MW PVA.	1:1
BF9	HPC, low MW PVA and F5-CH.	1:1:1

The mixture that gave the most convenient physical appearance was selected and further characterised as mentioned in section 2.2.12.

6.3 Results and discussion

6.3.1 Film preparation

Several mucoadhesive polymers have been investigated with and without the incorporation of plasticizer (i.e. glycerine). The development of the film was based on trial and error approach. Most of the polymeric solutions that were included in the trials, have been extensively used in the literature to produce films³²⁴⁻³²⁸, however, the choice was made depending on their tendency to produce a robust film with good mechanical integrity upon visual inspection of all prepared films under the same conditions (Table 6.2). HPMC 300 and HPMC 600 polymers totally failed to form films.

In literature, it was suggested that adding glycerine could increase the film elasticity and enhance flexibility, but on the other hand as a plasticizer it could interpose between polymer strands causing breakdown of polymer-polymer interaction and negatively affecting their film formation capability or reduce the obtained film strength ³²⁹. Therefore glycerine was added as plasticiser to HPMC 300 or HPMC 600 formulation, still it did not show any improvement and the polymers failed to produce an integrated film. Similar results were obtained when a mixture of HPC and plasticiser solution was cast, glycerine at very low percentage converted HPC (i.e. BF6) from forming a rigid and totally inflexible film to be in the form of a jelly-like mass, which did not solidify even after a longer drying time (i.e. overnight). However, drying it at a higher temperature resulted in a very porous and cracked film (Table 6.2).

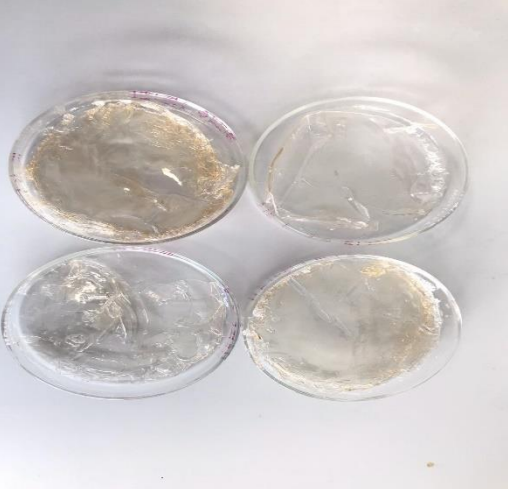
Although the mixture composed from HPC and PVA produced a non-porous and homogenous film, it lacked flexibility. While the mixture of equal ratio of HPC, PVA, and transfersomes (F5-CH) formed flexible, nonporous and homogeneous films with a very good reproducibility. Having the coated transfersomes (containing lipid and surfactant in its construction) could have enhanced the properties of the film.

It was reported in literature that the use of free surfactant could enhance achieving a uniform dispersion during the film casting and facilitates the recovery of transfersomes during the film redispersion (i.e. once it disintegrates) ^{330,331}. The uniformity enhancement is believed to be due to electrostatic stabilisation provided by free surfactant molecules ³³⁰. However, since surfactant molecules are bound within the transfersome bilayers, so their effect to enhance the film uniformity is limited to the few number of surfactant molecules that could leaked out of transfersomes. Additionally, the polymeric coating layer is suggested to enhance the film

mechanical integrity and flexibility, since including the uncoated transfersomes did not show a similar effect.

The films obtained after casting BF9 as a mixture of HPC, PVA and F5-CH transfersomes demonstrated good agreement with the reported literature ^{330,331}. Accordingly, BF9 was considered the formulation of choice and was produced in several batches for further characterisation.

Table 6.2 Descriptive results of film formation trials.

Formulation	Visual appearance	Description
BF1, BF2 & BF3		<p>- Very thin films were obtained by casting HPMC 300, HPMC 600 solution and the mixture of HPMC 600 with plasticiser, but the films were totally fragile and crispy. Although the drying time and temperature were attuned, but the same properties were observed.</p>

BF4 & BF5		<p>- The mixtures failed to form films, dry layers of precipitated polymeric solutions were observed after drying.</p>
BF6		<p>- HPC alone formed a very rigid film that lacked flexibility, and it was difficult to peel off the glass petri dish.</p>

BF7	 Two Petri dishes are shown, one above the other. Both contain a white, cracked, and somewhat sticky-looking film. The top dish shows a more uniform, though cracked, surface, while the bottom dish shows a more irregular, web-like crack pattern.	<p>- Adding plasticiser made the HPC-based film more cracked, sticky and more of a jelly-like mass.</p>
BF8 & BF9	 Two circular, smooth, yellowish films are shown, one above the other, resting on a light-colored, textured surface. The films appear uniform in color and texture, with no visible cracks or irregularities.	<p>- The mixture of HPC and PVA of low MW as a mixture with transfersomes successfully formed robust films that demonstrated enough strength and flexibility. They were easily peeled off the dish.</p>

6.3.2 Characterisation of films

Several batches were cast using formulation BF9 that proved to be the successful composition (HPC: PVA:F5-CH, i.e. v/v ratio) as intraday replicates and as fresh films over several days. Samples from many batches (total of 12) were characterised for weight uniformity, thickness, content uniformity, disintegration, pH, and tensile strength (Table 6.3).

Statistical analysis was performed for all results, however, data for weight uniformity, thickness, content uniformity and pH showed no significant differences between samples from intraday replicates or from batches produced over several days. Both disintegration time and tensile strength revealed a significant difference between samples produced over different days, as one of the produced batches demonstrated tensile strength of $581.47 \pm 29.67 \text{ N/cm}^2$ with the highest disintegration time of $4.63 \pm 0.62 \text{ min}$ with $p < 0.001$ compared to other batches. However, there is no pharmacopoeial test currently set to qualify fast disintegrating films, therefore, the majority of researchers have developed their own testing methods, and applying the standard pharmacopoeial tablet disintegration test was reported many times. Thus, less than 5 minutes disintegration time still complies with the pharmacopoeial standard of common tablets. Additionally, it was reported that film disintegration time proportionally increases with increasing the film thickness³³². Yet, the results of all batches revealed homogeneous thickness and weight with no significant differences. So, the increased disintegration time could be related to the film adherence to the wall of the chamber of the disintegration apparatus during reciprocation³³³. The thickness of the film was homogenous within films produced from the same batch, and within different batches, it is worth mentioning that the thickness value of any film is an average of several readings as described in the method and Figure 2.5.

Moreover, there is not any established standard for film mechanical properties such as tensile or puncture strength. Generally, the film should have good mechanical properties that withstand handling, allows easy placing on the buccal mucosa, and still disintegrates quickly. Therefore, both tensile and puncture strengths of the produced films could be considered good mechanical properties in comparison to marketed orodispersible film, taking into consideration the difference in disintegration times ^{323,334}.

The mean pH of a healthy oral mucosa was reported to be 6.78 ³³⁵, while the saliva pH was ranged between 6.2 to 7.6 ³³⁶. Therefore, the film pH of 7.92 was within the tolerated pH range of the mouth without inducing any soreness ³³⁶.

Table 6.3 Results of film characterisations including weight uniformity, thickness, content uniformity, disintegration time, pH, and tensile strength, n=12, mean values± SD.

Film property	Results (unit)
Weight uniformity	82.32 ± 7.6 mg
Thickness	0.178 ± 0.01 mm
Content uniformity	2.10 ± 0.17 mg 95% recovery of theoretical content (2.20 mg)
Disintegration time	2.75 ± 1.42 min
pH	7.92 ± 0.05
Tensile strength	464.68 ± 77.63 N/cm ²
Puncture strength	159.18 ± 36.76 N/cm ²

6.3.3 Film morphology

The film visual inspection showed two distinctive faces: a shiny smooth face and another pale yellow rough face, the latter was believed to be due to transfersomes having the EPC lipid that produce a yellowish colour. However, a detailed morphology of the produced film was

observed using SEM (Figure 6.1). The film appeared to be non-porous, having a smooth surface. Additionally there was a homogeneous spread of transferrins over the rough surface. Moreover, SEM images of the film edges proved that the film has two distinctive layers.

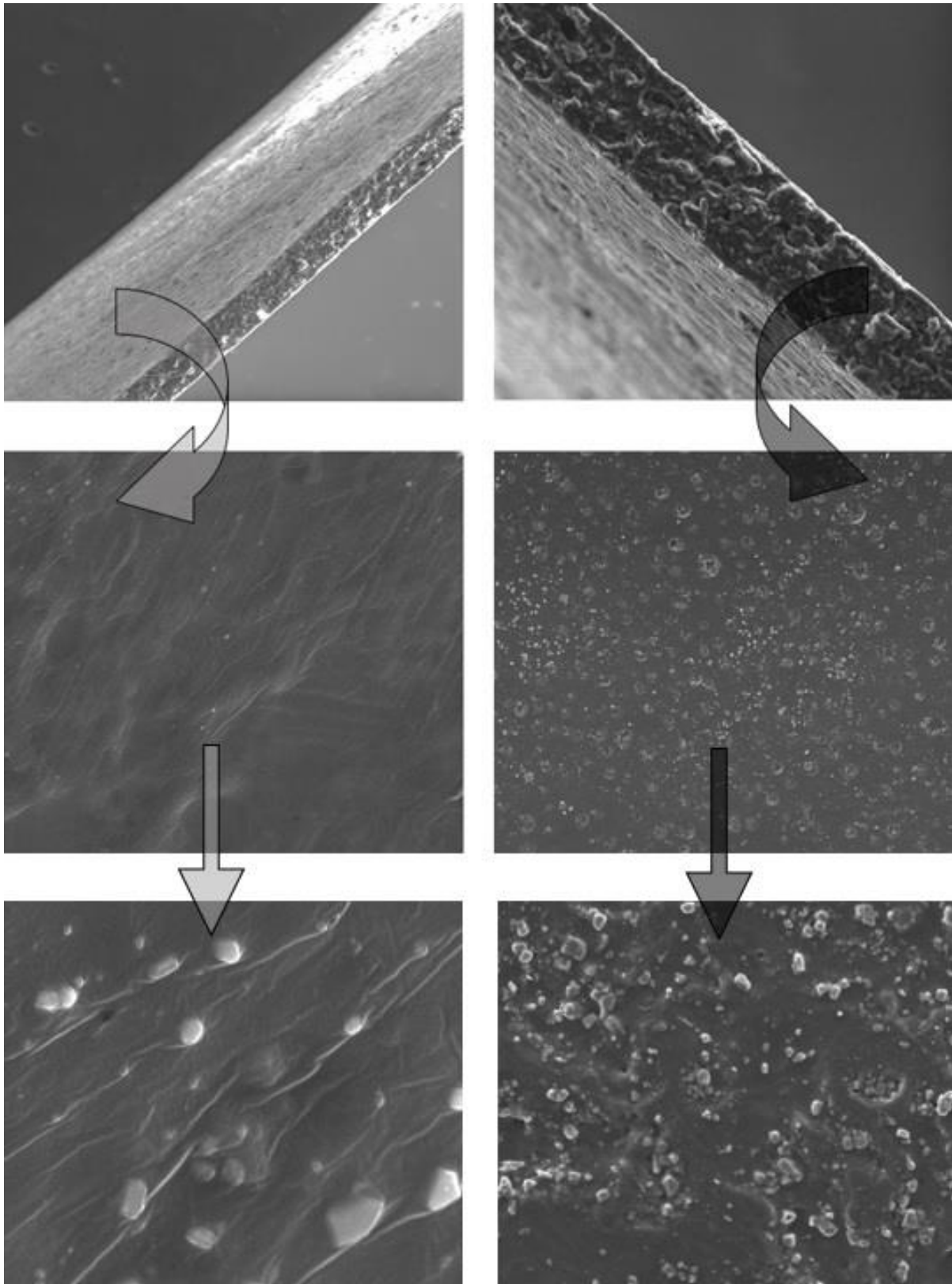


Figure 6.1 SEM images of produced film, top) images showed film edge confirming two layers, bottom) polymeric smooth surface with transfersomes embedded (left) and transfersomes rough surface (right).

However, to ensure the existence of intact transfersomes, samples from hydrated films were also checked by SEM and the images confirmed the presence of undamaged transfersomes in their spherical shape and intact layer (Figure 6.2).

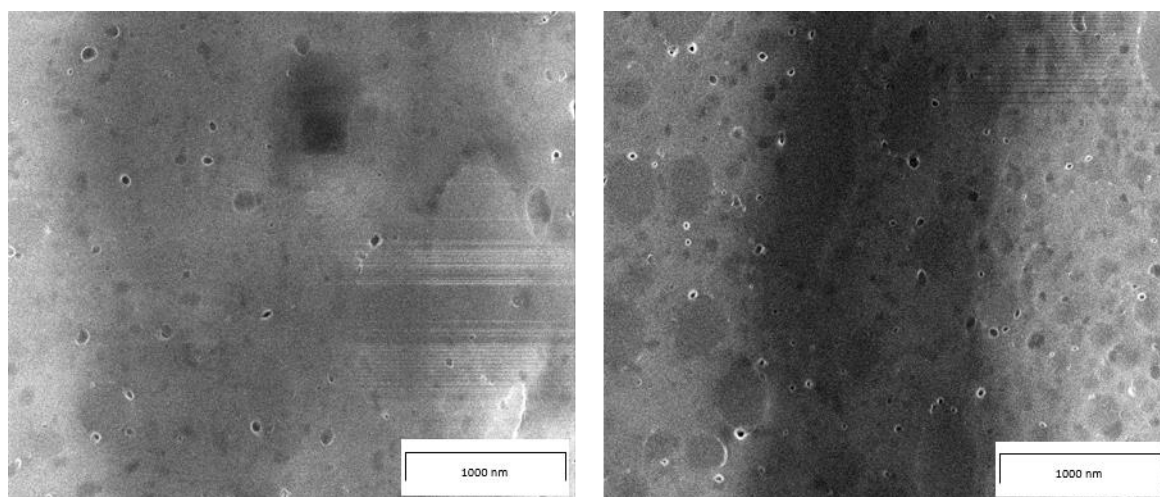


Figure 6.2 SEM images revealed the existence of intact transfersomes in two different dissolved film samples.

6.3.4 Drug release from film

The release of drug from the produced film was studied using the *ex vivo* model (i.e. using Franz diffusion cell with fresh animal mucosa). Although the drug release from transfersomes were studied in previous chapters (section 5.3.2), it was necessary to ensure the release profile from transfersomes (i.e. F5-CH) did not change after being mixed with the other polymers, such as HPC and PVA, and converted to a dry film. Several samples of the same batch and from different batches have been investigated. They demonstrated an immediate release of 13.6% after 1 h and a sustained release profile, with a 75% maximum recovery at the end of 24 h (Figure 6.3). The release profile exhibited similar trend to F5-CH release that showed a 14.90% release after 1 h with 80% after 24 h (Figure 5.5), without any significant difference in the drug release between the free F5-CH transfersomes and the one embedded

into the polymeric film. The obtained results showed that embedding transfersomes within a polymeric film did not affect their integrity and function as a delivery carrier.

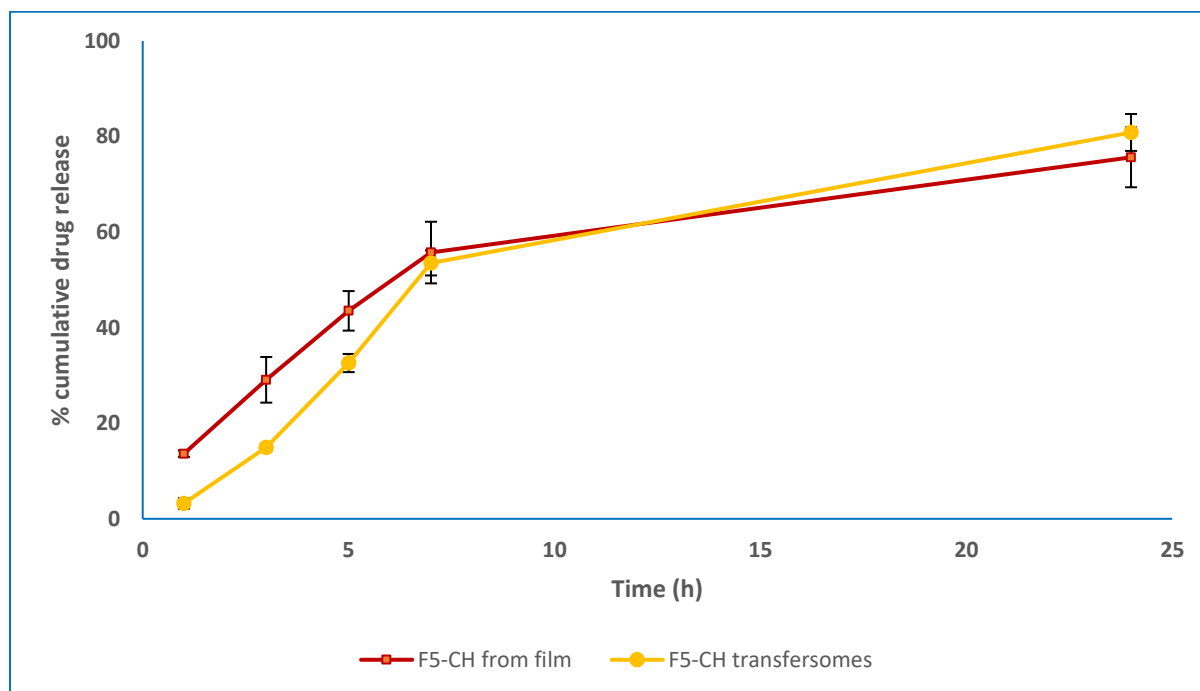


Figure 6.3 Release profile from film loaded with F5-CH transfersomes using Franz diffusion cell with fresh animal oesophagus epithelium and comparison with release from coated transfersomes (not from film), $n=3$, mean values \pm SD.

6.4 Conclusion

In this chapter, several polymers with reported mucoadhesive properties were investigated for the formation of buccal films. The solvent casting method was used to prepare the films. Upon visual inspection of the preliminary trials, a mixture of HPC and PVA with F5-CH was found to be the best formulation to produce a non-porous and homogeneous film. Therefore, several batches of the film were produced and further checked for their mechanical properties, content uniformity, disintegration, pH, morphology and release.

Overall, the produced film demonstrated good mechanical properties in comparison to the reported literature of marketed films, as well as fast disintegration, compatible pH and

uniform drug dispersion. Finally, the release profile of LA from coated transfersomes was unaffected by its loading within the polymeric film.

Chapter 7. General discussion and future work

7.1 Research overview

To meet the clinical purpose of having pain free dental practice with enhanced patient satisfaction, this research attempted to produce a novel needle-free dosage form to deliver LA by embedding several concepts together.

First concept: Nano lipid-based vesicles to sustain release of LA (Chapter 3)

Novel transfersomes were successfully optimised to sustain the release of lidocaine by using DOE approach through screening several preparation parameters. Transfersomes demonstrated nano size of less than 200 nm, with a uniform PDI ≤ 0.3 and good %EE of maximum 56% as well as a slow release of lidocaine over 24 h. Moreover, Taguchi DOE helped rank the preparation parameters according to their effect on both transfersomes size and %EE, which were found to be in the following order: EA ratio >EA type >lipid type (Figure 7.1). It was found that increasing the EA concentration up to 25% resulted in a reduction in transfersomes size; however, with a further increase in EA, would increase the size.

Additionally, a new HPLC method for lidocaine was developed and validated using a mobile phase of 30 % v/v PBS (0.01 M) and 70 % v/v Acetonitrile at a flow rate of 1 mL/min. Detection was carried out at 255 nm at 30 °C and the retention time was 2.84 minutes. Linearity was obtained over the range 0.1-2 mg/mL (R^2 0.9999). The method proved to meet the linearity, accuracy, sensitivity, intermediate precision and repeatability properties, and was shown to be valid for the analysis of lidocaine free-base according to ICH guidelines.

Second concept: Inducing a mucoadhesive coating layer (Chapter 4)

Several mucoadhesive polymers (HPMC K4M, HPMC K15M, and chitosan HCl) with reported mucoadhesive properties were evaluated to form a homogeneous coating layer around the

optimised transfersomes. A coating layer was successfully formed because all formulations showed an increased size after the coating. But transfersomes coated with HPMC K4M and K15M significantly failed to keep the nanosize or homogenous distribution that obtained with the uncoated ones. Chitosan HCl of 0.1% w/v concentration was observed to form a good coating layer with only a slight alteration to the transfersomes size and a significantly enhanced drug entrapment (84%) in comparison with uncoated transfersomes. The initial *in vitro* release testing showed a sustained release profile over 24 h with 23.4% immediate release during the first hour (Figure 7.1).

Third concept: Ensuring delivery system safety and employing more representative models for evaluation (Chapter 5)

A systematic method was used to study the safety profile of the delivery system based on a process of elimination. Toxicity screening of all ingredients at different concentrations was conducted using AB cytotoxicity test, followed by elimination of formulations containing toxic excipients such as DMPC and SDC; finally, transfersomes were produced using non-toxic concentrations and were evaluated for safety. This method enabled a greater understanding of the effect of each formulation component as well as the whole system rather than the incomplete picture previously reported in the literature.

Three different cell lines (MRC5, MRC5- SV2 and NOK) were employed to confirm the safety of coated transfersomes, which were proven to be completely safe and non-toxic at the intended concentration to be delivered.

Ex vivo testing using fresh animal mucosa (obtained from a slaughterhouse) was used to assess the delivery system permeability and draw a more precise profile than that obtained by using synthetic membrane (i.e. *in vitro* release test). The *ex vivo* model proved the

successful formation of a sustained delivery system, as the drug released from the uncoated transfersome (F5) and chitosan coated transfersomes (F5-CH) slowly with 94% and 80% drug accumulation after 24 h respectively (Figure 7.1).

This research attempted to develop cell-based model form normal oral keratinocytes. Although a successful model was obtained from NOK cells that was cheaper and more representative than the commercially available one, yet the model is a starting point for future development and improvement. The permeability results attained from employing the cell-based model showed a similar trend of sustained drug release to the *in vitro* release and *ex vivo* permeability results. However, further investigations are required to prove the accumulation and entrapment of coated transfersomes within the cell multilayers.

Fourth concept: Loading the novel and safe delivery system into a patient friendly dosage form (Chapter 6)

Fast disintegrating films that could be applied easily by patients or health-care professionals was the ultimate goal. Single layer films loaded with the coated transfersomes were developed using a mixture of mucoadhesive polymers (HPC and PVA). A simple film casting method was used and the produced films disintegrated at an average time of 2.75 min. They showed good mechanical properties and flexibility, in addition to having a pH of 7.9 that would be well tolerated in the buccal mucosa. The content uniformity was confirmed and the drug release from transfersomes was not affected by their loading into the polymeric film (Figure 7.1).

7.2 General summary of the research

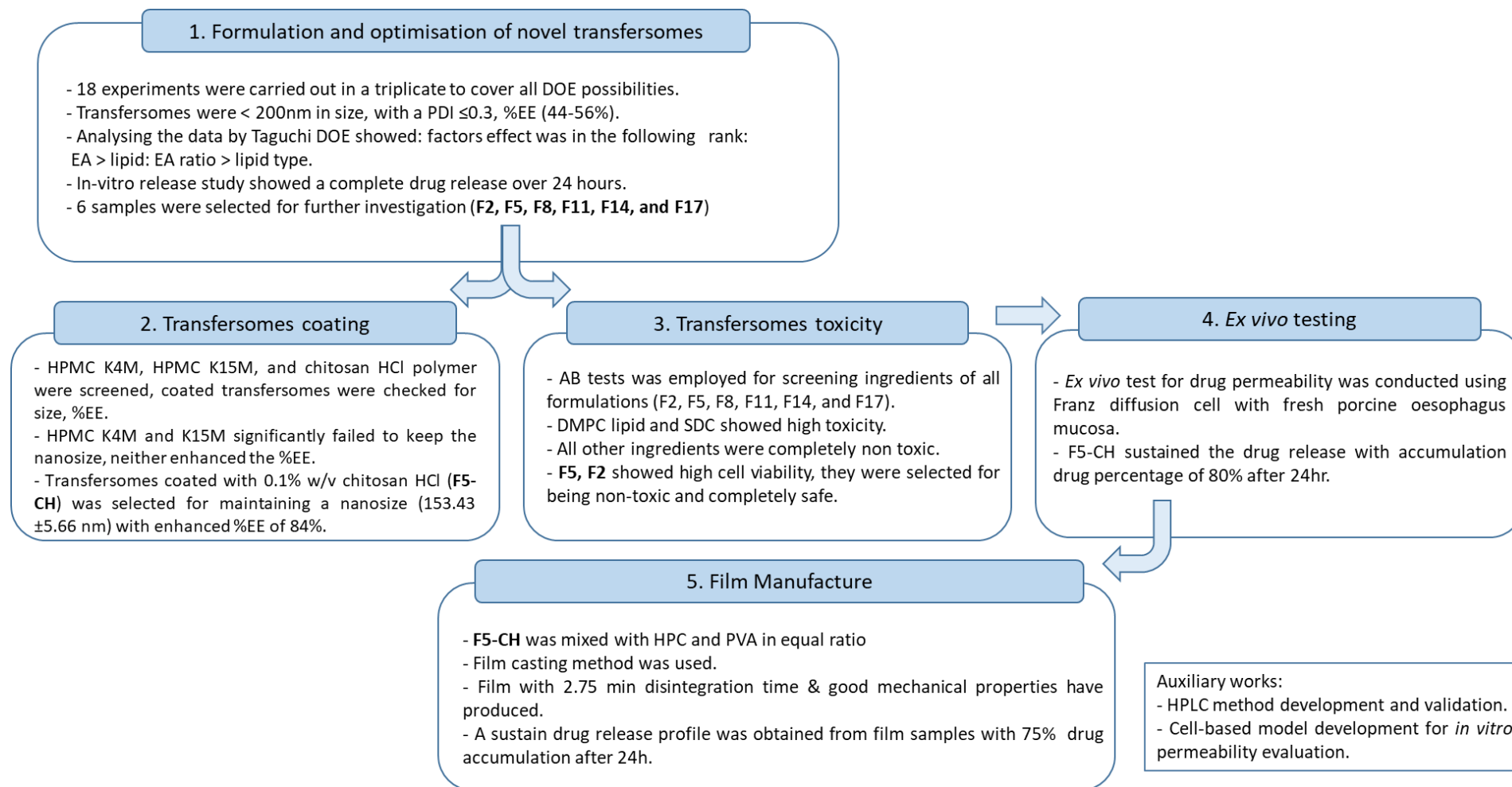


Figure 7.1 Schematic conclusion of the research.

7.3 Limitations and future work

Although this research has addressed the majority of the intended objectives, however, there were a few limitations that needed further investigation:

The main limitation of this research was finding a suitable method to purify loaded transfersomes from free drug. Although the free drug was measured every time, but that conducting all transfersomes characterisations in the absence of the free drug could be more reliable. However, few experiments have been carried out to separate free lidocaine from transfersomes such as using ultracentrifuge, centrifuge it using deuterium water (heavy water), and dialysis. Mostly all the methods used were either time consuming such as dialysis or they did not separate transfersomes from free drug like ultracentrifuge where transfersomes did not settle even at very high centrifuging force. Thus, this limitation opens a new space for development.

Moreover, there are some points requiring further development and investigation.

- 1) The developed transfersomes were characterised for most properties, however, studying their stability and finding the best storage conditions could enhance their profile and makes them more approachable.
- 2) Employing the novel transfersomes to load other LAs such as bupivacaine to prove that the trend obtained with lidocaine can be applied to several API's.
- 3) The cell-based model that was developed using NOK cells still needs further investigation. Time constraint was a main limitation of this project, therefore this model was not fully characterised, so further explorations such as ensuring the acquisition of multilayers that could be achieved by applying a fluorescence staining and checking by confocal

microscopy. Additionally, TEER value could be assessed to indicate the integrity of the model.

- 4) Buccal film was successfully prepared; however, it still needs further development by adding palatability enhancers to enhance the taste and smell, which could make it more appealing to patients.

References

1. Gupta H, Bhandari D, Sharma A. Recent trends in oral drug delivery: a review. *Recent patents on drug delivery & formulation*. 2009; 3(2):162-173.
2. Rossi S, Sandri G, Caramella CM. Buccal drug delivery: A challenge already won? *Drug Discovery Today: Technologies*. 2005; 2(1):59-65.
3. Hanif M, Zaman M, Chaurasiya V. Polymers used in buccal film: a review. *Designed Monomers and Polymers*. 2015; 18(2):105-111.
4. Sokolowski CJ, Giovannitti JA, Boynes SG. Needle Phobia: Etiology, Adverse Consequences, and Patient Management. *Dental Clinics of North America*. 2010; 54(4):731-744.
5. McMurtry CM, Pillai Riddell R, Taddio A, Racine N, Asmundson GJG, Noel M, Chambers CT, Shah V, HelpinKids, Adults T. Far From "Just a Poke": Common Painful Needle Procedures and the Development of Needle Fear. *Clin J Pain*. 2015; 31(10 Suppl):S3-S11.
6. Ballard A, Khadra C, Adler S, Doyon-Trottier E, Le May S. Efficacy of the Buzzy® device for pain management of children during needle-related procedures: a systematic review protocol. *Syst Rev*. 2018; 7(1):78-78.
7. Taddio A, Ipp M, Thivakaran S, Jamal A, Parikh C, Smart S, Sovran J, Stephens D, Katz J. Survey of the prevalence of immunization non-compliance due to needle fears in children and adults. *Vaccine*. 2012; 30(32):4807-4812.
8. Boyce D, Wempe H, Campbell C, Fuehne S, Zylstra E, Smith G, Wingard C, Jones R. ADVERSE EVENTS ASSOCIATED WITH THERAPEUTIC DRY NEEDLING. *Int J Sports Phys Ther*. 2020; 15(1):103-113.
9. Zambanini A, Feher MD. Needle Phobia in Type 1 Diabetes Mellitus. *Diabetic Medicine*. 1997; 14(4):321-323.
10. Sudhakar Y, Kuotsu K, Bandyopadhyay AK. Buccal bioadhesive drug delivery — A promising option for orally less efficient drugs. *Journal of Controlled Release*. 2006; 114(1):15-40.
11. Shojaei AH. Buccal mucosa as a route for systemic drug delivery: a review. *J Pharm Pharm Sci*. 1998; 1(1):15-30.
12. Hand AR, Frank ME. *Fundamentals of oral histology and physiology*, ed.: John Wiley & sons. 2014.
13. Johnston TP. *Anatomy and physiology of the oral mucosa*, ed.: Springer. 2015.
14. Patel VF, Liu F, Brown MB. Advances in oral transmucosal drug delivery. *Journal of Controlled Release*. 2011; 153(2):106-116.
15. Lai SK, Wang Y-Y, Hanes J. Mucus-penetrating nanoparticles for drug and gene delivery to mucosal tissues. *Advanced drug delivery reviews*. 2009; 61(2):158-171.
16. Salamat-Miller N, Chittchang M, Johnston TP. The use of mucoadhesive polymers in buccal drug delivery. *Advanced Drug Delivery Reviews*. 2005; 57(11):1666-1691.
17. Forstner J. Intestinal mucins in health and disease. *Digestion*. 1978; 17(3):234-263.
18. Patel DA, Patel M, Patel K, Patel N. Buccal mucosa as a route for systemic drug delivery: A review. *Int J Drug Dev & Res*. 2012; 4(2):99-116.
19. Roblegg E, Fröhlich E, Meindl C, Teubl B, Zaversky M, Zimmer A. Evaluation of a physiological in vitro system to study the transport of nanoparticles through the buccal mucosa. *Nanotoxicology*. 2012; 6(4):399-413.
20. Chen J, Duan H, Pan H, Yang X, Pan W. Two types of core/shell fibers based on carboxymethyl chitosan and Sodium carboxymethyl cellulose with self-assembled liposome for buccal delivery of carvedilol across TR146 cell culture and porcine buccal mucosa. *International Journal of Biological Macromolecules*. 2019; 128:700-709.
21. Abd El Azim H, Nafee N, Ramadan A, Khalafallah N. Liposomal buccal mucoadhesive film for improved delivery and permeation of water-soluble vitamins. *International journal of pharmaceutics*. 2015; 488(1):78-85.

22. Chinna Reddy P, Chaitanya KSC, Madhusudan Rao Y. A review on bioadhesive buccal drug delivery systems: current status of formulation and evaluation methods. *Daru*. 2011; 19(6):385-403.
23. Russo E, Selmin F, Baldassari S, Gennari CGM, Caviglioli G, Cilurzo F, Minghetti P, Parodi B. A focus on mucoadhesive polymers and their application in buccal dosage forms. *Journal of Drug Delivery Science and Technology*. 2016; 32:113-125.
24. Cilurzo F, Selmin F, Minghetti P, Rimoldi I, Demartin F, Montanari L. Fast-dissolving mucoadhesive microparticulate delivery system containing piroxicam. *Eur J Pharm Sci*. 2005; 24(4):355-361.
25. Cilurzo F, Selmin F, Minghetti P, Gennari CGM, Demartin F, Montanari L. Characterization and physical stability of fast-dissolving microparticles containing nifedipine. *European journal of pharmaceutics and biopharmaceutics : official journal of Arbeitsgemeinschaft fur Pharmazeutische Verfahrenstechnik eV*. 2008; 68(3):579-588.
26. Sander C, Madsen KD, Hyrup B, Nielsen HM, Rantanen J, Jacobsen J. Characterization of spray dried bioadhesive metformin microparticles for oromucosal administration. *European Journal of Pharmaceutics and Biopharmaceutics*. 2013; 85(3, Part A):682-688.
27. Monti D, Burgalassi S, Rossato MS, Albertini B, Passerini N, Rodriguez L, Chetoni P. Poloxamer 407 microspheres for orotransmucosal drug delivery. Part II: In vitro/in vivo evaluation. *International journal of pharmaceutics*. 2010; 400(1):32-36.
28. Giovino C, Ayensu I, Tetteh J, Boateng JS. Development and characterisation of chitosan films impregnated with insulin loaded PEG-b-PLA nanoparticles (NPs): A potential approach for buccal delivery of macromolecules. *International journal of pharmaceutics*. 2012; 428(1):143-151.
29. Cavallari C, Fini A, Ospitali F. Mucoadhesive multiparticulate patch for the intrabuccal controlled delivery of lidocaine. *European Journal of Pharmaceutics and Biopharmaceutics*. 2013; 83(3):405-414.
30. Al-Dhubiab BE, Nair AB, Kumria R, Attimarad M, Harsha S. Formulation and evaluation of nano based drug delivery system for the buccal delivery of acyclovir. *Colloids and Surfaces B: Biointerfaces*. 2015; 136:878-884.
31. Nidhi M, Patro MN, Kusumvalli S, Kusumdevi V. Development of transmucosal patch loaded with anesthetic and analgesic for dental procedures and in vivo evaluation. *Int J Nanomedicine*. 2016; 11:2901-2920.
32. Mouftah S, Abdel-Mottaleb MMA, Lamprecht A. Buccal delivery of low molecular weight heparin by cationic polymethacrylate nanoparticles. *International journal of pharmaceutics*. 2016; 515(1):565-574.
33. Abruzzo A, Cerchiara T, Bigucci F, Gallucci MC, Luppi B. Mucoadhesive Buccal Tablets Based on Chitosan/Gelatin Microparticles for Delivery of Propranolol Hydrochloride. *Journal of Pharmaceutical Sciences*. 2015; 104(12):4365-4372.
34. Ali J, Khar RK, Ahuja A. Formulation and characterisation of a buccoadhesive erodible tablet for the treatment of oral lesions. *Pharmazie*. 1998; 53(5):329-334.
35. Almeida L, Oshiro Júnior JA, Silva M, Nóbrega F, Andrade J, Santos W, Ribeiro A, Conceição M, Veras G, Medeiros AC. Tablet of Ximenia Americana L. Developed from Mucoadhesive Polymers for Future Use in Oral Treatment of Fungal Infections. *Polymers (Basel)*. 2019; 11(2):379.
36. Fini A, Bergamante V, Ceschel GC. Mucoadhesive gels designed for the controlled release of chlorhexidine in the oral cavity. *Pharmaceutics*. 2011; 3(4):665-679.
37. Nafee NA, Boraie MA, Ismail FA, Mortada LM. Design and characterization of mucoadhesive buccal patches containing cetylpyridinium chloride. *Acta Pharm*. 2003; 53(3):199-212.
38. Perioli L, Ambrogi V, Angelici F, Ricci M, Giovagnoli S, Capuccella M, Rossi C. Development of mucoadhesive patches for buccal administration of ibuprofen. *Journal of Controlled Release*. 2004; 99(1):73-82.
39. Yehia SA, El-Gazayerly ON, Basalious EB. Fluconazole mucoadhesive buccal films: in vitro/in vivo performance. *Current drug delivery*. 2009; 6(1):17-27.

40. Morales JO, McConville JT. Manufacture and characterization of mucoadhesive buccal films. *European Journal of Pharmaceutics and Biopharmaceutics*. 2011; 77(2):187-199.
41. Asane GS, Nirmal SA, Rasal KB, Naik AA, Mahadik MS, Rao YM. Polymers for Mucoadhesive Drug Delivery System: A Current Status. *Drug development and industrial pharmacy*. 2008; 34(11):1246-1266.
42. Ahmadi F, Oveisi Z, Samani SM, Amoozgar Z. Chitosan based hydrogels: characteristics and pharmaceutical applications. *Res Pharm Sci*. 2015; 10(1):1-16.
43. Tiwari G, Tiwari R, Sriwastawa B, Bhati L, Pandey S, Pandey P, Bannerjee SK. Drug delivery systems: An updated review. *Int J Pharm Investig*. 2012; 2(1):2-11.
44. Onoue S, Yamada S, Chan H-K. Nanodrugs: pharmacokinetics and safety. *Int J Nanomedicine*. 2014; 9:1025-1037.
45. Singh R, Vyas SP. Topical liposomal system for localized and controlled drug delivery. *Journal of Dermatological Science*. 1996; 13(2):107-111.
46. Bansal S, Kashyap CP, Aggarwal G, Harikumar S. A comparative review on vesicular drug delivery system and stability issues. *Int J Res Pharm Chem*. 2012; 2(3):704-713.
47. Abdus S, Sultana Y, Aqil M. Liposomal Drug Delivery Systems: An Update Review. *Current Drug Delivery*. 2007; 4(4):297-305.
48. Jain S, Jain V, Mahajan S. Lipid based vesicular drug delivery systems. *Advances in Pharmaceutics*. 2014.
49. Kraft JC, Freeling JP, Wang Z, Ho RJY. Emerging Research and Clinical Development Trends of Liposome and Lipid Nanoparticle Drug Delivery Systems. *Journal of Pharmaceutical Sciences*. 2014; 103(1):29-52.
50. Biju S, Talegaonkar S, Mishra P, Khar R. Vesicular systems: an overview. *Indian Journal of Pharmaceutical Sciences*. 2006; 68(2).
51. Akbarzadeh A, Rezaei-Sadabady R, Davaran S, Joo SW, Zarghami N, Hanifehpour Y, Samiei M, Kouhi M, Nejati-Koshki K. Liposome: classification, preparation, and applications. *Nanoscale Res Lett*. 2013; 8(1):102-102.
52. El Maghraby GMM, Williams AC, Barry BW. Oestradiol skin delivery from ultradeformable liposomes: refinement of surfactant concentration. *International journal of pharmaceutics*. 2000; 196(1):63-74.
53. Hayashi K, Shimanouchi T, Kato K, Miyazaki T, Nakamura A, Umakoshi H. Span 80 vesicles have a more fluid, flexible and "wet" surface than phospholipid liposomes. *Colloids and Surfaces B: Biointerfaces*. 2011; 87(1):28-35.
54. Hua S. Lipid-based nano-delivery systems for skin delivery of drugs and bioactives. *Front Pharmacol*. 2015; 6:219-219.
55. Bnyan R, Khan I, Ehtezazi T, Saleem I, Gordon S, O'Neill F, Roberts M. Surfactant Effects on Lipid-Based Vesicles Properties. *Journal of Pharmaceutical Sciences*. 2018; 107(5):1237-1246.
56. Lian T, Ho RJY. Trends and Developments in Liposome Drug Delivery Systems. *Journal of Pharmaceutical Sciences*. 2001; 90(6):667-680.
57. Bulbake U, Doppalapudi S, Kommineni N, Khan W. Liposomal Formulations in Clinical Use: An Updated Review. *Pharmaceutics*. 2017; 9(2):12.
58. Kazi KM, Mandal AS, Biswas N, Guha A, Chatterjee S, Behera M, Kuotsu K. Niosome: A future of targeted drug delivery systems. *J Adv Pharm Technol Res*. 2010; 1(4):374-380.
59. Marianecchi C, Di Marzio L, Rinaldi F, Celia C, Paolino D, Alhaique F, Esposito S, Carafa M. Niosomes from 80s to present: The state of the art. *Advances in Colloid and Interface Science*. 2014; 205:187-206.
60. Jain S, Jain P, Umamaheshwari RB, Jain NK. Transfersomes a novel vesicular carrier for enhanced transdermal delivery: development, characterization, and performance evaluation. *Drug development and industrial pharmacy*. 2003; 29(9):1013-1026.

61. Ascenso A, Raposo S, Batista C, Cardoso P, Mendes T, Praça FG, Bentley MVLB, Simões S. Development, characterization, and skin delivery studies of related ultradeformable vesicles: transfersomes, ethosomes, and transethosomes. *Int J Nanomedicine*. 2015; 10:5837-5851.
62. Pawar AY. Transfersome: a novel technique which improves transdermal permeability. *Asian Journal of Pharmaceutics (AJP): Free full text articles from Asian J Pharm*. 2016; 10(04).
63. Maheshwari RGS, Tekade RK, Sharma PA, Darwhekar G, Tyagi A, Patel RP, Jain DK. Ethosomes and ultradeformable liposomes for transdermal delivery of clotrimazole: A comparative assessment. *Saudi Pharm J*. 2012; 20(2):161-170.
64. Pratima NA, Shailee T. Ethosomes: A Novel Tool for Transdermal Drug Delivery. *International Journal of Research in Pharmacy & Science*. 2012; 2(1).
65. Chen ZX, Li B, Liu T, Wang X, Zhu Y, Wang L, Wang XH, Niu X, Xiao Y, Sun Q. Evaluation of paeonol-loaded transethosomes as transdermal delivery carriers. *European Journal of Pharmaceutical Sciences*. 2017; 99:240-245.
66. Palozza P, Muzzalupo R, Trombino S, Valdannini A, Picci N. Solubilization and stabilization of β -carotene in niosomes: delivery to cultured cells. *Chemistry and Physics of Lipids*. 2006; 139(1):32-42.
67. Verma P, Pathak K. Therapeutic and cosmeceutical potential of ethosomes: An overview. *J Adv Pharm Technol Res*. 2010; 1(3):274-282.
68. Khan I, Yousaf S, Subramanian S, Korale O, Alhnan MA, Ahmed W, Taylor KMG, Elhissi A. Proliposome powders prepared using a slurry method for the generation of beclometasone dipropionate liposomes. *International journal of pharmaceutics*. 2015; 496(2):342-350.
69. Khan I, Yousaf S, Subramanian S, Alhnan MA, Ahmed W, Elhissi A. Proliposome Powders for the Generation of Liposomes: the Influence of Carbohydrate Carrier and Separation Conditions on Crystallinity and Entrapment of a Model Antiasthma Steroid. *AAPS PharmSciTech*. 2018; 19(1):262-274.
70. Zhdanov RI, Podobed OV, Vlassov VV. Cationic lipid–DNA complexes—lipoplexes—for gene transfer and therapy. *Bioelectrochemistry*. 2002; 58(1):53-64.
71. Tadros TF. *Applied Surfactants: Principles and Applications* Wiley, ed.: VCH Verlag GmbH & Co Weinheim. 2005.
72. Rosen MJ, Kunjappu JT. *Surfactants and interfacial phenomena*, ed.: John Wiley & Sons. 2012.
73. Gadberry JF. Other Types of Surfactants. *Chemistry and Technology of Surfactants*. 2006:153.
74. Kronberg B, Lindman B. *Surfactants and polymers in aqueous solution*, ed.: John Wiley & Sons Ltd., Chichester. 2003.
75. Summerton E, Zimbitas G, Britton M, Bakalis S. Low temperature stability of surfactant systems. *Trends in Food Science & Technology*. 2017; 60:23-30.
76. Tsubone K, Rosen MJ. Structural Effect on Surface Activities of Anionic Surfactants Having N-acyl-N-methylamide and Carboxylate Groups. *Journal of Colloid and Interface Science*. 2001; 244(2):394-398.
77. Perger T-M, Bešter-Rogač M. Thermodynamics of micelle formation of alkyltrimethylammonium chlorides from high performance electric conductivity measurements. *Journal of Colloid and Interface Science*. 2007; 313(1):288-295.
78. Zdziennicka A, Szymczyk K, Krawczyk J, Jańczuk B. Critical micelle concentration of some surfactants and thermodynamic parameters of their micellization. *Fluid Phase Equilibria*. 2012; 322:126-134.
79. Purkait MK, DasGupta S, De S. Performance of TX-100 and TX-114 for the separation of chrysoidine dye using cloud point extraction. *Journal of Hazardous Materials*. 2006; 137(2):827-835.
80. Chauhan S, Kaur M, Kumar K, Chauhan MS. Study of the effect of electrolyte and temperature on the critical micelle concentration of dodecyltrimethylammonium bromide in aqueous medium. *The Journal of Chemical Thermodynamics*. 2014; 78:175-181.
81. Chauhan S, Sharma K. Effect of temperature and additives on the critical micelle concentration and thermodynamics of micelle formation of sodium dodecyl benzene sulfonate and

- dodecyltrimethylammonium bromide in aqueous solution: a conductometric study. *The Journal of Chemical Thermodynamics*. 2014; 71:205-211.
82. Southall NT, Dill KA, Haymet ADJ. A View of the Hydrophobic Effect. *The Journal of Physical Chemistry B*. 2002; 106(3):521-533.
 83. Maibaum L, Dinner AR, Chandler D. Micelle Formation and the Hydrophobic Effect. *The Journal of Physical Chemistry B*. 2004; 108(21):6778-6781.
 84. Myers D. *Surfactant science and technology*, ed.: John Wiley & Sons. 2005.
 85. Som I, Bhatia K, Yasir M. Status of surfactants as penetration enhancers in transdermal drug delivery. *J Pharm Bioallied Sci*. 2012; 4(1):2-9.
 86. Raffa P, Wever DAZ, Picchioni F, Broekhuis AA. Polymeric Surfactants: Synthesis, Properties, and Links to Applications. *Chemical Reviews*. 2015; 115(16):8504-8563.
 87. Lutz JF. Solution self-assembly of tailor-made macromolecular building blocks prepared by controlled radical polymerization techniques. *Polymer international*. 2006; 55(9):979-993.
 88. Griffin WC. Classification of surface-active agents by "HLB". *J Soc Cosmet Chem*. 1949; 1:311-326.
 89. Trotta M, Peira E, Debernardi F, Gallarate M. Elastic liposomes for skin delivery of dipotassium glycyrrhizinate. *International journal of pharmaceutics*. 2002; 241(2):319-327.
 90. Kumar GP, Rajeshwarrao P. Nonionic surfactant vesicular systems for effective drug delivery—an overview. *Acta Pharmaceutica Sinica B*. 2011; 1(4):208-219.
 91. Chaudhary H, Kohli K, Kumar V. Nano-transfersomes as a novel carrier for transdermal delivery. *International journal of pharmaceutics*. 2013; 454(1):367-380.
 92. Singh S, Vardhan H, Kotla NG, Maddiboyina B, Sharma D, Webster TJ. The role of surfactants in the formulation of elastic liposomal gels containing a synthetic opioid analgesic. *Int J Nanomedicine*. 2016; 11:1475-1482.
 93. Freitas C, Müller RH. Effect of light and temperature on zeta potential and physical stability in solid lipid nanoparticle (SLN™) dispersions. *International journal of pharmaceutics*. 1998; 168(2):221-229.
 94. Al Shuwaili AH, Rasool BKA, Abdulrasool AA. Optimization of elastic transfersomes formulations for transdermal delivery of pentoxifylline. *European Journal of Pharmaceutics and Biopharmaceutics*. 2016; 102:101-114.
 95. Barbosa RM, Severino P, Preté PSC, Santana MHA. Influence of different surfactants on the physicochemical properties of elastic liposomes. *Pharmaceutical Development and Technology*. 2017; 22(3):360-369.
 96. van den Bergh BAI, Bouwstra JA, Junginger HE, Wertz PW. Elasticity of vesicles affects hairless mouse skin structure and permeability. *Journal of Controlled Release*. 1999; 62(3):367-379.
 97. van den Bergh BAI, Vroom J, Gerritsen H, Junginger HE, Bouwstra JA. Interactions of elastic and rigid vesicles with human skin in vitro: electron microscopy and two-photon excitation microscopy. *Biochimica et Biophysica Acta (BBA) - Biomembranes*. 1999; 1461(1):155-173.
 98. Duangjit S, Pamornpathomkul B, Opanasopit P, Rojanarata T, Obata Y, Takayama K, Ngawhirunpat T. Role of the charge, carbon chain length, and content of surfactant on the skin penetration of meloxicam-loaded liposomes. *Int J Nanomedicine*. 2014; 9:2005-2017.
 99. Ali MH, Moghaddam B, Kirby DJ, Mohammed AR, Perrie Y. The role of lipid geometry in designing liposomes for the solubilisation of poorly water soluble drugs. *International journal of pharmaceutics*. 2013; 453(1):225-232.
 100. Park S-I, Lee E-O, Kim JW, Kim YJ, Han SH, Kim J-D. Polymer-hybridized liposomes anchored with alkyl grafted poly(asparagine). *Journal of colloid and interface science*. 2011; 364(1):31-38.
 101. Gupta M, Vaidya B, Mishra N, Vyas SP. Effect of Surfactants on the Characteristics of Fluconazole Niosomes for Enhanced Cutaneous Delivery. *Artificial Cells, Blood Substitutes, and Biotechnology*. 2011; 39(6):376-384.

102. Van Hal DA, Bouwstra JA, van Rensen A, Jeremiassé E, de Vringer T, Junginger HE. Preparation and characterization of nonionic surfactant vesicles. *Journal of colloid and interface science*. 1996; 178(1):263-273.
103. Varshosaz J, Pardakhty A, Hajhashemi V-i, Najafabadi AR. Development and Physical Characterization of Sorbitan Monoester Niosomes for Insulin Oral Delivery. *Drug Delivery*. 2003; 10(4):251-262.
104. Taymouri S, Varshosaz J. Effect of different types of surfactants on the physical properties and stability of carvedilol nano-niosomes. *Adv Biomed Res*. 2016; 5:48-48.
105. Socaciu C, Jessel R, Diehl HA. Competitive carotenoid and cholesterol incorporation into liposomes: effects on membrane phase transition, fluidity, polarity and anisotropy. *Chemistry and Physics of Lipids*. 2000; 106(1):79-88.
106. Moazeni E, Gilani K, Sotoudegan F, Pardakhty A, Najafabadi AR, Ghalandari R, Fazeli MR, Jamalifar H. Formulation and in vitro evaluation of ciprofloxacin containing niosomes for pulmonary delivery. *Journal of Microencapsulation*. 2010; 27(7):618-627.
107. Saitejaswi R, Swapna S, Madhu B, Bakshi V. Formulation and evaluation of lornoxicam loaded transfersome gel. *Eur J Biomed Pharm Sci*. 2016; 3:144-150.
108. Mishra D, Garg M, Dubey V, Jain S, Jain NK. Elastic Liposomes Mediated Transdermal Delivery of an Anti-Hypertensive Agent: Propranolol Hydrochloride. *Journal of Pharmaceutical Sciences*. 2007; 96(1):145-155.
109. Hao Y, Zhao F, Li N, Yang Y, Li Ka. Studies on a high encapsulation of colchicine by a niosome system. *International journal of pharmaceutics*. 2002; 244(1):73-80.
110. Patel R, Singh S, Singh S, Sheth N, Gendle R. Development and characterization of curcumin loaded transfersome for transdermal delivery. *Journal of pharmaceutical sciences and research*. 2009; 1(4):71.
111. Malakar J, Sen SO, Nayak AK, Sen KK. Formulation, optimization and evaluation of transferosomal gel for transdermal insulin delivery. *Saudi Pharm J*. 2012; 20(4):355-363.
112. El-Laithy HM, Shoukry O, Mahran LG. Novel sugar esters proniosomes for transdermal delivery of vinpocetine: Preclinical and clinical studies. *European Journal of Pharmaceutics and Biopharmaceutics*. 2011; 77(1):43-55.
113. Zheng W-s, Fang X-q, Wang L-l, Zhang Y-j. Preparation and quality assessment of itraconazole transfersomes. *International journal of pharmaceutics*. 2012; 436(1):291-298.
114. Bernsdorff C, Wolf A, Winter R, Gratton E. Effect of hydrostatic pressure on water penetration and rotational dynamics in phospholipid-cholesterol bilayers. *Biophys J*. 1997; 72(3):1264-1277.
115. Mohammed AR, Weston N, Coombes AGA, Fitzgerald M, Perrie Y. Liposome formulation of poorly water soluble drugs: optimisation of drug loading and ESEM analysis of stability. *International journal of pharmaceutics*. 2004; 285(1):23-34.
116. Cipolla D, Wu H, Gonda I, Eastman S, Redelmeier T, Chan H-K. Modifying the Release Properties of Liposomes Toward Personalized Medicine. *Journal of Pharmaceutical Sciences*. 2014; 103(6):1851-1862.
117. Guinedi AS, Mortada ND, Mansour S, Hathout RM. Preparation and evaluation of reverse-phase evaporation and multilamellar niosomes as ophthalmic carriers of acetazolamide. *International journal of pharmaceutics*. 2005; 306(1):71-82.
118. Junyaprasert VB, Singhsa P, Suksiriworapong J, Chantasart D. Physicochemical properties and skin permeation of Span 60/Tween 60 niosomes of ellagic acid. *International journal of pharmaceutics*. 2012; 423(2):303-311.
119. Bala I, Bhardwaj V, Hariharan S, Kumar MNVR. Analytical methods for assay of ellagic acid and its solubility studies. *Journal of Pharmaceutical and Biomedical Analysis*. 2006; 40(1):206-210.
120. Uchegbu IF, Vyas SP. Non-ionic surfactant based vesicles (niosomes) in drug delivery. *International journal of pharmaceutics*. 1998; 172(1):33-70.

121. Manosroi A, Wongtrakul P, Manosroi J, Sakai H, Sugawara F, Yuasa M, Abe M. Characterization of vesicles prepared with various non-ionic surfactants mixed with cholesterol. *Colloids and Surfaces B: Biointerfaces*. 2003; 30(1):129-138.
122. Tabbakhian M, Tavakoli N, Jaafari MR, Daneshamouz S. Enhancement of follicular delivery of finasteride by liposomes and niosomes: 1. In vitro permeation and in vivo deposition studies using hamster flank and ear models. *International journal of pharmaceutics*. 2006; 323(1):1-10.
123. Yoshioka T, Sternberg B, Florence AT. Preparation and properties of vesicles (niosomes) of sorbitan monoesters (Span 20, 40, 60 and 80) and a sorbitan triester (Span 85). *International journal of pharmaceutics*. 1994; 105(1):1-6.
124. Mokhtar M, Sammour OA, Hammad MA, Megrab NA. Effect of some formulation parameters on flurbiprofen encapsulation and release rates of niosomes prepared from proniosomes. *International journal of pharmaceutics*. 2008; 361(1):104-111.
125. El Zaafarany GM, Awad GAS, Holayel SM, Mortada ND. Role of edge activators and surface charge in developing ultradeformable vesicles with enhanced skin delivery. *International journal of pharmaceutics*. 2010; 397(1):164-172.
126. Bayindir ZS, Yuksel N. Characterization of niosomes prepared with various nonionic surfactants for paclitaxel oral delivery. *Journal of Pharmaceutical Sciences*. 2010; 99(4):2049-2060.
127. Mahale NB, Thakkar PD, Mali RG, Walunj DR, Chaudhari SR. Niosomes: Novel sustained release nonionic stable vesicular systems — An overview. *Advances in Colloid and Interface Science*. 2012; 183-184:46-54.
128. Aboud HM, Ali AA, El-Menshawe SF, Elbary AA. Nanotransfersomes of carvedilol for intranasal delivery: formulation, characterization and in vivo evaluation. *Drug Delivery*. 2016; 23(7):2471-2481.
129. Shaji J, Lal M. Preparation, optimization and evaluation of transferosomal formulation for enhanced transdermal delivery of a COX-2 inhibitor. *Int J Pharm Pharm Sci*. 2014; 6(1):467-477.
130. Yang Y, Ou R, Guan S, Ye X, Hu B, Zhang Y, Lu S, Zhou Y, Yuan Z, Zhang J, Li Q-g. A novel drug delivery gel of terbinafine hydrochloride with high penetration for external use. *Drug Delivery*. 2015; 22(8):1086-1093.
131. Elsayed MMA, Abdallah OY, Naggat VF, Khalafallah NM. Deformable liposomes and ethosomes: Mechanism of enhanced skin delivery. *International journal of pharmaceutics*. 2006; 322(1):60-66.
132. Kang SN, Hong S-S, Kim S-Y, Oh H, Lee M-K, Lim S-J. Enhancement of liposomal stability and cellular drug uptake by incorporating tributyrin into celecoxib-loaded liposomes. *Asian Journal of Pharmaceutical Sciences*. 2013; 8(2):128-133.
133. A. Namdeo NKJ. Niosomal delivery of 5-fluorouracil. *Journal of Microencapsulation*. 1999; 16(6):731-740.
134. Uchegbu IF, Double JA, Turton JA, Florence AT. Distribution, metabolism and tumoricidal activity of doxorubicin administered in sorbitan monostearate (Span 60) niosomes in the mouse. *Pharmaceutical research*. 1995; 12(7):1019-1024.
135. Bragagni M, Mennini N, Ghelardini C, Mura P. Development and characterization of niosomal formulations of doxorubicin aimed at brain targeting. *Journal of Pharmacy & Pharmaceutical Sciences*. 2012; 15(1):184-196.
136. Rajnish A, Ajay S. Release Studies of Ketoprofen Niosome Formulation. *J Chem*. 2010; 2(1):79-82.
137. Confalonieri E, Soraci A, Becaluba M, Denzoin L, Rodriguez E, Riccio B, Tapia O. The disposition of free and niosomally encapsulated Rac-flurbiprofen in dairy bovines. *Journal of veterinary pharmacology and therapeutics*. 2010; 33(1):9-14.
138. El-Menshawe SF, Hussein AK. Formulation and evaluation of meloxicam niosomes as vesicular carriers for enhanced skin delivery. *Pharmaceutical Development and Technology*. 2013; 18(4):779-786.
139. Huang Y, Han G, Wang H, Liang W. Cationic niosomes as gene carriers: preparation and cellular uptake in vitro. *Pharmazie*. 2005; 60(6):473-474.

140. Abu-Huwajj R, Assaf S, Salem M, Sallam A. Potential Mucoadhesive Dosage Form of Lidocaine Hydrochloride: II. In Vitro and In Vivo Evaluation. *Drug development and industrial pharmacy*. 2007; 33(4):437-448.
141. Ganem-Quintanar A, Quintanar-Guerrero D, Falson-Rieg F, Buri P. Ex vivo oral mucosal permeation of lidocaine hydrochloride with sucrose fatty acid esters as absorption enhancers. *International journal of pharmaceutics*. 1998; 173(1-2):203-210.
142. Uchegbu IF, Florence AT. Non-ionic surfactant vesicles (niosomes): Physical and pharmaceutical chemistry. *Advances in Colloid and Interface Science*. 1995; 58(1):1-55.
143. Mohanty A, Dey J. Effect of the Headgroup Structure on the Aggregation Behavior and Stability of Self-Assemblies of Sodium N-[4-(n-Dodecyloxy)benzoyl]-l-aminoacidates in Water. *Langmuir*. 2007; 23(3):1033-1040.
144. Gianasi E, Cociancich F, Uchegbu IF, Florence AT, Duncan R. Pharmaceutical and biological characterisation of a doxorubicin-polymer conjugate (PK1) entrapped in sorbitan monostearate Span 60 niosomes. *International journal of pharmaceutics*. 1997; 148(2):139-148.
145. Nasr M, Mansour S, Mortada ND, Elshamy AA. Vesicular aceclofenac systems: A comparative study between liposomes and niosomes. *Journal of Microencapsulation*. 2008; 25(7):499-512.
146. Hofland HEJ, Bouwstra JA, Gooris GS, Spies F, Talsma H, Junginger HE. Nonionic Surfactant Vesicles: A Study of Vesicle Formation, Characterization, and Stability. *Journal of Colloid and Interface Science*. 1993; 161(2):366-376.
147. Sakai T, Ikoshi R, Toshida N, Kagaya M. Thermodynamically Stable Vesicle Formation and Vesicle-to-Micelle Transition of Single-Tailed Anionic Surfactant in Water. *The Journal of Physical Chemistry B*. 2013; 117(17):5081-5089.
148. Pattni BS, Chupin VV, Torchilin VP. New Developments in Liposomal Drug Delivery. *Chemical Reviews*. 2015; 115(19):10938-10966.
149. Reeves JP, Dowben RM. Formation and properties of thin-walled phospholipid vesicles. *Journal of Cellular Physiology*. 1969; 73(1):49-60.
150. Biswas S, Dodwadkar NS, Deshpande PP, Torchilin VP. Liposomes loaded with paclitaxel and modified with novel triphenylphosphonium-PEG-PE conjugate possess low toxicity, target mitochondria and demonstrate enhanced antitumor effects in vitro and in vivo. *Journal of Controlled Release*. 2012; 159(3):393-402.
151. Popa R, Vrânceanu M, Nikolaus S, Nirschl H, Lenewit G. Entrance Effects at Nanopores of Nanocapsules Functionalized with Poly(ethylene glycol) and Their Flow through Nanochannels. *Langmuir*. 2008; 24(22):13030-13036.
152. Machado AR, de Assis LM, Machado MIR, de Souza-Soares LA. Importance of lecithin for encapsulation processes. *African Journal of Food Science*. 2014; 8(4):176-183.
153. Stano P, Bufali S, Pisano C, Bucci F, Barbarino M, Santaniello M, Carminati P, Luisi PL. Novel Camptothecin Analogue (Gimatecan)-Containing Liposomes Prepared by the Ethanol Injection Method. *Journal of liposome research*. 2004; 14(1-2):87-109.
154. Maherani B, Arab-Tehrany E, R Mozafari M, Gaiani C, Linder M. Liposomes: a review of manufacturing techniques and targeting strategies. *Current nanoscience*. 2011; 7(3):436-452.
155. Meure LA, Foster NR, Dehghani F. Conventional and Dense Gas Techniques for the Production of Liposomes: A Review. *AAPS PharmSciTech*. 2008; 9(3):798.
156. Mozafari MR. Liposomes: an overview of manufacturing techniques. *Cellular and Molecular Biology Letters*. 2005; 10(4):711.
157. Laouini A, Jaafar-Maalej C, Limaryem-Blouza I, Sfar S, Charcosset C, Fessi H. Preparation, characterization and applications of liposomes: state of the art. *Journal of colloid Science and Biotechnology*. 2012; 1(2):147-168.
158. van Swaay D, DeMello A. Microfluidic methods for forming liposomes. *Lab on a Chip*. 2013; 13(5):752-767.
159. Jahn A, Stavis SM, Hong JS, Vreeland WN, DeVoe DL, Gaitan M. Microfluidic Mixing and the Formation of Nanoscale Lipid Vesicles. *ACS Nano*. 2010; 4(4):2077-2087.

160. Patil YP, Jadhav S. Novel methods for liposome preparation. *Chemistry and Physics of Lipids*. 2014; 177:8-18.
161. Rogobete AF, Dragomirescu M, Bedreag OH, Sandesc D, Cradigati CA, Sarandan M, Papurica M, Popovici SE, Vernic C, Preda G. New aspects of controlled release systems for local anaesthetics: A review. *Trends in Anaesthesia and Critical Care*. 2016; 9:27-34.
162. Becker DE, Reed KL. Essentials of local anesthetic pharmacology. *Anesth Prog*. 2006; 53(3):98-110.
163. Mumba JM, Kabambi FK, Ngaka CT. *Pharmacology of Local Anaesthetics and Commonly Used Recipes in Clinical Practice*, ed.: IntechOpen. 2017.
164. Becker DE, Reed KL. Local anesthetics: review of pharmacological considerations. *Anesth Prog*. 2012; 59(2):90-103.
165. Chahar P, Cummings KC, 3rd. Liposomal bupivacaine: a review of a new bupivacaine formulation. *J Pain Res*. 2012; 5:257-264.
166. Zorzetto L, Brambilla P, Marcello E, Bloise N, De Gregori M, Cobianchi L, Peloso A, Allegri M, Visai L, Petrini P. From micro- to nanostructured implantable device for local anesthetic delivery. *Int J Nanomedicine*. 2016; 11:2695-2709.
167. Larsen SW, Østergaard J, Friberg-Johansen H, Jessen MNB, Larsen C. In vitro assessment of drug release rates from oil depot formulations intended for intra-articular administration. *European Journal of Pharmaceutical Sciences*. 2006; 29(5):348-354.
168. Fredholt K, Larsen DH, Larsen C. Modification of in vitro drug release rate from oily parenteral depots using a formulation approach. *European Journal of Pharmaceutical Sciences*. 2000; 11(3):231-237.
169. Larsen SW, Frost AB, Østergaard J, Marcher H, Larsen C. On the mechanism of drug release from oil suspensions in vitro using local anesthetics as model drug compounds. *European Journal of Pharmaceutical Sciences*. 2008; 34(1):37-44.
170. Richard BM, Rickert DE, Newton PE, Ott LR, Haan D, Brubaker AN, Cole PI, Ross PE, Rebelatto MC, Nelson KG. Safety evaluation of EXPAREL (DepoFoam bupivacaine) administered by repeated subcutaneous injection in rabbits and dogs: species comparison. *Journal of drug delivery*. 2011; 2011.
171. Liu X, Ma X, Kun E, Guo X, Yu Z, Zhang F. Influence of lidocaine forms (salt vs. freebase) on properties of drug–eudragit® L100-55 extrudates prepared by reactive melt extrusion. *International journal of pharmaceutics*. 2018; 547(1):291-302.
172. Estebe J-P. Intravenous lidocaine. *Best Practice & Research Clinical Anaesthesiology*. 2017; 31(4):513-521.
173. Holgado MA, Arias JL, Cózar MJ, Alvarez-Fuentes J, Gañán-Calvo AM, Fernández-Arévalo M. Synthesis of lidocaine-loaded PLGA microparticles by flow focusing: Effects on drug loading and release properties. *International journal of pharmaceutics*. 2008; 358(1):27-35.
174. Klose D, Siepmann F, Willart JF, Descamps M, Siepmann J. Drug release from PLGA-based microparticles: Effects of the “microparticle:bulk fluid” ratio. *International journal of pharmaceutics*. 2010; 383(1):123-131.
175. Vladislavljević GT, Shahmohamadi H, Das DB, Ekanem EE, Tauanov Z, Sharma L. Glass capillary microfluidics for production of monodispersed poly (dl-lactic acid) and polycaprolactone microparticles: Experiments and numerical simulations. *Journal of Colloid and Interface Science*. 2014; 418:163-170.
176. Görner T, Gref R, Michenot D, Sommer F, Tran MN, Dellacherie E. Lidocaine-loaded biodegradable nanospheres. I. Optimization of the drug incorporation into the polymer matrix. *Journal of Controlled Release*. 1999; 57(3):259-268.
177. Polakovič M, Görner T, Gref R, Dellacherie E. Lidocaine loaded biodegradable nanospheres: II. Modelling of drug release. *Journal of Controlled Release*. 1999; 60(2):169-177.
178. Ramos Campos EV, Silva de Melo NF, Guilherme VA, de Paula E, Rosa AH, de Araújo DR, Fraceto LF. Preparation and Characterization of Poly(ε-Caprolactone) Nanospheres Containing the Local Anesthetic Lidocaine. *Journal of Pharmaceutical Sciences*. 2013; 102(1):215-226.

179. Huang Y-Y, Chung T-W, Tzeng T-w. Drug release from PLA/PEG microparticulates. *International journal of pharmaceutics*. 1997; 156(1):9-15.
180. Wang J, Zhang L, Chi H, Wang S. An alternative choice of lidocaine-loaded liposomes: lidocaine-loaded lipid-polymer hybrid nanoparticles for local anesthetic therapy. *Drug Delivery*. 2016; 23(4):1254-1260.
181. Fundueanu G, Constantin M, Ascenzi P. Poly(N-isopropylacrylamide-co-acrylamide) cross-linked thermoresponsive microspheres obtained from preformed polymers: Influence of the physico-chemical characteristics of drugs on their release profiles. *Acta Biomaterialia*. 2009; 5(1):363-373.
182. Fundueanu G, Constantin M, Asmarandei I, Harabagiu V, Ascenzi P, Simionescu BC. The thermosensitivity of pH/thermoresponsive microspheres activated by the electrostatic interaction of pH-sensitive units with a bioactive compound. *Journal of Biomedical Materials Research Part A*. 2013; 101(6):1661-1669.
183. Ganguly S, Dash AK. A novel in situ gel for sustained drug delivery and targeting. *International journal of pharmaceutics*. 2004; 276(1):83-92.
184. Fernandes Fraceto L, de Matos Alves Pinto L, Franzoni L, Albert Carmo Braga A, Spisni A, Schreier S, de Paula E. Spectroscopic evidence for a preferential location of lidocaine inside phospholipid bilayers. *Biophysical Chemistry*. 2002; 99(3):229-243.
185. Babaie S, Ghanbarzadeh S, Davaran S, Kouhsoltani M, Hamishehkar H. Nanoethosomes for Dermal Delivery of Lidocaine. *Adv Pharm Bull*. 2015; 5(4):549-556.
186. Babaei S, Ghanbarzadeh S, Adib Z, Kouhsoltani M, Davaran S, Hamishehkar H. Enhanced skin penetration of lidocaine through encapsulation into nanoethosomes and nanostructured lipid carriers: a comparative study. *Die Pharmazie-An International Journal of Pharmaceutical Sciences*. 2016; 71(5):247-251.
187. Zhu X, Li F, Peng X, Zeng K. Formulation and evaluation of lidocaine base ethosomes for transdermal delivery. *Anesth Analg*. 2013; 117(2):352-357.
188. Omar MM, Hasan OA, El Sisi AM. Preparation and optimization of lidocaine transferosomal gel containing permeation enhancers: a promising approach for enhancement of skin permeation. *Int J Nanomedicine*. 2019; 14:1551-1562.
189. Giovannitti JA, Jr., Rosenberg MB, Phero JC. Pharmacology of Local Anesthetics Used in Oral Surgery. *Oral and Maxillofacial Surgery Clinics*. 2013; 25(3):453-465.
190. Dawling S, Flanagan RJ, Widdop B. Fatal lignocaine poisoning: report of two cases and review of the literature. *Hum Toxicol*. 1989; 8(5):389-392.
191. Kudo K, Nishida N, Kiyoshima A, Ikeda N. A fatal case of poisoning by lidocaine overdose--analysis of lidocaine in formalin-fixed tissues: a case report. *Med Sci Law*. 2004; 44(3):266-271.
192. Beecroft C, Davies G. Systemic toxic effects of local anaesthetics. *Anaesthesia & Intensive Care Medicine*. 2010; 11(3):98-100.
193. Odedra D, Lyons G. Local anaesthetic toxicity. *Current Anaesthesia & Critical Care*. 2010; 21(1):52-54.
194. Tong YCI, Kaye AD, Urman RD. Liposomal bupivacaine and clinical outcomes. *Best Practice & Research Clinical Anaesthesiology*. 2014; 28(1):15-27.
195. Liu D-Z, Sheu M-T, Chen C-H, Yang Y-R, Ho H-O. Release characteristics of lidocaine from local implant of polyanionic and polycationic hydrogels. *Journal of Controlled Release*. 2007; 118(3):333-339.
196. Kumarswamy A, Moretti A, Paquette D, Padilla R, Everett E, Nares S. In vivo assessment of osseous wound healing using a novel bone putty containing lidocaine in the surgical management of tooth extractions. *Int J Dent*. 2012; 2012:894815-894815.
197. Second YLK, Neelakantan P. Local anesthetics in dentistry--newer methods of delivery. *Int J Pharm Clin Res*. 2014; 6(1):4-6.
198. Johnson M, Martinson M. Efficacy of electrical nerve stimulation for chronic musculoskeletal pain: a meta-analysis of randomized controlled trials. *Pain*. 2007; 130(1-2):157-165.

199. Kanebako M, Inagi T, Takayama K. Transdermal delivery of indomethacin by iontophoresis. *Biological and Pharmaceutical Bulletin*. 2002; 25(6):779-782.
200. Ohzeki K, Kitahara M, Suzuki N, Taguchi K, Yamazaki Y, Akiyama S, Takahashi K, Kanzaki Y. Local anesthetic cream prepared from lidocaine-tetracaine eutectic mixture. *Yakugaku Zasshi*. 2008; 128(4):611-616.
201. Arapostathis KN, Dabarakis NN, Coolidge T, Tsirlis A, Kotsanos N. Comparison of acceptance, preference, and efficacy between jet injection INJEX and local infiltration anesthesia in 6 to 11 year old dental patients. *Anesth Prog*. 2010; 57(1):3-12.
202. Jain S, Jain P, Umamaheshwari RB, Jain NK. Transfersomes a novel vesicular carrier for enhanced transdermal delivery: development, characterization, and performance evaluation. *Drug development and industrial pharmacy*. 2003; 29(9):1013-1026.
203. El Zaafarany GM, Awad GA, Holayel SM, Mortada ND. Role of edge activators and surface charge in developing ultradeformable vesicles with enhanced skin delivery. *International journal of pharmaceutics*. 2010; 397(1-2):164-172.
204. Ahmed TA. Preparation of transfersomes encapsulating sildenafil aimed for transdermal drug delivery: Plackett-Burman design and characterization. *Journal of liposome research*. 2015; 25(1):1-10.
205. Bnyan R, Khan I, Ehtezazi T, Saleem I, Gordon S, O'Neill F, Roberts M. Formulation and optimisation of novel transfersomes for sustained release of local anaesthetic. *Journal of Pharmacy and Pharmacology*. 2019; 71(10):1508-1519.
206. Chen H, Pan H, Li P, Wang H, Wang X, Pan W, Yuan Y. The potential use of novel chitosan-coated deformable liposomes in an ocular drug delivery system. *Colloids and Surfaces B: Biointerfaces*. 2016; 143:455-462.
207. Jøraholmen MW, Vanić Ž, Tho I, Škalko-Basnet N. Chitosan-coated liposomes for topical vaginal therapy: Assuring localized drug effect. *International journal of pharmaceutics*. 2014; 472(1-2):94-101.
208. Stetefeld J, McKenna SA, Patel TR. Dynamic light scattering: a practical guide and applications in biomedical sciences. *Biophys Rev*. 2016; 8(4):409-427.
209. Zhu X, Gao T. Chapter 10 - Spectrometry, ed.: Elsevier. 2019:237-264.
210. Bhattacharjee S. DLS and zeta potential - What they are and what they are not? *J Control Release*. 2016; 235:337-351.
211. Dong MW. 3 - HPLC Instrumentation in Pharmaceutical Analysis: Status, Advances, and Trends, ed.: Academic Press. 2005:47-75.
212. Lozano-Sánchez J, Borrás-Linares I, Sass-Kiss A, Segura-Carretero A. Chapter 13 - Chromatographic Technique: High-Performance Liquid Chromatography (HPLC), ed.: Academic Press. 2018:459-526.
213. Ahuja S. 1 - Overview: Handbook of Pharmaceutical Analysis by HPLC, ed.: Academic Press. 2005:1-17.
214. Sahu PK, Ramiseti NR, Cecchi T, Swain S, Patro CS, Panda J. An overview of experimental designs in HPLC method development and validation. *Journal of Pharmaceutical and Biomedical Analysis*. 2018; 147:590-611.
215. Paithankar H. HPLC METHOD VALIDATION FOR PHARMACEUTICALS: A REVIEW. *International Journal of Universal Pharmacy and Biosciences*. 2013; 2:229-240.
216. Guideline IHT. International conference on harmonization, Geneva, Switzerland, 2005, pp 11-12.
217. Tang CY, Yang Z. Chapter 8 - Transmission Electron Microscopy (TEM), ed.: Elsevier. 2017:145-159.
218. Xu Q, Kanellopoulos N. Nanoporous Materials : Advanced Techniques for Characterization, Modeling, and Processing, ed., Baton Rouge, UNITED STATES: CRC Press LLC. 2011.
219. Egerton R. Physical Principles of Electron Microscopy: An Introduction to TEM, SEM, and AEM, ed.: Springer US. 2011.

220. Abd Mutalib M, Rahman MA, Othman MHD, Ismail AF, Jaafar J. Chapter 9 - Scanning Electron Microscopy (SEM) and Energy-Dispersive X-Ray (EDX) Spectroscopy, ed.: Elsevier. 2017:161-179.
221. Yoshida A, Kaburagi Y, Hishiyama Y. Chapter 5 - Scanning Electron Microscopy, ed.: Butterworth-Heinemann. 2016:71-93.
222. Kunda NK, Alfagih IM, Dennison SR, Tawfeek HM, Somavarapu S, Hutcheon GA, Saleem IY. Bovine serum albumin adsorbed PGA-co-PDL nanocarriers for vaccine delivery via dry powder inhalation. *Pharm Res.* 2015; 32(4):1341-1353.
223. Tawfeek HM, Evans AR, Iftikhar A, Mohammed AR, Shabir A, Somavarapu S, Hutcheon GA, Saleem IY. Dry powder inhalation of macromolecules using novel PEG-co-polyester microparticle carriers. *Int J Pharm.* 2013; 441(1-2):611-619.
224. Refai H, Hassan D, Abdelmonem R. Development and characterization of polymer-coated liposomes for vaginal delivery of sildenafil citrate. *Drug Delivery.* 2017; 24(1):278-288.
225. Fatokun AA, Liu JO, Dawson VL, Dawson TM. Identification through high-throughput screening of 4'-methoxyflavone and 3',4'-dimethoxyflavone as novel neuroprotective inhibitors of parthanatos. *Br J Pharmacol.* 2013; 169(6):1263-1278.
226. Zhu C, Xiong Z, Chen X, Lu Z, Zhou G, Wang D, Bao J, Hu X. Soluble vascular endothelial growth factor (VEGF) receptor-1 inhibits migration of human monocytic THP-1 cells in response to VEGF. *Inflammation Research.* 2011; 60(8):769-774.
227. Shojaei AH. Buccal mucosa as a route for systemic drug delivery: a review. *Journal Of Pharmacy & Pharmaceutical Sciences: A Publication Of The Canadian Society For Pharmaceutical Sciences, Société Canadienne Des Sciences Pharmaceutiques.* 1998; 1(1):15-30.
228. Giovannitti Jr JA, Rosenberg MB, Phero JC. Pharmacology of Local Anesthetics Used in Oral Surgery. *Oral and Maxillofacial Surgery Clinics of North America.* 2013; 25(3):453-465.
229. Bnyan R, Khan I, Ehtezazi T, Saleem I, Gordon S, O'Neill F, Roberts M. Surfactant Effects on Lipid-Based Vesicles Properties. *J Pharm Sci.* 2018.
230. Yang SC, Zhu JB. Preparation and characterization of camptothecin solid lipid nanoparticles. *Drug Dev Ind Pharm.* 2002; 28(3):265-274.
231. Tekade RK, Chougule MB. Formulation development and evaluation of hybrid nanocarrier for cancer therapy: Taguchi orthogonal array based design. *Biomed Res Int.* 2013; 2013:712678.
232. Maghsoodloo S, Ozdemir G, Jordan V, Huang C-H. Strengths and limitations of taguchi's contributions to quality, manufacturing, and process engineering. *Journal of Manufacturing Systems.* 2004; 23(2):73-126.
233. Lee SH, Heng D, Ng WK, Chan H-K, Tan RBH. Nano spray drying: A novel method for preparing protein nanoparticles for protein therapy. *International journal of pharmaceutics.* 2011; 403(1):192-200.
234. Asghar A, Abdul Raman AA, Daud WMAW. A Comparison of Central Composite Design and Taguchi Method for Optimizing Fenton Process. *The Scientific World Journal.* 2014; 2014:869120.
235. Chawla V, Saraf SA. Rheological studies on solid lipid nanoparticle based carbopol gels of aceclofenac. *Colloids and Surfaces B: Biointerfaces.* 2012; 92:293-298.
236. López-Cacho JM, González-R PL, Talero B, Rabasco AM, González-Rodríguez ML. Robust Optimization of Alginate-Carbopol 940 Bead Formulations. *The Scientific World Journal.* 2012; 2012:605610.
237. Alfagih I, Kunda N, Alanazi F, Dennison SR, Somavarapu S, Hutcheon GA, Saleem IY. Pulmonary Delivery of Proteins Using Nanocomposite Microcarriers. *Journal of Pharmaceutical Sciences.* 2015; 104(12):4386-4398.
238. Abdelwahab NS, Nouruddin W, Fatatry H, Osman W. Determination of Thiomersal, Lidocaine and Phenylephrine in their Ternary Mixture. *J Chromatogr Sep Tech.* 2013; 4(8):1-6.
239. Carafa M, Santucci E, Lucania G. Lidocaine-loaded non-ionic surfactant vesicles: characterization and in vitro permeation studies. *International journal of pharmaceutics.* 2002; 231(1):21-32.

240. Qin WW, Jiao Z, Zhong MK, Shi XJ, Zhang J, Li ZD, Cui XY. Simultaneous determination of procaine, lidocaine, ropivacaine, tetracaine and bupivacaine in human plasma by high-performance liquid chromatography. *Journal of chromatography B, Analytical technologies in the biomedical and life sciences*. 2010; 878(15-16):1185-1189.
241. Ricci Júnior E, Bentley MVLB, Marchetti JM. HPLC assay of lidocaine in in vitro dissolution test of the Poloxamer 407 gels. *Rev Farm Bioquim Univ Sao Paulo*. 2002; 38:107-111.
242. Shaalan RA, Belal TS. HPLC-DAD stability indicating determination of nitrofurazone and lidocaine hydrochloride in their combined topical dosage form. *Journal of chromatographic science*. 2010; 48(8):647-653.
243. Sakdiset P, Okada A, Todo H, Sugibayashi K. Selection of phospholipids to design liposome preparations with high skin penetration-enhancing effects. *J Drug Deliv Sci Technol*. 2018; 44:58-64.
244. Barbosa RM, Severino P, Prete PS, Santana MH. Influence of different surfactants on the physicochemical properties of elastic liposomes. *Pharm Dev Technol*. 2017; 22(3):360-369.
245. Zeb A, Qureshi OS, Kim H-S, Cha J-H, Kim H-S, Kim J-K. Improved skin permeation of methotrexate via nanosized ultradeformable liposomes. *Int J Nanomedicine*. 2016; 11:3813-3824.
246. Bragagni M, Mennini N, Maestrelli F, Cirri M, Mura P. Comparative study of liposomes, transfersomes and ethosomes as carriers for improving topical delivery of celecoxib. *Drug Delivery*. 2012; 19(7):354-361.
247. Sarfraz M, Afzal A, Yang T, Gai Y, Raza SM, Khan MW, Cheng Y, Ma X, Xiang G. Development of Dual Drug Loaded Nanosized Liposomal Formulation by A Reengineered Ethanolic Injection Method and Its Pre-Clinical Pharmacokinetic Studies. *Pharmaceutics*. 2018; 10(3):151.
248. Malam Y, Loizidou M, Seifalian AM. Liposomes and nanoparticles: nanosized vehicles for drug delivery in cancer. *Trends in Pharmacological Sciences*. 2009; 30(11):592-599.
249. Hunter RJ. *Zeta potential in colloid science: principles and applications*, ed.: Academic press. 2013.
250. Shah R, Eldridge D, Palombo E, Harding I. Optimisation and Stability Assessment of Solid Lipid Nanoparticles using Particle Size and Zeta Potential. *Journal of Physical Science*. 2014; 25(1).
251. Friedman S, Kolusheva S, Volinsky R, Zeiri L, Schrader T, Jelinek R. Lipid/polydiacetylene films for colorimetric protein surface-charge analysis. *Anal Chem*. 2008; 80(20):7804-7811.
252. Tsermentseli KS, Kontogiannopoulos NK, Papageorgiou PV, Assimopoulou NA. Comparative Study of PEGylated and Conventional Liposomes as Carriers for Shikonin. *Fluids*. 2018; 3(2).
253. Han H-K, Shin H-J, Ha DH. Improved oral bioavailability of alendronate via the mucoadhesive liposomal delivery system. *European Journal of Pharmaceutical Sciences*. 2012; 46(5):500-507.
254. Epstein H, Gutman D, Cohen-Sela E, Haber E, Elmalak O, Koroukhov N, Danenberg HD, Golomb G. Preparation of Alendronate Liposomes for Enhanced Stability and Bioactivity: In Vitro and In Vivo Characterization. *The AAPS Journal*. 2008; 10(4):505-515.
255. Olmsted SS, Padgett JL, Yudin AI, Whaley KJ, Moench TR, Cone RA. Diffusion of macromolecules and virus-like particles in human cervical mucus. *Biophys J*. 2001; 81(4):1930-1937.
256. Natarajan JV, Nugraha C, Ng XW, Venkatraman S. Sustained-release from nanocarriers: a review. *Journal of Controlled Release*. 2014; 193:122-138.
257. Harris D, Robinson JR. Drug Delivery via the Mucous Membranes of the Oral Cavity. *Journal of Pharmaceutical Sciences*. 1992; 81(1):1-10.
258. Gandhi RB, Robinson JR. Oral cavity as a site for bioadhesive drug delivery. *Advanced Drug Delivery Reviews*. 1994; 13(1):43-74.
259. Sugihara H, Yamamoto H, Kawashima Y, Takeuchi H. Effectiveness of submicronized chitosan-coated liposomes in oral absorption of indomethacin. *Journal of liposome research*. 2012; 22(1):72-79.
260. Takeuchi H, Thongborisute J, Matsui Y, Sugihara H, Yamamoto H, Kawashima Y. Novel mucoadhesion tests for polymers and polymer-coated particles to design optimal mucoadhesive drug delivery systems. *Advanced Drug Delivery Reviews*. 2005; 57(11):1583-1594.

261. Thirawong N, Thongborisute J, Takeuchi H, Sriamornsak P. Improved intestinal absorption of calcitonin by mucoadhesive delivery of novel pectin–liposome nanocomplexes. *Journal of Controlled Release*. 2008; 125(3):236-245.
262. Mortazavi SA. An in vitro assessment of mucus/mucoadhesive interactions. *International journal of pharmaceutics*. 1995; 124(2):173-182.
263. Huang Y, Leobandung W, Foss A, Peppas NA. Molecular aspects of muco- and bioadhesion:: Tethered structures and site-specific surfaces. *Journal of Controlled Release*. 2000; 65(1):63-71.
264. Lee JW, Park JH, Robinson JR. Bioadhesive-Based Dosage Forms: The Next Generation. *Journal of Pharmaceutical Sciences*. 2000; 89(7):850-866.
265. Bernkop-Schnürch A, Schwarz V, Steininger S. Polymers with thiol groups: A new generation of mucoadhesive polymers? *Pharmaceutical Research*. 1999; 16(6):876-881.
266. Takeuchi H, Yamamoto H, Niwa T, Hino T, Kawashima Y. Mucoadhesion of Polymer-Coated Liposomes to Rat Intestine in Vitro. *Chemical and Pharmaceutical Bulletin*. 1994; 42(9):1954-1956.
267. Yamada T, Onishi H, Machida Y. In vitro and in vivo evaluation of sustained release chitosan-coated ketoprofen microparticles. *Yakugaku Zasshi*. 2001; 121(3):239-245.
268. Lehr CM, Bouwstra JA, Schacht EH, Junginger HE. In vitro evaluation of mucoadhesive properties of chitosan and some other natural polymers. *International journal of pharmaceutics*. 1992; 78(1-3):43-48.
269. Mendes AC, Sevilla Moreno J, Hanif M, E L Douglas T, Chen M, Chronakis IS. Morphological, Mechanical and Mucoadhesive Properties of Electrospun Chitosan/Phospholipid Hybrid Nanofibers. *Int J Mol Sci*. 2018; 19(8):2266.
270. Smart JD. The basics and underlying mechanisms of mucoadhesion. *Advanced Drug Delivery Reviews*. 2005; 57(11):1556-1568.
271. Solomonidou D, Cremer K, Krumme M, Kreuter J. Effect of carbomer concentration and degree of neutralization on the mucoadhesive properties of polymer films. *Journal of Biomaterials Science, Polymer Edition*. 2001; 12(11):1191-1205.
272. Madsen F, Eberth K, Smart JD. A rheological examination of the mucoadhesive/mucus interaction: The effect of mucoadhesive type and concentration. *Journal of Controlled Release*. 1998; 50(1-3):167-178.
273. Hoffmann A, Daniels R. Ultra–fast disintegrating ODTs comprising viable probiotic bacteria and HPMC as a mucoadhesive. *European Journal of Pharmaceutics and Biopharmaceutics*. 2019; 139:240-245.
274. Iorgulescu G. Saliva between normal and pathological. Important factors in determining systemic and oral health. *J Med Life*. 2009; 2(3):303-307.
275. Nafee NA, Ismail FA, Boraie NA, Mortada LM. Mucoadhesive buccal patches of miconazole nitrate: in vitro/in vivo performance and effect of ageing. *International journal of pharmaceutics*. 2003; 264(1):1-14.
276. Mortazavi SAR. Investigation of various parameters influencing the duration of mucoadhesion of some polymer containing discs. *DARU Journal of Pharmaceutical Sciences*. 2002:7.
277. Drumond N, Stegemann S. Polymer adhesion predictions for oral dosage forms to enhance drug administration safety. Part 1: In vitro approach using particle interaction methods. *Colloids and Surfaces B: Biointerfaces*. 2018; 165:9-17.
278. Lehr C-M, Bouwstra JA, Schacht EH, Junginger HE. In vitro evaluation of mucoadhesive properties of chitosan and some other natural polymers. *International journal of pharmaceutics*. 1992; 78(1):43-48.
279. Akbari J, Saeedi M, Enayatifard R, Doost M. Development and evaluation of mucoadhesive chlorhexidine tablet formulations. *Tropical Journal of Pharmaceutical Research*. 2010; 9(4).
280. Lochhead R. Water-soluble polymers: solution adsorption and interaction characteristics. *Cosmetics and toiletries*. 1992; 107(9):131-156.
281. Guo J-x, Ping Q-n, Jiang G, Huang L, Tong Y. Chitosan-coated liposomes: characterization and interaction with leuprolide. *International journal of pharmaceutics*. 2003; 260(2):167-173.

282. Li N, Zhuang C, Wang M, Sun X, Nie S, Pan W. Liposome coated with low molecular weight chitosan and its potential use in ocular drug delivery. *International journal of pharmaceutics*. 2009; 379(1):131-138.
283. Li J, Wang X, Zhang T, Wang C, Huang Z, Luo X, Deng Y. A review on phospholipids and their main applications in drug delivery systems. *Asian Journal of Pharmaceutical Sciences*. 2015; 10(2):81-98.
284. Mu X, Zhong Z. Preparation and properties of poly(vinyl alcohol)-stabilized liposomes. *International journal of pharmaceutics*. 2006; 318(1):55-61.
285. Minh NC, Nguyen VH, Schwarz S, Stevens WF, Trung TS. Preparation of water soluble hydrochloric chitosan from low molecular weight chitosan in the solid state. *International Journal of Biological Macromolecules*. 2019; 121:718-726.
286. Li N, Zhuang C-Y, Wang M, Sui C-G, Pan W-S. Low molecular weight chitosan-coated liposomes for ocular drug delivery: In vitro and in vivo studies. *Drug Delivery*. 2012; 19(1):28-35.
287. Lin M, Qi X-R. 2018. Purification Method of Drug-Loaded Liposome. In Lu W-L, Qi X-R, editors. *Liposome-Based Drug Delivery Systems*, ed., Berlin, Heidelberg: Springer Berlin Heidelberg. p 1-11.
288. Nicolazzo JA, Finnin BC. In vivo and in vitro models for assessing drug absorption across the buccal mucosa, ed.: Springer. 2008:89-111.
289. Fagerholm U, Johansson M, Lennernäs H. Comparison between permeability coefficients in rat and human jejunum. *Pharmaceutical research*. 1996; 13(9):1336-1342.
290. Tsutsumi K, Obata Y, Takayama K, Isowa K, Nagai T. Permeation of several drugs through keratinized epithelial-free membrane of hamster cheek pouch. *International journal of pharmaceutics*. 1999; 177(1):7-14.
291. Nielsen HM, Rassing MR. TR146 cells grown on filters as a model of human buccal epithelium: IV. Permeability of water, mannitol, testosterone and β -adrenoceptor antagonists. Comparison to human, monkey and porcine buccal mucosa. *International journal of pharmaceutics*. 2000; 194(2):155-167.
292. Squier CA, Wertz PW. Structure and function of the oral mucosa and implications for drug delivery. *Drugs and the pharmaceutical sciences*. 1996; 74:1-26.
293. Mashru R, Sutariya V, Sankalia M, Sankalia J. Transbuccal delivery of lamotrigine across porcine buccal mucosa: in vitro determination of routes of buccal transport. *J Pharm Pharm Sci*. 2005; 8(1):54-62.
294. Vande Vannet B, Mohebbian N, Wehrbein H. Toxicity of used orthodontic archwires assessed by three-dimensional cell culture. *European Journal of Orthodontics*. 2006; 28(5):426-432.
295. Vande Vannet B, Hanssens J-L, Wehrbein H. The use of three-dimensional oral mucosa cell cultures to assess the toxicity of soldered and welded wires. *European Journal of Orthodontics*. 2007; 29(1):60-66.
296. Rampersad SN. Multiple applications of Alamar Blue as an indicator of metabolic function and cellular health in cell viability bioassays. *Sensors (Basel)*. 2012; 12(9):12347-12360.
297. Smistad G, Jacobsen J, Sande SA. Multivariate toxicity screening of liposomal formulations on a human buccal cell line. *International journal of pharmaceutics*. 2007; 330(1):14-22.
298. Filion MC, Phillips NC. Toxicity and immunomodulatory activity of liposomal vectors formulated with cationic lipids toward immune effector cells. *Biochimica et Biophysica Acta (BBA)-Biomembranes*. 1997; 1329(2):345-356.
299. Inácio ÂS, Mesquita KA, Baptista M, Ramalho-Santos J, Vaz WLC, Vieira OV. In vitro surfactant structure-toxicity relationships: implications for surfactant use in sexually transmitted infection prophylaxis and contraception. *PLoS One*. 2011; 6(5):e19850-e19850.
300. Vlachy N, Touraud D, Heilmann J, Kunz W. Determining the cytotoxicity of cationic surfactant mixtures on HeLa cells. *Colloids and Surfaces B: Biointerfaces*. 2009; 70(2):278-280.
301. Noudeh GD, Khazaeli P, Mirzaei S, Sharififar F, Nasrollahosaiani S. Determination of the toxicity effect of sorbitan esters surfactants group on biological membrane. *J Biol Sci*. 2009; 9:423-430.

302. Arechabala B, Coiffard C, Rivalland P, Coiffard LJM, Roeck-Holtzhauer YD. Comparison of cytotoxicity of various surfactants tested on normal human fibroblast cultures using the neutral red test, MTT assay and LDH release. *Journal of Applied Toxicology*. 1999; 19(3):163-165.
303. Zhou Y, Doyen R, Lichtenberger LM. The role of membrane cholesterol in determining bile acid cytotoxicity and cytoprotection of ursodeoxycholic acid. *Biochim Biophys Acta*. 2009; 1788(2):507-513.
304. Ibrahim MA, Shazly GA, Aleanizy FS, Alqahtani FY, Elosaily GM. Formulation and evaluation of docetaxel nanosuspensions: In-vitro evaluation and cytotoxicity. *Saudi Pharm J*. 2019; 27(1):49-55.
305. Palumbo P, Melchiorre E, La Torre C, Miconi G, Cinque B, Marchesani G, Zoccali V, Maione M, Macchiarelli G, Vitale A. Effects of phosphatidylcholine and sodium deoxycholate on human primary adipocytes and fresh human adipose tissue. *International journal of immunopathology and pharmacology*. 2010; 23(2):481-489.
306. Nishina K, Mikawa K, Morikawa O, Obara H, Mason R. The effects of intravenous anesthetics and lidocaine on proliferation of cultured type II pneumocytes and lung fibroblasts. *Anesthesia & Analgesia*. 2002; 94(2):385-388.
307. Johnson ME, Uhl CB, Spittler K-H, Wang H, Gores GJ. Mitochondrial injury and caspase activation by the local anesthetic lidocaine. *Anesthesiology: The Journal of the American Society of Anesthesiologists*. 2004; 101(5):1184-1194.
308. Chang Y-S, Tseng S-Y, Tseng S-H, Wu C-L. Cytotoxicity of lidocaine or bupivacaine on corneal endothelial cells in a rabbit model. *Cornea*. 2006; 25(5):590-596.
309. Kyung Kim D, Jankowski RJ, Pruchnic R, de Miguel F, Yoshimura N, Honda M, Furuta A, Chancellor MB. In Vitro and In Vivo Effect of Lidocaine on Rat Muscle-Derived Cells for Treatment of Stress Urinary Incontinence. *Urology*. 2009; 73(2):437-441.
310. Alvi IA, Madan J, Kaushik D, Sardana S, Pandey RS, Ali A. Comparative study of transfersomes, liposomes, and niosomes for topical delivery of 5-fluorouracil to skin cancer cells: preparation, characterization, in-vitro release, and cytotoxicity analysis. *Anticancer Drugs*. 2011; 22(8):774-782.
311. Mahor S, Rawat A, Dubey PK, Gupta PN, Khatra K, Goyal AK, Vyas SP. Cationic transfersomes based topical genetic vaccine against hepatitis B. *International journal of pharmaceuticals*. 2007; 340(1):13-19.
312. Islam N, Ferro V. Recent advances in chitosan-based nanoparticulate pulmonary drug delivery. *Nanoscale*. 2016; 8(30):14341-14358.
313. Mohammed MA, Syeda JTM, Wasan KM, Wasan EK. An Overview of Chitosan Nanoparticles and Its Application in Non-Parenteral Drug Delivery. *Pharmaceutics*. 2017; 9(4):53.
314. Pistone S, Goycoolea FM, Young A, Smistad G, Hiorth M. Formulation of polysaccharide-based nanoparticles for local administration into the oral cavity. *European Journal of Pharmaceutical Sciences*. 2017; 96:381-389.
315. Diaz del Consuelo I, Pizzolato G-P, Falson F, Guy RH, Jacques Y. Evaluation of pig esophageal mucosa as a permeability barrier model for buccal tissue. *Journal of Pharmaceutical Sciences*. 2005; 94(12):2777-2788.
316. Caon T, Simões CMO. Effect of Freezing and Type of Mucosa on Ex Vivo Drug Permeability Parameters. *AAPS PharmSciTech*. 2011; 12(2):587-592.
317. Prestin S, Rothschild SI, Betz CS, Kraft M. Measurement of epithelial thickness within the oral cavity using optical coherence tomography. *Head Neck*. 2012; 34(12):1777-1781.
318. Stasio DD, Lauritano D, Iquebal H, Romano A, Gentile E, Lucchese A. Measurement of Oral Epithelial Thickness by Optical Coherence Tomography. *Diagnostics (Basel)*. 2019; 9(3):90.
319. Di Colo G, Zambito Y, Zaino C. Polymeric enhancers of mucosal epithelia permeability: synthesis, transepithelial penetration-enhancing properties, mechanism of action, safety issues. *Journal of pharmaceutical sciences*. 2008; 97(5):1652-1680.
320. Chen M-C, Mi F-L, Liao Z-X, Hsiao C-W, Sonaje K, Chung M-F, Hsu L-W, Sung H-W. Recent advances in chitosan-based nanoparticles for oral delivery of macromolecules. *Advanced drug delivery reviews*. 2013; 65(6):865-879.

321. Sandri G, Rossi S, Ferrari F, Bonferoni MC, Muzzarelli C, Caramella C. Assessment of chitosan derivatives as buccal and vaginal penetration enhancers. *European Journal of Pharmaceutical Sciences*. 2004; 21(2):351-359.
322. Preis M, Woertz C, Schneider K, Kukawka J, Broscheit J, Roewer N, Breitzkreutz J. Design and evaluation of bilayered buccal film preparations for local administration of lidocaine hydrochloride. *European Journal of Pharmaceutics and Biopharmaceutics*. 2014; 86(3):552-561.
323. Alopeus JF, Hellfritsch M, Gutowski T, Scherließ R, Almeida A, Sarmiento B, Škalko-Basnet N, Tho I. Mucoadhesive buccal films based on a graft co-polymer – A mucin-retentive hydrogel scaffold. *European Journal of Pharmaceutical Sciences*. 2020; 142:105142.
324. Fonseca-Santos B, Chorilli M. An overview of polymeric dosage forms in buccal drug delivery: State of art, design of formulations and their in vivo performance evaluation. *Materials Science and Engineering: C*. 2018; 86:129-143.
325. Zulfakar MH, Goh JY, Rehman K. Development and mechanical characterization of eugenol–cetalkonium chloride sustained release mucoadhesive oral film. *Polymer Composites*. 2016; 37(11):3200-3209.
326. Timur SS, Yüksel S, Akca G, Şenel S. Localized drug delivery with mono and bilayered mucoadhesive films and wafers for oral mucosal infections. *International journal of pharmaceutics*. 2019; 559:102-112.
327. Hiorth M, Nilsen S, Tho I. Bioadhesive Mini-Tablets for Vaginal Drug Delivery. *Pharmaceutics*. 2014; 6(3):494-511.
328. Kamel R, Mahmoud A, El-Feky G. Double-phase hydrogel for buccal delivery of tramadol. *Drug development and industrial pharmacy*. 2012; 38(4):468-483.
329. Liew KB, Tan YTF, Peh K-K. Effect of polymer, plasticizer and filler on orally disintegrating film. *Drug development and industrial pharmacy*. 2014; 40(1):110-119.
330. Krull SM, Ma Z, Li M, Davé RN, Bilgili E. Preparation and characterization of fast dissolving pullulan films containing BCS class II drug nanoparticles for bioavailability enhancement. *Drug development and industrial pharmacy*. 2016; 42(7):1073-1085.
331. Vuddanda PR, Montenegro-Nicolini M, Morales JO, Velaga S. Effect of surfactants and drug load on physico-mechanical and dissolution properties of nanocrystalline tadalafil-loaded oral films. *European Journal of Pharmaceutical Sciences*. 2017; 109:372-380.
332. Speer I, Steiner D, Thabet Y, Breitzkreutz J, Kwade A. Comparative study on disintegration methods for oral film preparations. *European Journal of Pharmaceutics and Biopharmaceutics*. 2018; 132:50-61.
333. Ernest T. 2014. Use of hypromellose and hydroxypropyl cellulose to develop an age appropriate platform technology for the administration of medicines to children. ed.: Liverpool John Moores University.
334. Preis M, Knop K, Breitzkreutz J. Mechanical strength test for orodispersible and buccal films. *International journal of pharmaceutics*. 2014; 461(1):22-29.
335. Aframian DJ, Davidowitz T, Benoliel R. The distribution of oral mucosal pH values in healthy saliva secretors. *Oral Dis*. 2006; 12(4):420-423.
336. Baliga S, Muglikar S, Kale R. Salivary pH: A diagnostic biomarker. *J Indian Soc Periodontol*. 2013; 17(4):461-465.

Publications and Conferences

Journal Papers

- **Ruba Bnyan**, Iftikhar Khan, Touraj Ehtezazi, Imran Saleem, Sarah Gordon, Francis O'Neill, and Matthew Roberts. "Formulation and optimisation of novel transfersomes for sustained release of local anaesthetic." Journal of Pharmacy and Pharmacology (2019), [DOI: 10.1111/jphp.13149](https://doi.org/10.1111/jphp.13149)
- **Ruba Bnyan**, Iftikhar Khan, Touraj Ehtezazi, Imran Saleem, Sarah Gordon, Francis O'Neill, and Matthew Roberts. "Surfactant effects on lipid-based vesicles properties." Journal of pharmaceutical sciences 107, no. 5 (2018): 1237-1246, [DOI: 10.1016/j.xphs.2018.01.005](https://doi.org/10.1016/j.xphs.2018.01.005)

Additional research papers

- **Ruba Bnyan**, Laura Cesarini, Iftikhar Khan, Matthew Roberts and Touraj Ehtezazi. "The Effect of Ethanol Evaporation on the Properties of Inkjet Produced Liposomes" DARU J Pharm Sci 28, 271–280 (2020), [Doi.org/10.1007/s40199-020-00340-1](https://doi.org/10.1007/s40199-020-00340-1)
- Iftikhar Khan, Maria Apostolou, **Ruba Bnyan**, Chahinez Houacine, Abdelbary Elhissi, Sakib S Yousaf "Paclitaxel-loaded Micro or Nano Transfersome Formulations into Novel Tablets for Pulmonary Drug Delivery via Nebulization" International Journal Of Pharmaceutics (2019), [DOI:10.1016/j.ijpharm.2019.118919](https://doi.org/10.1016/j.ijpharm.2019.118919)
- Iftikhar Khan, Katie Lau, **Ruba Bnyan**, Chahinez Houacine, Matthew Roberts, Abdullah Israb, Abdelbary Elhissi, Sakib S Yousaf "A Facile and Novel Approach to Manufacture Paclitaxel-loaded Proliposome Tablet Formulations of Micro or Nano vesicles for Nebulization" Pharmaceutical Research 37, 116 (2020), [Doi.org/10.1007/s11095-020-02840-w](https://doi.org/10.1007/s11095-020-02840-w) .
- Marafi Ansam, **Ruba Bnyan**, Sakib Yousaf, and Iftikhar Khan. "Anti-Aging Liposomal formulation: A Mini Review" Novel Approaches in Drug Designing & Development (2018) 3(3): 555614, [DOI: 10.19080/NAPDD.2018.03.555614](https://doi.org/10.19080/NAPDD.2018.03.555614)

Conferences

- **Ruba Bnyan**, Iftikhar Khan, Touraj Ehtezazi, Imran Saleem, Sarah Gordon, Francis O'Neill, and Matthew Roberts. "A novel carrier system via deformable liposomes using local anaesthetic for buccal delivery" PharmSci conference (2019) Greenwich, UK.
- **Ruba Bnyan**, Iftikhar Khan, Touraj Ehtezazi, Imran Saleem, Sarah Gordon, Francis O'Neill, and Matthew Roberts. "Transfersomes for buccal delivery of local anaesthetic (LA)" United Kingdom and Ireland Controlled Release Society (UKICRS) Symposium (2019) Liverpool, UK.

- **Ruba Bnyan**, Iftikhar Khan, Touraj Ehtezazi, Imran Saleem, Sarah Gordon, Francis O'Neill, and Matthew Roberts. "#Dentist Fear... #Needle Phobia ... NO MORE ! Local Anaesthetic Transfersomes" International women day, celebrating women in research held by LJMU (2018), Liverpool, UK.
- **Ruba Bnyan**, Iftikhar Khan, Touraj Ehtezazi, Imran Saleem, and Matthew Roberts. "Transfersomes as novel carriers for sustained buccal delivery of local anaesthetic" 16th International Conference and Exhibition on Pharmaceutics & Novel Drug Delivery Systems (2018) Berlin, Germany.
- **Ruba Bnyan**, Iftikhar Khan, Touraj Ehtezazi, Imran Saleem, Sarah Gordon, Francis O'Neill, and Matthew Roberts. "#Dentist Fear... #Needle Phobia ... NO MORE! Local Anaesthetic Transfersomes" 4th Annual keele Nanopharmaceutics Symposium (2018), Keele, UK.
- **Ruba Bnyan**, Iftikhar Khan, Touraj Ehtezazi, Imran Saleem, and Matthew Roberts. "Formulation and optimization of transfersomesfor sustained buccal delivery of local anaesthetic" Faculty of science research and seminar day, LJMU (2017), Liverpool, UK.
- **Ruba Bnyan**, Iftikhar Khan, Touraj Ehtezazi, Imran Saleem, and Matthew Roberts. "Formulation and optimization of transfersomesfor sustained buccal delivery of local anaesthetic" The pharmaceutical analysis postgraduate research awards and careers Symposium held by the Joint Pharmaceutical Analysis Group (JPAG), (2017), London, UK.

[Research related awards](#)

- Three minute thesis competition (3MT) **awarded twice, 1st winner** for the School of Pharmacy, and **runner up** for the university, LJMU, 2019.
- Awarded **travel funds** (twice of £350 each) to attend conferences from the doctoral academy, LJMU, 2018 and 2019.
- Awarded a **runner up prize** for a poster presentation in the Faculty of Science postgraduate Research Seminar and Poster Day, LJMU, 2017.